A correlation study of proton decay signatures induced through the gauge boson and scalar leptoquark mediations

Džaferović-Mašić, Emina

Doctoral thesis / Doktorski rad

2024

University of Zagreb

Emina Džaferović-Mašić

A CORRELATION STUDY OF PROTON DECAY SIGNATURES INDUCED THROUGH THE GAUGE BOSON AND SCALAR LEPTOQUARK MEDIATIONS

DOCTORAL DISSERTATION

Supervisor:

Prof. dr. sc. Ilja Doršner

Zagreb, 2024

University of Zagreb

PRIRODOSLOVNO-MATEMATIČKI FAKULTET
ODSJEK ZA FIZIKU

Emina Džaferović-Mašić

KORELACIJSKA STUDIJA TRAGOVA PROTONSKOG RASPADA IZMJENOM BAŽDARNIH BOZONA I SKALARNIH LEPTOKVARKOVA

DOKTORSKI RAD

Mentor:

Prof. dr. sc. Ilja Doršner

Zagreb, 2024

Acknowledgments

This doctoral journey has been a couple of years now long adventure. Every adventure starts by choice, followed by excitement and lots of challenges on that road. But no matter how strong, ambitious and decisive a person is, the journey itself is not feasible without others' guidance, help, advice, humour, laugh, critique, proofreading or just a nice meal and enjoyable break. Hence, before the official opening of thesis' lines and introduction into what has been done in previous years, I need to mention some of the people who helped me on my scientific adventure called postdoctoral education.

One might say this story started in 2017 with my enrolment into postdoctoral studies at the University of Zagreb and choosing prof. dr. sc. Ilja Doršner as my supervisor, but I would go way back to 2009 when I first met my supervisor and knew what I will be doing in next decades - particle physics. Therefore, 2017 was continuation of my work with prof. dr. sc. Ilja Doršner, enriched with his enormous experience, ideas, commitment, and selfless and generous help at every step of the way. In fact, I am deeply grateful to him for accepting me as his doctoral student and mentee, for trusting me with his remarkably prodigious model of $SU(5)$ group that was a home-basis for my doctoral research. Prof. dr. sc. Ilja Doršner had so much patience for my rhythm and pace of work and research, for my questions and doubts and so much more. Without his ideas and his guidance, this work could not be accomplished.

Furthermore, none of my steps in academia and in much wider space of action would not be accomplished if there weren't for my parents Nefisa and Jusuf Džaferović. They have been so supportive in so many ways, that no book would be enough to write it down. I embrace the opportunity to thank them for patience and understanding, their sacrifice and faith in all these years for my work, research and contemplation over old and new ideas, aspirations and goals.

These ideas, aspirations and goals were at the same time under a great responsibility for me since I had a younger brother who looked upon me and probably got affected by some of my work as well. Therefore, I want to thank Emir Džaferović for being there for me, for understanding and supporting me by traveling with me to Zagreb, by being with me during my oral exams and lot more.

I want to express my love and sincere and whole hearted gratitude towards my husband Adnan Mašić who was at the same time a family and a colleague, who helped me with practical advice and his rich experience in physics research and academia in general. Our discussions were always fruitful and enhanced with new outcomes and encouraging motivation.

I am grateful to prof.dr.sc. Krešimir Kumerički, who was at the time of my enrolment into postdoctoral studies, Chief of Doctoral studies at the Department of Physics, for giving me the opportunity to be

CURRICULUM VITAE

prof. dr. sc. Ilja Doršner

CROSBI: https://www.bib.irb.hr/pregled/znanstvenici/341315

Ilja Doršner was born on April 16, 1971, in Sarajevo, Bosnia and Herzegovina. He obtained his BSc in Physics in 1997 from University of Sarajevo. As an undergraduate he spent 9 months in Naples, Italy, at University of Naples "Federico II" working in the High Energy Physics group of prof. Franco Buccella. From 1997 to 1998 he was Teaching Assistant at University of Sarajevo. He enrolled in PhD program in Physics at University of Delaware, USA, in 1998, where he obtained PhD in 2003. The title of his PhD thesis was "Selected Topics in High Energy Physics: Flavor, Neutrino and Extra-dimensional Models" and his mentor was prof. Stephen M. Barr. The following six years he was postdoctoral fellow at the Abdus Salam International Centre for Theoretical Physics (2003-2006), Pennsylvania State University (2006-2007), and Institute Jozef Štefan (2007-2009). He was a professor of physics from 2009 through 2014 at Faculty of Science of University of Sarajevo. His is currently a professor at Faculty of Electrical Engineering, Mechanical Engineering and Naval Architecture of University of Split and a researcher at Institute Jozef Štefan, Slovenia.

Ilja Doršner has been working in the field of High Energy Physics on the phenomenology of the Standard Model of elementary particle physics and its extensions. He has, in particular, worked extensively on grand unified models, generation of neutrino masses, stability of proton, physics of leptoquarks and flavor physics. He (co)authored more than 50 published articles in journals indexed in Current Contents (CC). His articles have been cited more than 2200 times according to SCI-Expanded and more than 3400 times according to INSPIRE (SLAC) database. His Google Scholar h-index is 32 and the total number of Google Scholar citations exceeds 3900.

He gave around 40 invited talks at international conferences and workshops and at least 20 seminars at various international academic institutions. He was Regular Associate at the Abdus Salam International Centre for Theoretical Physics from 2010 through 2014, Scientific Associate at CERN in 2017, and Corresponding Associate at CERN in 2021. He is a recipient of an annual prize for science of Republic of

Croatia for 2016. He is referee for Journal of High Energy Physics, Nuclear Physics B, Physical Review D, Physical Review Letters, European Physical Journal C, Frontiers in High-Energy and Astroparticle Physics, Europhysics Letters, and Physics Letters B. He authored one textbook on Symmetries in Physics.

CURRICULUM VITAE

Emina Džaferović-Mašić, mag. phy.

CROSBI: https://www.croris.hr/osobe/profil/41403

Emina Džaferović-Mašić was born on March 25, 1987, in Sarajevo, Bosnia and Herzegovina where she went to elementary and high school and discovered her love and passion for art, literature and science, mathematics and physics in particular. At the age of ten she enrolled in various competitions at all levels winning 1st, 2nd and 3rd places. One of the special prizes is Bronze Medal in Mediterranean Mathematics Olympiad.

She has finished her undergraduate (in 2010) and graduate studies (in 2013) in Physics at the University of Sarajevo, Department of Physics in the field of Theoretical Physics, more precisely in High Energy Physics. In addition to this, she has finished undergraduate (in 2015) and graduate studies (2017) in French Language and Literature at the University of Sarajevo, Department of Roman Languages.

During her undergraduate and graduate studies, she has participated in numerous summer schools and camps in theoretical physics at the University of Sarajevo (2010, 2011, 2012), at the Institute Jozef Štefan (2010), at CERN (2010), at the Abdus Salam International Centre for Theoretical Physics (2011), at the University Cergy-Pontoise (2015), and at the University of Zagreb (2017).

Emina Džaferović-Mašić is also a poet with a number of published books of poetry such as: "The Outspoken Silences", "When Dawn Rarefies the Air", "In the Storefront Without Glass", etc.

In the field of physics, she has published the following: Expression of expanded uncertainty in accreditation scope regarding ILAC P14 (Conference paper, 2022), Teaching physics for high-school students through real-life questions and situations (Conference paper, 2022), Parameter space exploration of the minimal SU(5) unification (Scientific Paper, 2021), Improvements in theoretical background and practical experiment on atomic spectra for high school and university students (Conference paper, 2020), Visualization of data from network of sensors: appropriate spatial interpolation method (Scientific Paper, 2018), Experimental study of temperature inversions above urban area using unmanned aerial vehicle (Scientific Paper, 2018), Physics at ILC and comparison of its capabilities with LHC (Conference Abstract,

2018), Challenges on teaching particle physics in high school (Conference Abstract, 2018), Temperature inversion measurements in Sarajevo valley using unmanned aerial vehicles (Scientific Paper, 2016), Phenomenology of Scalar Leptoquarks (graduate thesis, 2013), Neutrino Oscillations in Vacuum and Matter (undergraduate thesis, 2010).

Abstract

Proton decay is one of the most significant predictions of models of grand unification and, at the same time, the source of one of the most important constraints on the otherwise viable parameter space of these theories. In the model considered in this thesis, and within which the correlation study of the proton decay signatures was performed, there are only two sources of proton instability. The first source are vector bosons X and Y, while the second source is a scalar leptoquark. The aim of the thesis is to study predictions for two-body proton decay partial lifetimes due to the exchanges of both X and Y vector bosons and one scalar leptoquark. The model of interest yields all unitary transformations, Yukawa couplings, and gauge coupling strength that are necessary to generate accurate partial lifetime predictions as a function of mediator's mass. The research hypothesis is that the predicted patterns for two-body proton decays might be different for these two types of mediators. This would then allow for unambiguous experimental answer to the question of what the dominant source of proton decay in this model of unification is. It should thus be considered to be the most important outcome of this doctoral research. Therefore, we present results of correlation study between two sources of proton instability in reference to experimental limits and future expectations in this field.

KEY WORDS: $SU(5)$ model, proton decay, scalar leptoquark, gauge boson, partial proton lifetime, proton decay width, correlation study

Sažetak

Raspad protona jedno je od najznačajnijih predviđanja modela velikog ujedinjenja, a istovremeno, i izvor jednog od najvažnijih ograničenja na inače održiv prostor parametara ovih teorija. U modelu koji se razmatra u ovoj doktorskoj tezi, a unutar kojeg je provedena korelacijska studija za tragove protonskog raspada, postoje samo dva izvora nestabilnosti protona. Prvi izvor su vektorski bozoni X i Y, dok je drugi izvor skalarni leptokvark. Cilj doktorskog rada je proučavati predviđanja za parcijalne živote raspada protona na dvije čestice izmjenom X i Y vektorskih bozona, i skalarnog leptokvarka. Model od interesa daje sve unitarne transformacije, Yukawina vezanja i jakost baždarnih vezanja koja su potrebna za generiranje predikcija točnog parcijalnog životnog vijeka protona. Hipoteza istraživanja je da bi predviđeni obrasci raspada protona na dvije čestice mogli biti različiti za ove dvije vrste medijatora. To bi onda omogućilo nedvosmislen eksperimentalni odgovor na pitanje koji je dominantni izvor raspada protona u ovom modelu ujedinjenja. Ovo bi stoga bio najvažniji rezultat ovog doktorskog istraživanja. Zato predstavljamo rezultate studije korelacije između dvaju izvora protonske nestabilnosti u odnosu na eksperimentalne granice i buduća očekivanja u ovom području.

KLJUČNE RIJEČI: $SU(5)$ model, raspad protona, skalarni leptokvark, baždarni bozoni, parcijalno vrijeme života protona, širina raspada protona, studija korelacije

Prošireni sažetak

Ključne riječi: $SU(5)$ model, raspad protona, skalarni leptokvark, baždarni bozoni, parcijalno vrijeme života protona, širina raspada protona, studija korelacije

Uvod

Velike ujedinjene teorije [1, 2, 3, 4, 5, 6] (GUT) su teorijski okviri koji nastoje ujediniti tri temeljne sile Standardnog Modela fizike elementarnih čestica — elektromagnetske, slabe i jake interakcije — u jednu. Unutar tih okvira, temeljni sastojci materije, kvarkovi i leptoni, također su djelomično ili potpuno unificirani. Jedno od značajnih predviđanja ovakvih teorija je da protoni nisu apsolutno stabilni. Raspad protona je stoga ključni potpis baš ovih teorija koji čak nudi potencijalni put za testiranje iako su relevantne energetske ljestvice daleko izvan izravnog dosega trenutnim ili bilo kojim drugim eksperimentalnim mogućnostima. Otkriće protonskog raspada bio bi revolucionarni pomak u polju fizike čestica i važan razvoj u našem razumijevanju svemira.

Georgi-Glashow model [3] odigrao je ključnu ulogu u ranom razvoju velikih teorija ujedinjenja. Međutim, ovaj model, koji se sastoji samo od adjungiranog skalarnog polja za slamanje GUT simetrija i fundamentalnog Higgsa za slamanje elektroslabe simetrije, nije kompatibilan s eksperimentalnim podacima zbog svoje jednostavnosti. Stoga je potrebno proširiti postojeći Georgi-Glashow model vodeći računa o jednostavnosti samog modela.

Jedan od takvih modela na temelju $SU(5)$ baždarne simetrije koji predstavlja jednu od teorija velikog ujedinjenja, je opisan u [7]. Ova minimalna realizacija koristi samo prvih pet najmanjih reprezentacija dimenzija 5, 10, 15, 24 i 35. Ima ograničen broj parametara modela, a što ga čini vrlo prediktivnim modelom. Zanimljivo je da osim dva superteška bozona, samo jedan skalarni leptokvark sudjeluje u protonskom raspadu. Ova specifična značajka, daje predviđanja u vezi s ujedinjenjem skala i vremenu poluživota protona u ovisnosti od kanala raspada.

Studija predstavljena u ovom radu se bavi protonskim raspadom putem osam kanala, ispitujući stopu raspada i vrijeme poluživota. Usporedbom sa stvarnim podatcima dobivenim u eksperimentima kao što je Super-Kamiokande, bili smo u mogućnosti dati predikcije za ono što bi se moglo vidjeti u eksperimentima

u narednom vremenskom periodu. Naime, na osnovu tipa opaženog kanala u eksperimentu, moguće je reći da li je protonski raspad ostvaren izmjenom baždarnog bozona ili skalarnog leptokvarka.

Model

Model koji je predstavljen u referenci [7], a unutar kojeg radimo u ovoj doktorskoj tezi, sadrži skalarna $(5_H, 24_H$ i $35_H)$, fermionska $(\overline{5}_{Fi}, 10_{Fi}$ i $15_F + \overline{15}_F)$ i baždarna polja (24_G), gdje je $i = 1, 2, 3$. Kompletan sadržaj polja u ovom modelu je dan u Tablici 1.

Tablica 1: Sastav i građa modela, dekompozicija prema baždarnoj grupi Standardnog Modela i pridruženi koeficijenti β-funkcije. $i(= 1, 2, 3)$ predstavlja indeks generacije.

Skalarna polja			Fermionska polja		
$SU(5)$	Standardni Model	(b_3, b_2, b_1)	$SU(5)$	Standardni Model	(b_3, b_2, b_1)
$\Lambda = 5_H$	$\Lambda_1 \left(1, 2, +\frac{1}{2}\right)$	$\left(0, \frac{1}{6}, \frac{1}{10}\right)$	$F_i = \overline{5}_{Fi}$	$L_i \left(1, 2, -\frac{1}{2}\right)$	$\left(0, 1, \frac{3}{5}\right)$
	$\Lambda_3 \left(3, 1, -\frac{1}{3}\right)$	$\left(\frac{1}{6}, 0, \frac{1}{15}\right)$		$d_i^c \left(\overline{3}, 1, +\frac{1}{3}\right)$	$\left(1, 0, \frac{2}{5}\right)$
$\phi = 24_H$	$\phi_0 (1, 1, 0)$	$(0, 0, 0)$	$T_i = 10_{Fi}$	$Q_i \left(3, 2, +\frac{1}{6}\right)$	$\left(2, 3, \frac{1}{5}\right)$
	$\phi_1 (1, 3, 0)$	$\left(0, \frac{1}{3}, 0\right)$		$u_i^c \left(\overline{3}, 1, -\frac{2}{3}\right)$	$\left(1, 0, \frac{8}{5}\right)$
	$\phi_3 \left(3, 2, -\frac{5}{6}\right)$	$\left(\frac{1}{6}, \frac{1}{4}, \frac{5}{12}\right)$		$e_i^c (1, 1, +1)$	$\left(0, 0, \frac{6}{5}\right)$
	$\phi_{\overline{3}} \left(\overline{3}, 2, +\frac{5}{6}\right)$	$\left(\frac{1}{6}, \frac{1}{4}, \frac{5}{12}\right)$	$\Sigma = 15_F$	$\Sigma_1 (1, 3, +1)$	$\left(0, \frac{4}{3}, \frac{6}{5}\right)$
	$\phi_8 (8, 1, 0)$	$\left(\frac{1}{2}, 0, 0\right)$		$\Sigma_3 \left(3, 2, +\frac{1}{6}\right)$	$\left(\frac{2}{3}, 1, \frac{1}{15}\right)$
$\Phi = 35_H$	$\Phi_1 \left(1, 4, -\frac{3}{2}\right)$	$\left(0, \frac{5}{3}, \frac{9}{5}\right)$		$\Sigma_6 \left(6, 1, -\frac{2}{3}\right)$	$\left(\frac{5}{3}, 0, \frac{16}{15}\right)$
	$\Phi_3 \left(\overline{3}, 3, -\frac{2}{3}\right)$	$\left(\frac{1}{2}, 2, \frac{4}{5}\right)$	$\overline{\Sigma} = \overline{15}_F$	$\overline{\Sigma}_1 (1, 3, -1)$	$\left(0, \frac{4}{3}, \frac{6}{5}\right)$
	$\Phi_6 \left(\overline{6}, 2, +\frac{1}{6}\right)$	$\left(\frac{5}{3}, 1, \frac{1}{15}\right)$		$\overline{\Sigma}_3 \left(\overline{3}, 2, -\frac{1}{6}\right)$	$\left(\frac{2}{3}, 1, \frac{1}{15}\right)$
	$\Phi_{10} \left(\overline{10}, 1, +1\right)$	$\left(\frac{5}{2}, 0, 2\right)$		$\overline{\Sigma}_6 \left(\overline{6}, 1, +\frac{2}{3}\right)$	$\left(\frac{5}{3}, 0, \frac{16}{15}\right)$

Lagranžijan skalarnog dijela je dan u sljedećoj jednadžbi:

$$
\begin{aligned}
\mathcal{L}_V = &- \mu_\Lambda^2 \left(\Lambda_\alpha^* \Lambda^\alpha\right) + \lambda_0^\Lambda \left(\Lambda_\alpha^* \Lambda^\alpha\right)^2 + \mu_1 \Lambda_\alpha^* \Lambda^\beta \phi_\beta^\alpha + \lambda_1^\Lambda \left(\Lambda_\alpha^* \Lambda^\alpha\right) \left(\phi_\gamma^\beta \phi_\beta^\gamma\right) + \lambda_2^\Lambda \Lambda_\alpha^* \Lambda^\beta \phi_\beta^\gamma \phi_\gamma^\alpha \\
&- \mu_\phi^2 \left(\phi_\gamma^\beta \phi_\beta^\gamma\right) + \mu_2 \phi_\beta^\alpha \phi_\gamma^\beta \phi_\alpha^\gamma + \lambda_0^\phi \left(\phi_\gamma^\beta \phi_\beta^\gamma\right)^2 + \lambda_1^\phi \phi_\beta^\alpha \phi_\gamma^\beta \phi_\delta^\gamma \phi_\alpha^\delta + \mu_\Phi^2 \left(\Phi^{*\alpha\beta\gamma} \Phi_{\alpha\beta\gamma}\right) \\
&+ \lambda_0^\Phi \left(\Phi^{*\alpha\beta\gamma} \Phi_{\alpha\beta\gamma}\right)^2 + \lambda_1^\Phi \Phi^{*\alpha\beta\gamma} \Phi_{\alpha\beta\delta} \Phi^{*\delta\rho\sigma} \Phi_{\rho\sigma\gamma} + \lambda_0 \left(\Phi^{*\alpha\beta\gamma} \Phi_{\alpha\beta\gamma}\right) \left(\phi_\rho^\delta \phi_\delta^\rho\right) \\
&+ \lambda_0' \left(\Phi^{*\alpha\beta\gamma} \Phi_{\alpha\beta\gamma}\right) \left(\Lambda_\rho^* \Lambda^\rho\right) + \lambda_0'' \Phi^{*\alpha\beta\gamma} \Phi_{\beta\gamma\delta} \Lambda^\delta \Lambda_\alpha^* + \mu_3 \Phi^{*\alpha\beta\gamma} \Phi_{\beta\gamma\delta} \phi_\alpha^\delta \\
&+ \lambda_1 \Phi^{*\alpha\beta\gamma} \Phi_{\alpha\delta\rho} \phi_\beta^\delta \phi_\gamma^\rho + \lambda_2 \Phi^{*\alpha\beta\rho} \Phi_{\alpha\beta\delta} \phi_\rho^\gamma \phi_\gamma^\delta + \left\{\lambda' \Lambda^\alpha \Lambda^\beta \Lambda^\gamma \Phi_{\alpha\beta\gamma} + \text{h.c.}\right\},
\end{aligned}
\tag{1}
$$

gdje je $\Lambda = 5_H$, $\phi = 24_H$, $\Phi = 35_H$, a $\alpha, \beta, \gamma, \delta, \sigma, \rho = 1, 2, 3, 4, 5$ označavaju $SU(5)$ indekse.

Potpuni Yukawa dio Lagranžijana je:

$$
\begin{aligned}
\mathcal{L}_Y = &\left\{Y_{ij}^u T_i^{\alpha\beta} T_j^{\gamma\delta} \Lambda^\rho \epsilon_{\alpha\beta\gamma\delta\rho} + Y_{ij}^d T_i^{\alpha\beta} F_{\alpha j} \Lambda_\beta^* + Y_i^a \Sigma^{\alpha\beta} F_{\alpha i} \Lambda_\beta^* + Y_i^b \overline{\Sigma}_{\beta\gamma} F_{\alpha i} \Phi^{*\alpha\beta\gamma} \right. \\
&\left. + Y_i^c T_i^{\alpha\beta} \overline{\Sigma}_{\beta\gamma} \phi_\alpha^\gamma + \text{h.c.}\right\} + M_\Sigma \overline{\Sigma}_{\alpha\beta} \Sigma^{\alpha\beta} + y \overline{\Sigma}_{\alpha\beta} \Sigma^{\beta\gamma} \phi_\gamma^\alpha,
\end{aligned}
\tag{2}
$$

gdje su specificirane kontrakcije i u $SU(5)$ prostoru i u prostoru ukusa. Y^u i Y^d su općenito 3×3 kompleksne Yukawa matrice, Y^a, Y^b i Y^c su kompleksni Yukawa vektori duljine 3, pri čemu je y realan

broj. Relevantni matrični elementi su označeni s Y_{ij}^u, Y_{ij}^d, Y_i^a, Y_i^b, Y_i^c i y, gdje $i, j = 1, 2, 3$ predstavljaju indekse generacije.

U ovom modelu $SU(5)$ simetrija se direktno slama na baždarnu grupu Standardnog Modela $SU(3) \times SU(2) \times U(1)$ kada polje $\phi_0 \in 24_H$ dobije specifičnu vakuumski očekivanu vrijednost (VEV). Simetrija Standardnog Modela se zatim narušava na elektroslaboj skali pomoću vakuumske očekivane vrijednosti polja $\Lambda_1 \in 5_H$ na $SU(3) \times U(1)_{\text{em}}$ što možemo predstaviti na sljedeći način:

$$SU(5) \xrightarrow{\langle 24_H \rangle} SU(3) \times SU(2) \times U(1) \xrightarrow{\langle 5_H \rangle} SU(3) \times U(1)_{\text{em}} . \tag{3}$$

Relevantne VEV vrijednosti za ovaj rad su:

$$\langle 24_H \rangle = v_{24} \text{diag} \left(-1, -1, -1, 3/2, 3/2 \right), \tag{4}$$

$$\langle 5_H \rangle = (0 \quad 0 \quad 0 \quad 0 \quad v_5/\sqrt{2})^T, \tag{5}$$

gdje $v_5 \approx 246 \, \text{GeV}$ daje mase poljima baždarnih bozona Standardnog Modela $W_\mu^\pm$ i Z_μ. Mase superteških baždarnih bozona $X_\mu^{\pm 4/3} \in 24_G$ i $Y_\mu^{\pm 1/3} \in 24_G$ su

$$M_X = M_Y = \sqrt{\frac{25}{8}} g_{\text{GUT}} v_{24}, \tag{6}$$

gdje g_{GUT} predstavlja baždarnu konstantu vezanja pri skali ujedinjenja.

Mase fermiona

U procesu generiranja masa, u ovom modelu se koristimo s tri različita mehanizma u ovisnosti od toga da li govorimo o nabijenim ili neutralnim fermionima.

Sektor nabijenih fermiona

U Georgi-Glashow $SU(5)$ modelu su fermioni Standardnog Modela dati kroz dvije reprezentacije:

$$\overline{5}_F = \begin{pmatrix} d_1^C \\ d_2^C \\ d_3^C \\ e \\ -\nu_e \end{pmatrix}, \quad 10_F = \frac{1}{\sqrt{2}} \begin{pmatrix} 0 & u_3^C & -u_2^C & u_1 & d_1 \\ -u_3^C & 0 & u_1^C & u_2 & d_2 \\ u_2^C & -u_1^C & 0 & u_3 & d_3 \\ -u_1 & -u_2 & -u_3 & 0 & e^C \\ -d_1 & -d_2 & -d_3 & -e^C & 0 \end{pmatrix}, \tag{7}$$

gdje su sva polja lijeve kiralnosti u odnosu na Lorentzove transformacije.

Nakon slamanja elektroslabe simetrije putem VEV vrijednosti polja datog jednadžbom (5), prva dva

člana u jednadžbi (2) generiraju sljedeće masene matrice za gornje kvarkove, nabijene leptone i donje kvarkove:

$$M_U = \sqrt{2}v_5 \left(Y^u + Y^{u\,T} \right), \tag{8}$$

$$M_E = \frac{v_5}{2} Y^{d\,T}, \tag{9}$$

$$M_D = \frac{v_5}{2} Y^d. \tag{10}$$

Jednadžbe (9) i (10) predviđaju $m_e = m_d$, $m_\mu = m_s$ i $m_\tau = m_b$, gdje ove masene relacije vrijede na skali ujedinjenja M_{GUT}. Da bismo uspjeli dobiti eksperimentima utvrđeno neslaganje između masa donjih kvarkova i nabijenih leptona, morat ćemo uvesti korekcije ili na M_E ili na M_D, ili za oboje. Ovakve korekcije u modelu u ovom radu dolaze od interakcija između nabijenih fermiona Standardnog Modela u $\overline{5}_{F\,i}$ i $10_{F\,j}$ s fermionima iz $15_F + \overline{15}_F$ [7, 8].

Članovi miješanja potrebni za dalji račun dolaze od kontrakcija u trećem, četvrtom i petom članu iz (2) i glase:

$$\mathcal{L}_Y \supset - Y^a_i \left(\Sigma^0 \nu_i \frac{h^0}{\sqrt{2}} + \Sigma^{e^C} e_i^- \frac{v_5}{\sqrt{2}} + \Sigma^d d_i^C \frac{v_5}{\sqrt{2}} \right)$$
$$- Y^b_i \, \overline{\Sigma}^0 \nu_i \frac{\Phi^0_{\mathrm{Re}}}{\sqrt{2}} - \frac{5 v_{24}}{4} Y^c_i \left(d_i \overline{\Sigma}^d + u_i \overline{\Sigma}^u \right), \tag{11}$$

pri čemu su vlastita stanja električnog naboja $\Sigma^0, \Sigma^{e^C} \in \Sigma_1(1,3,1)$ i $\Sigma^u, \Sigma^d \in \Sigma_3(3,2,1/6)$.

U ovom modelu i analizi smo zainteresirani za slučaj u kojem je $M_{\Sigma_i} \gg v_5$. U ovom limitu 3×3 masene matrice nabijenih fermiona Standardnog Modela izgledaju ovako:

$$M_U = \left(\mathbb{1} + \epsilon^2 \, Y^c Y^{c\dagger} \right)^{-\frac{1}{2}} \sqrt{2}v_5(Y^u + Y^{u\,T}), \tag{12}$$

$$M_E = \frac{1}{2}v_5 Y^{d\,T}, \tag{13}$$

$$M_D = \left(\mathbb{1} + \epsilon^2 \, Y^c Y^{c\dagger} \right)^{-\frac{1}{2}} \left(M_E^T + \frac{1}{\sqrt{2}} v_5 \, \epsilon \, Y^c Y^a \right), \tag{14}$$

gdje je

$$\epsilon = \frac{5}{4} \frac{v_{24}}{M_{\Sigma_3}}. \tag{15}$$

Neutrinski sektor

Neutrinske mase se ostvaruju na razini vodećeg reda i na razini jedne petlje. Na razini vodećeg reda masena matrica bi glasila:

$$(M_N)_{ij}^{\text{v.r.}} = -\frac{\lambda' v_5^4}{4 M_{\Sigma_1} M_{\Phi_1}^2} \left(Y_i^a Y_j^b + Y_i^b Y_j^a \right). \tag{16}$$

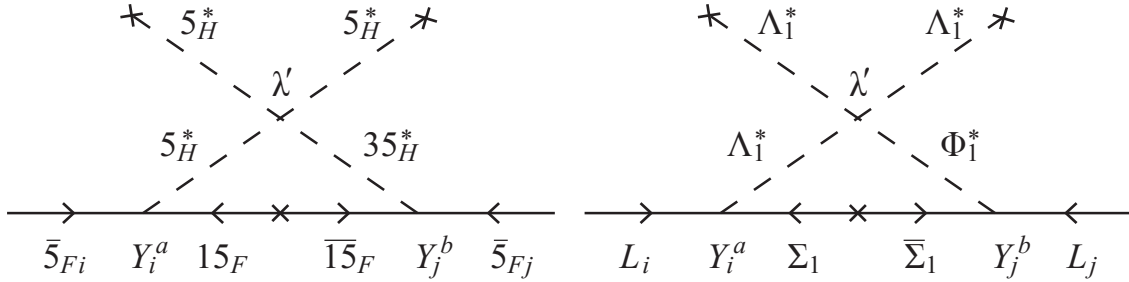dok bi na razini jedne petlje imala sljedeći izraz:

$$(M_N)_{ij}^{\text{j.p.}} = \frac{\lambda' v_5^2}{64\pi^2} (Y_i^a Y_j^b + Y_i^b Y_j^a) \frac{M_{\Sigma_1}}{M_{\Phi_1}^2 - M_h^2} \left\{ \frac{M_{\Phi_1}^2 \ln \frac{M_{\Sigma_1}^2}{M_{\Phi_1}^2}}{M_{\Sigma_1}^2 - M_{\Phi_1}^2} - \frac{M_h^2 \ln \frac{M_{\Sigma_1}^2}{M_h^2}}{M_{\Sigma_1}^2 - M_h^2} \right\}, \tag{17}$$

pri čemu je M_h masa Higgsovog bozona iz Standardnog Modela. Kada je $M_{\Phi_1}, M_{\Sigma_1} \gg M_h$, imamo

$$(M_N)_{ij}^{\text{j.p.}} = m_0 (Y_i^a Y_j^b + Y_i^b Y_j^a), \tag{18}$$

gdje uvodimo maseni parametar m_0 koji regulira masenu skalu za neutrine:

$$m_0 = \frac{\lambda' v_5^2}{64\pi^2} \frac{M_{\Sigma_1}}{M_{\Sigma_1}^2 - M_{\Phi_1}^2} \ln \frac{M_{\Sigma_1}^2}{M_{\Phi_1}^2}. \tag{19}$$

Slika 1: Feynmanovi dijagrami dominantnog doprinosa neutrinskim masama unutar $SU(5)$ (lijeva slika) i na razini Standardnog Modela (desna slika).

Može se primijetiti da su oba doprinosa proporcionalna kombinaciji $Y_i^a Y_j^b + Y_i^b Y_j^a$. Upravo zbog ovoga je najlakši od tri neutrina zapravo bezmasivan, pa možemo pisati:

$$(M_N)_{ij} = m_0 \left(Y_i^a Y_j^b + Y_i^b Y_j^a \right) = \left(N \, \text{diag}(0, m_2, m_3) \, N^T \right)_{ij}, \tag{20}$$

gdje je N unitarna matrica, a m_2 i m_3 su vlastita stanja mase neutrina. Unitarna matrica N se može napisati i kao:

$$N = \text{diag}(e^{i\gamma_1}, e^{i\gamma_2}, e^{i\gamma_3}) V_{\text{PMNS}}^*, \tag{21}$$

gdje je V_{PMNS} Pontecorvo-Maki-Nakagawa-Sakata (PMNS) unitarna matrica miješanja s tri kuta, dvije Majorana faze i jednom CP Diracovom fazom.

Fermionski fit

Masene matrice M_U, M_E, M_D i M_N dimenzije 3×3 za fermione Standardnog Modela, date u jednadžbama (12), (13), (14), i (20), mogu se dijagonalizirati na sljedeći način:

$$M_U = U_L M_U^{\text{diag}} U_R^{\dagger}, \tag{22}$$

$$M_D = D_L M_D^{\text{diag}} D_R^{\dagger}, \tag{23}$$

$$M_E = E_L M_E^{\text{diag}} E_R^{\dagger}, \tag{24}$$

$$M_N = N M_N^{\text{diag}} N^T, \tag{25}$$

gdje su U_L, U_R, D_L, D_R, E_L, E_R i N unitarne matrice pomoću kojih se odvija prijelaz iz baze ukusa u masenu bazu.

Numerička studija u ovom radu osigurava ulazne parametre u D_L, D_R i N, dok osobitosti samog modela daju:

$$U_L = D_L \text{diag}(1, e^{i\eta_1}, e^{i\eta_2}) V_{\text{CKM}}^T \text{diag}(e^{i\kappa_1}, e^{i\kappa_2}, e^{i\kappa_3}) \equiv D_L D(\eta) V_{\text{CKM}}^T D(\kappa) \tag{26}$$

$$U_R = U_L^* \text{diag}(e^{i\xi_1}, e^{i\xi_2}, e^{i\xi_3}) \equiv U_L^* D(\xi), \tag{27}$$

$$E_L = \mathbb{1}, \tag{28}$$

$$E_R = \mathbb{1}, \tag{29}$$

pri čemu je V_{CKM} Cabibbo-Kobayashi-Maskawa (CKM) matrica miješanja, koja sadrži jednu CP Diracovu fazu δ^{CKM}. U jednadžbama (26) i (27) uvodimo odgovarajuću notaciju za matrice s fazama na dijagonali $D(\eta)$, $D(\kappa)$, i $D(\xi)$. Zanimljivo je primijetiti da je upravo simetrija matrice M_U ta koja povezuje U_L i U_R, kako je dato u jednadžbi (27).

Pri izvedbi numeričke analize, koristimo mase nabijenih leptona na skali M_{GUT} kao ulazne podatke za određivanje dijagonalne matrice Y^d putem $Y^d = 2\, \text{diag}(m_e, m_\mu, m_\tau)/v_5$. Budući da masena matrica za donje kvarkove i masena matrica za neutrine imaju istu Yukawa matricu Y^a, moramo koristiti kombinirana prilagodba ova dva sektora pri čemu tražimo minimum funkcije χ^2:

$$\chi^2 = \sum_{j=1}^{8} \left(\frac{T_j - O_j}{E_j} \right)^2, \tag{30}$$

gdje T_j, O_j i E_j predstavljaju teoretsko predviđanje, izmjerenu centralnu vrijednost i eksperimentalnu $1\,\sigma$ grešku za fizikalnu veličinu j, redom. Indeks j se koristi za mase donjih kvarkova i parametre u neutrinskom sektoru.

Ono što model općenito daje su vrijednosti masa nabijenih leptona, gornjih kvarkova, i vrijednosti za CKM parametre. Uz to, provodi se i kombinirana numerička analiza za parametre neutrinskih masa, za

mase donjih kvarkova i za PMNS parametre. Ključni rezultat ovakve numeričke analize za razmatranja u dijelu protonskog raspada su zapravo unitarne transformacije U_L, U_R, D_L i D_R, pri čemu prve dvije matrice sadrže pet i tri napoznatih faza, redom, kao i numeričko određivanje svih Yukawa vezivanja u ovom modelu. Osam dodatnih faza koje numerička analiza ne može odrediti su η_1, η_2, κ_1, κ_2, κ_3, ξ_1, ξ_2 i ξ_3, gdje su, u biti, jedine relevantne faze za studiju protonskog raspada η_1 i η_2.

Protonski raspad

Glavna ideja u ovoj analizi protonskog raspada leži u identifikaciji dominirajućeg ili dominirajućih kanala za oba tipa medijacije - izmjenom baždarnih bozona ili skalarnih leptokvarkova - koje analiziramo u modelu, ali i uspoređujemo s aktualnim eksperimentalnim granicama i budućim očekivanjima, a što je utemeljeno na podatcima prikupljenim u periodu od deset godina u Hyper-Kamiokande kolaboraciji. Upravo takav sažetak podataka je dan u Tablici 2.

Protonski raspad izmjenom baždarnih bozona

Eksplicitni izrazi koje koristimo za računanje brzine raspada protona i vremena poluživota za svih osam kanala raspada izmjenom baždarnih bozona $X_\mu^{+4/3}, Y_\mu^{+1/3} \in (\overline{3}, 2, +5/6)$ su dati u jednadžbama ispod:

$$
\begin{aligned}
\Gamma(p \to \pi^0 e_\beta^+) = {} & \frac{(m_p^2 - m_\pi^2)^2}{m_p^3} \frac{\pi}{2} A_L^2 \frac{\alpha_{\text{GUT}}^2}{M_{\text{GUT}}^4} \\
& \times \left\{ \left| A_{SR} \langle \pi^0 | (ud)_R u_L | p \rangle c(e_\beta, d^C) \right|^2 + \left| A_{SL} \langle \pi^0 | (ud)_L u_L | p \rangle c(e_\beta^C, d) \right|^2 \right\}.
\end{aligned}
\tag{31}
$$

$$
\Gamma(p \to \pi^+ \bar{\nu}) = \frac{(m_p^2 - m_\pi^2)^2}{m_p^3} \frac{\pi}{2} A_L^2 \frac{\alpha_{\text{GUT}}^2}{M_{\text{GUT}}^4} A_{SR}^2 |\langle \pi^+ | (ud)_R d_L | p \rangle|^2 \sum_{i=1}^{3} |c(\nu_i, d, d^C)|^2.
\tag{32}
$$

$$
\begin{aligned}
\Gamma(p \to \eta e_\beta^+) = {} & \frac{(m_p^2 - m_\eta^2)^2}{m_p^3} \frac{\pi}{2} A_L^2 \frac{\alpha_{\text{GUT}}^2}{M_{\text{GUT}}^4} \\
& \times \left\{ \left| A_{SR} \langle \eta | (ud)_R u_L | p \rangle c(e_\beta, d^C) \right|^2 + \left| A_{SL} \langle \eta | (ud)_L u_L | p \rangle c(e_\beta^C, d) \right|^2 \right\}.
\end{aligned}
\tag{33}
$$

$$
\begin{aligned}
\Gamma(p \to K^0 e_\beta^+) = {} & \frac{(m_p^2 - m_K^2)^2}{m_p^3} \frac{\pi}{2} A_L^2 \frac{\alpha_{\text{GUT}}^2}{M_{\text{GUT}}^4} \\
& \times \left\{ \left| A_{SR} \langle K^0 | (us)_R u_L | p \rangle c(e_\beta, s^C) \right|^2 + \left| A_{SL} \langle K^0 | (us)_L u_L | p \rangle c(e_\beta^C, s) \right|^2 \right\}.
\end{aligned}
\tag{34}
$$

Tablica 2: Aktualna granica na parcijalna vremena poluživota protona pri protonskom raspadu za sve dvo-čestične procese i buduća očekivanja za desetogodišnji period prikupljanja podataka sa 90% C.L..

kanal raspada	aktualna vrijednost τ_p [godine]	buduća osjetljivost τ_p [godine]
$p \to \pi^0 e^+$	2.4×10^{34} [9]	7.8×10^{34} [10]
$p \to \pi^0 \mu^+$	1.6×10^{34} [9]	7.7×10^{34} [10]
$p \to \eta^0 e^+$	1.0×10^{34} [11]	4.3×10^{34} [10]
$p \to \eta^0 \mu^+$	4.7×10^{33} [11]	4.9×10^{34} [10]
$p \to K^0 e^+$	1.1×10^{33} [12]	-
$p \to K^0 \mu^+$	3.6×10^{33} [13]	-
$p \to \pi^+ \overline{\nu}$	3.9×10^{32} [14]	-
$p \to K^+ \overline{\nu}$	6.6×10^{33} [15]	9.6×10^{33} [16] & 3.2×10^{34} [10]

$$
\Gamma(p \to K^+ \bar{\nu}) = \frac{(m_p^2 - m_K^2)^2}{m_p^3} \frac{\pi}{2} A_L^2 \frac{\alpha_{\text{GUT}}^2}{M_{\text{GUT}}^4}
$$

$$
\times \left\{ A_{SR}^2 \left| \langle K^+ | (us)_R d_L | p \rangle \right|^2 \sum_{i=1}^{3} \left| c(\nu_i, d, s^C) \right|^2 \right.
$$

$$
\left. + A_{SL}^2 \left| \langle K^+ | (ud)_R s_L | p \rangle \right|^2 \sum_{i=1}^{3} \left| c(\nu_i, s, d^C) \right|^2 \right\} . \tag{35}
$$

Protonski raspad izmjenom skalarnih leptokvarkova

Eksplicitni izrazi koje koristimo za računanje brzine raspada protona i vremena poluživota za svih osam kanala raspada izmjenom skalarnih leptokvarkova su dati u jednadžbama ispod:

$$
\Gamma(p \to \pi^0 e_\beta^+) = \frac{(m_p^2 - m_\pi^2)^2}{32\pi m_p^3 M_{\Lambda_3}^4} A_L^2
$$

$$
\times \left\{ \left| A_{SR} a(d^C, e_\beta) \langle \pi^0 | (du)_R u_L | p \rangle + A_{SL} a(d, e_\beta) \langle \pi^0 | (du)_L u_L | p \rangle \right|^2 \right.
$$

$$
\left. + \left| A_{SL} a(d, e_\beta^C) \langle \pi^0 | (du)_L u_L | p \rangle + A_{SR} a(d^C, e_\beta^C) \langle \pi^0 | (du)_R u_L | p \rangle \right|^2 \right\} . \tag{36}
$$

$$\Gamma(p \to \pi^+ \bar{\nu}) = \frac{(m_p^2 - m_\pi^2)^2}{32\pi m_p^3 M_{\Lambda_3}^4} A_L^2$$

$$\times \sum_{i=1}^{3} \left| A_{SR} a(d, d^C, \nu_i) \langle \pi^+ | (du)_R d_L | p \rangle + A_{SL} a(d, d, \nu_i) \langle \pi^+ | (du)_L d_L | p \rangle \right|^2 . \qquad (37)$$

$$\Gamma(p \to \eta^0 e_\beta^+) = \frac{(m_p^2 - m_\eta^2)^2}{32\pi m_p^3 M_{\Lambda_3}^4} A_L^2$$

$$\times \left\{ \left| A_{SL} a(d, e_\beta) \langle \eta | (ud)_L u_L | p \rangle + A_{SR} a(d^C, e_\beta) \langle \eta | (ud)_R u_L | p \rangle \right|^2 \right.$$

$$\left. + \left| A_{SL} a(d^C, e_\beta^C) \langle \eta | (ud)_L u_L | p \rangle + A_{SR} a(d, e_\beta^C) \langle \eta | (ud)_R u_L | p \rangle \right|^2 \right\} . \qquad (38)$$

$$\Gamma(p \to K^0 e_\beta^+) = \frac{(m_p^2 - m_K^2)^2}{64\pi m_p^3 M_{\Lambda_3}^4} A_L^2$$

$$\times \left\{ \left| A_{SR} a(s^C, e_\beta) \langle K^0 | (us)_R u_L | p \rangle + A_{SL} a(s, e_\beta) \langle K^0 | (us)_L u_L | p \rangle \right. \right.$$

$$\left. - A_{SR} a(s, e_\beta^C) \langle K^0 | (us)_R u_L | p \rangle - A_{SL} a(s^C, e_\beta^C) \langle K^0 | (us)_L u_L | p \rangle \right|^2$$

$$+ \left| A_{SR} a(s^C, e_\beta) \langle K^0 | (us)_R u_L | p \rangle + A_{SL} a(s, e_\beta) \langle K^0 | (us)_L u_L | p \rangle \right.$$

$$\left. \left. + A_{SR} a(s, e_\beta^C) \langle K^0 | (us)_R u_L | p \rangle + A_{SL} a(s, e_\beta^C) \langle K^0 | (us)_L u_L | p \rangle \right|^2 \right\} . \qquad (39)$$

$$\Gamma(p \to K^+ \bar{\nu}) = \frac{(m_p^2 - m_K^2)^2}{32\pi m_p^3 M_{\Lambda_3}^4} A_L^2$$

$$\times \sum_{i=1}^{3} \left| A_{SL} \left(a(s, d, \nu_i) \langle K^+ | (us)_L d_L | p \rangle + a(d, s, \nu_i) \langle K^+ | (ud)_L s_L | p \rangle \right) \right.$$

$$\left. + A_{SR} \left(a(d, s^C, \nu_i) \langle K^+ | (us)_R d_L | p \rangle + a(s, d^C, \nu_i) \langle K^+ | (ud)_R s_L | p \rangle \right) \right|^2 . \qquad (40)$$

Zaključci ove studije pokazuju da u slučaju protonskog raspada putem dominantnog kanala $p \to \pi^0 e^+$ možemo zaključiti da se radi o izmjeni baždardnog bozona, s mogućnošću da se opazi i još jedan kanal $p \to \eta^0 e^+$. Alternativa je da se protonski raspad desi putem $p \to K^+ \bar{\nu}$ kanala, što bi značilo da se ovaj raspad desio izmjenom skalarnog leptokvarka, uz mogućnost $p \to \pi^0 \mu^+$ procesa. Detekcija oba kanala $p \to \pi^0 e^+$ i $p \to K^+ \bar{\nu}$ bi mogla naglasiti kanal $p \to \pi^0 \mu^+$ kroz konstruktivnu interferenciju. Upravo ovi glavni zaključci u ovom specifičnom modelu, kao i studije protonskog raspada su prikazani na slici 2:
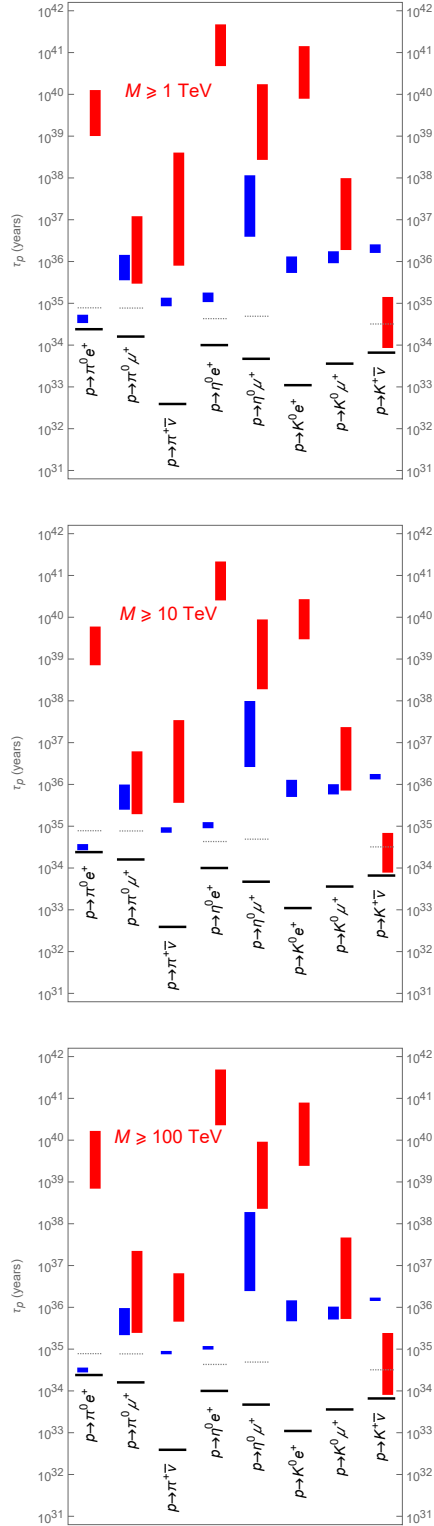
Slika 2: Korelacija potpisa protonskog raspada putem baždarnih bozona i skalarnog leptokvarka unutar scenarija $M \geq 1\,\mathrm{TeV}$, $M \geq 10\,\mathrm{TeV}$ i $M \geq 100\,\mathrm{TeV}$. Tanke crne crte predstavljaju trenutna eksperimentalna granica, plave okomite trake su predviđanja za kanale protonskog raspada izmjenom baždarnog bozona, crvene okomite trake su odgovarajuća predviđanja za kanale protonskog raspada izmjenom skalarnog leptokvarka, a sive isprekidane crte predstavljaju buduće eksperimentalne osjetljivosti nakon desetogodišnjeg razdoblja.

Contents

III Results   87

7 Specific $SU(5)$ Model   89

8 Correlation between proton decay signatures   99

IV Summary and conclusions   119

9 Discussion   121

Appendices   123

A Einstein index notation   125

B Dirac algebra and gamma matrices   129

C Fierz Transformations   133

List of Figures

List of Tables

Part I

Introduction

Chapter 1

Introduction

I have not yet lost a feeling of
wonder, and of delight, that this
delicate motion should reside in
all the things around us, revealing
itself only to him who looks for it.
I remember, in the winter of our
first experiments, just seven years
ago, looking on snow with new
eyes. There the snow lay around
my doorstep — great heaps of
protons quietly precessing in the
earth's magnetic field. To see the
world for a moment as something
rich and strange is the private
reward of many a discovery.

Edward M. Purcell

Everything that we observe around us seems to have an expiration date. It can only be expected that the same happens with the particles forming nucleus of every atom that builds up everything in and around us. In particle physics we refer to expiration date of a particle as its lifetime. If particle decays in different ways, we introduce a concept of partial lifetimes. Particles, through decay, give birth or transform to some other particles, if kinematically allowed.

There are some particles that we have not seen to decay so far. For example, electron is an elementary particle that builds up literally everything and yet we haven't observed its decay. Proton is a composite particle that also seems to be absolutely stable. Nevertheless, various physical theories that go beyond what we know today, predict proton decay and give an estimate on its lifetime.

In this thesis, we will explore and discuss proton decay within one specific $SU(5)$ model, where in the final states we have two particles. Now, process itself can have different final states and may proceed via different mediators. We will be analyzing proton decay induced through the gauge boson and scalar leptoquark mediations.

In order to do so, we will start with theoretical background, where we present the acclaimed physical theory in this field referred to as the Standard Model. Since proton decay is something theorized in physics beyond the Standard Model, in Chapter 3 we venture beyond the Standard Model, where among other theories lies $SU(5)$ Georgi-Glashow model. However, this model has its flaws and, hence, does not phenomenologically work. We dive into this exploration in Chapter 4.

Proton decay is one of the most important predictions of Grand Unification Theories (GUTs), and it has been studied extensively for decades. We talk about that in Chapter 5. There we discuss, analyze, and derive in detail expressions for two main types of mediation of proton decay — via gauge bosons and via scalar leptoquark.

However, the way the proton will decay and how to detect this decay is still an open question, both for the theory and experiment. In Chapter 6 we present some of the previously conducted experiments in the field, but also the future experiments that search for proton decay. Chapter 7 is dedicated to our specific $SU(5)$ model with the description of its particle content, symmetry breaking, unification, and mass generation mechanisms. Chapter 8 is devoted to the correlation study between two main ways for proton to decay, together with associated proton lifetimes and expectations in experiments. Our conclusions are presented in fourth part of this thesis — Summary and conclusions.

Part II

Theoretical Background

Chapter 2

Standard Model

> It's extraordinary to think that if
> you walked into a room and said
> you had never heard of Hamlet,
> you would be regarded as a
> Philistine. But you could walk
> into the same room and say, 'I
> don't know what a proton is,' and
> people would just laugh and say,
> 'Why should you know?'
>
> *Robert Winston*

Pillars of physics describing the world we live in and the world that lives within us and deeper, are physical entities such as particles of matter, forces between them and fields they feel and interact with.

Standard Model is the theory that, so far, describes in the most viable manner algorithm of the particle content of the Universe we know of and the forces and fields in the nature. This is the theory that has been forged for decades by many great names in the world of physics such as Chen Ning Yang, Robert Mills, Chien-Shiung Wu, Sheldon Glashow, Abdus Salam, Steven Weinberg, Abraham Pais, Sam Treiman, Philip Warren Anderson, Robert Brout, François Englert, Peter Higgs, Yoichiro Nambu, Jeffrey Goldstone and many more.

2.1 Particle content

Standard Model is a chiral gauge theory incorporating all known building blocks of matter and describing three out of four fundamental forces in nature: electromagnetic, weak and strong interactions [17, 18, 19]. The mechanism of this theory is based on the gauge group $SU(3) \times SU(2) \times U(1)$, where $SU(3)$ is a

gauge group for strong interactions and $SU(2) \times U(1)$ is a gauge group for electroweak interactions.

Table 2.1: Standard Model particles

FERMIONS				BOSONS	
	families			SPIN	SPIN
	1st	2nd	3rd	1	0
quarks	u	c	t	gluons	H
	d	s	b	g	
leptons	e	μ	τ	$W^\pm$	
	ν_e	ν_μ	ν_τ	Z	

A simplistic categorisation of building blocks of the Standard Model would be to introduce two types of particles: **fermions** that obey Fermi-Dirac statistics and build up the matter fields and experience the force, and **bosons** that obey Bose-Einstein statistics with a distinction between gauge bosons of spin 1 that are force carriers and Higgs boson of spin 0 that is responsible for symmetry breaking of the Standard Model. All the particles of the Standard Model can be summarized in simplified manner in Table 2.1. More specifically, the particle content of the Standard Model is presented in Table 2.2.

Table 2.2: Standard Model field content ($i = 1, 2, 3$ denotes the generations, $\alpha = 1, 2, 3$ denotes the color, $a = 1, 2, 3$ and $A = 1, ..., 8$)

Fields	SPIN (j)	$SU(3)$	$SU(2)$	$U(1)$	B	L
$Q_{L\alpha}^i = \begin{pmatrix} u_{L\alpha}^i \\ d_{L\alpha}^i \end{pmatrix}$	$\frac{1}{2}$	3	2	$+\frac{1}{6}$	$+\frac{1}{3}$	0
$u_{R\alpha}^i$	$\frac{1}{2}$	3	1	$+\frac{2}{3}$	$+\frac{1}{3}$	0
$d_{R\alpha}^i$	$\frac{1}{2}$	3	1	$-\frac{1}{3}$	$+\frac{1}{3}$	0
$l_L^i = \begin{pmatrix} \nu_L^i \\ e_L^i \end{pmatrix}$	$\frac{1}{2}$	1	2	$-\frac{1}{2}$	0	$+1$
e_R^i	$\frac{1}{2}$	1	1	-1	0	$+1$
H	0	1	2	$+\frac{1}{2}$	0	0
G_μ^A	1	8	1	0	0	0
W_μ^a	1	1	3	0	0	0
B_μ	1	1	1	0	0	0

One can see, from Table 2.2, that the Standard Model fermions comprise six $SU(2)$ doublets $Q_{L\alpha}^i$ and $l_{L\alpha}^i$ and nine $SU(3)$ singlets $u_{R\alpha}^i$, $d_{R\alpha}^i$, and $e_{R\alpha}^i$. Left-handed $Q_{L\alpha}^i$ consists of quarks $u_{L\alpha}^i$ and $d_{L\alpha}^i$, whereas l_L^i consists of charged lepton e_L^i and neutrino ν_L^i. Index i denotes generations of fermions referred to in Ta-

ble 2.1 as families. Our notation is such that $(u^1_{L,R}, u^2_{L,R}, u^3_{L,R}) = (u_{L,R}, c_{L,R}, t_{L,R})$, $(d^1_{L,R}, d^2_{LR}, d^3_{L,R}) = (d_{L,R}, s_{L,R}, b_{L,R})$, $(e^1_{L,R}, e^2_{L,R}, e^3_{L,R}) = (e_{L,R}, \mu_{L,R}, \tau_{L,R})$, and $(\nu^1_L, \nu^2_L, \nu^3_L) = (\nu_{eL}, \nu_{\mu L}, \nu_{\tau L})$. Quarks transform as triplets of $SU(3)$, therefore, they belong to the fundamental representation of that group. There are furthermore eight generators of $SU(3)$ group and G^A_μ are eight carriers of interaction that are associated with them. These are referred to as gluons. There are also three additional vector bosons W^a_μ of $SU(2)$ group and one B_μ carrier of $U(1)$ interaction. W^a_μ and B_μ are mediators of the electroweak force. Finally, there is a single scalar boson field H that is a doublet of $SU(2)$ that accomplishes electroweak symmetry breaking. It is referred to as the Higgs boson.

2.2   Lagrangian

Standard Model is a gauge theory. More specifically, it is a quantum field theory. Lagrangian of the Standard Model can be written in the following form:

$$\mathcal{L}_{\text{SM}} = \mathcal{L}_{\text{gauge}} + \mathcal{L}_{\text{kinetic}} + \mathcal{L}_{\text{Higgs}} + \mathcal{L}_{\text{Yukawa}} \tag{2.1}$$

where separate contributions are [20, 21]:

$$\mathcal{L}_{\text{gauge}} = -\frac{1}{4} G^A_{\mu\nu} G^{A\,\mu\nu} - \frac{1}{4} W^a_{\mu\nu} W^{a\,\mu\nu} - \frac{1}{4} B_{\mu\nu} B^{\mu\nu} \tag{2.2}$$

$$\mathcal{L}_{\text{kinetic}} = i \left(\overline{Q}^i_L \slashed{D} Q^i_L + \overline{u}^i_R \slashed{D} u^i_R + \overline{d}^i_R \slashed{D} d^i_R + \overline{l}^i_L \slashed{D} l^i_L + \overline{e}^i_R \slashed{D} e^i_R \right) \tag{2.3}$$

$$\mathcal{L}_{\text{Higgs}} = (D_\mu H)^\dagger (D^\mu H) - \lambda \left(H^\dagger H - \frac{v^2}{2} \right)^2 \tag{2.4}$$

$$\mathcal{L}_{\text{Yukawa}} = - \left(g^{ij}_u \overline{Q}_{Li} \epsilon H^* u_{Rj} - g^{ij}_d \overline{Q}_{iL} H d_{Rj} - g^{ij}_e \overline{L}_{Li} H e_{Rj} \right) + \text{h.c.} \tag{2.5}$$

Fermions featured in Eq. (2.5) are in the so-called flavor basis. In order to go to the mass eigenstate basis, we need to redefine them in the following way:

$$u'_{L,R} = U^\dagger_{L,R} u_{L,R} \Rightarrow u_{L,R} = U_{L,R} u'_{L,R} \Rightarrow \overline{u}_{L,R} = \overline{u}'_{L,R} U^\dagger_{L,R} \tag{2.6}$$

$$d'_{L,R} = D^\dagger_{L,R} d_{L,R} \Rightarrow d_{L,R} = D_{L,R} d'_{L,R} \Rightarrow \overline{d}_{L,R} = \overline{d}'_{L,R} D^\dagger_{L,R} \tag{2.7}$$

$$e'_{L,R} = E^\dagger_{L,R} e_{L,R} \Rightarrow e_{L,R} = E_{L,R} e'_{L,R} \Rightarrow \overline{e}_{L,R} = \overline{e}'_{L,R} E^\dagger_{L,R} \tag{2.8}$$

$$\nu'_L = N\nu_L \Rightarrow \nu_L = N\nu'_L \Rightarrow \overline{\nu}_L = \overline{\nu}'_L N^\dagger \tag{2.9}$$

where $U_{L,R}$, $D_{L,R}$, $E_{L,R}$, and N are 3×3 unitary matrices in flavor space.

Where do these unitary transformations manifest themselves in the Standard Model? It turns out that there are only two terms in Lagrangian where we can observe these transformations and these correspond to interactions of left-handed quarks and left-handed leptons with $W^\pm$ bosons, as we will show later on. We note that right-handed transformations U_R, D_R, and E_R are not physical in the Standard Model in a sense that they are not present in any observable.

With redefinition of states given in Eq. (2.6), and taking into account that the vacuum expectation value (VEV) of Higgs is $\langle H \rangle = (0 \quad v)^T$, we get in the up-type quark sector that corresponds to the first term in Lagrangian of Eq. (2.5) the following:

$$\overline{u}'_{Li} \left(U^\dagger_L g_u U_R \right)_{ij} u'_{Rj} v \equiv \overline{u}'_L g^{\text{diag}}_u v\, u'_R \tag{2.10}$$

where

$$g^{\text{diag}}_u v = m^{\text{diag}}_u = \begin{pmatrix} m_u & 0 & 0 \\ 0 & m_c & 0 \\ 0 & 0 & m_t \end{pmatrix} \approx m_t \begin{pmatrix} 10^{-5} & 0 & 0 \\ 0 & 10^{-2} & 0 \\ 0 & 0 & 1 \end{pmatrix} \tag{2.11}$$

represents mass matrix for the up-type quarks. We will analogously do the same procedure for the down-type quarks:

$$\overline{d}'_{Li} \left(D^\dagger_L g_d D_R \right)_{ij} d'_{Rj} v \equiv \overline{d}'_L g^{\text{diag}}_d v\, d'_{Rj} \tag{2.12}$$

where

$$g^{\text{diag}}_d v = m^{\text{diag}}_d = \begin{pmatrix} m_d & 0 & 0 \\ 0 & m_s & 0 \\ 0 & 0 & m_b \end{pmatrix} \approx m_b \begin{pmatrix} 10^{-3} & 0 & 0 \\ 0 & 10^{-2} & 0 \\ 0 & 0 & 1 \end{pmatrix} \tag{2.13}$$

The kinetic Lagrangian of Eq. (2.3) yields the following interactions:

$$\overline{u}_{Li} \gamma_\mu W^\mu d_{Li} + \overline{u}_{Li} \gamma_\mu Z^\mu u_{Li} + \overline{e}_{Li} \gamma_\mu W^\mu \nu_{Li} + \overline{\nu}_{Li} \gamma_\mu Z^\mu \nu_{Li} \tag{2.14}$$

where first and third terms are charged currents and second and forth terms are neutral currents. With

redefinition of states presented in Eqs. (2.6)–(2.9), this becomes:

$$\overline{u}'_L U_L^\dagger \gamma_\mu W^\mu D_L d'_L + \overline{u}'_L U_L^\dagger \gamma_\mu Z^\mu U_L u'_L + \overline{e}'_L E_L^\dagger \gamma_\mu W^\mu N_L \nu'_L + \overline{\nu}'_L N_L^\dagger \gamma_\mu Z^\mu N_L \nu'_L \tag{2.15}$$

with

$$U_L^\dagger D_L = V_{\text{CKM}} \quad \text{and} \quad E_L^\dagger N_L = U_{\text{PMNS}} \tag{2.16}$$

where V_{CKM} is the Cabibbo–Kobayashi–Maskawa matrix. V_{CKM} was introduced by Nicola Cabibbo, and enriched for one more generation by Makoto Kobayashi and Toshihide Maskawa. For a historical overview, see Ref. [22]. It is a unitary matrix that gives exact values on the strength of flavor changing between quarks. U_{PMNS} is the Pontecorvo–Maki–Nakagawa–Sakata matrix that contains information on neutrino oscillations firstly predicted by Bruno Pontecorvo. It was introduced in the current form in 1962 by Ziro Maki, Masami Nakagawa, and Shoichi Sakata. V_{CKM} and U_{PMNS}, as defined in Eq. (2.16) are both given as a mismatch of two unitary left-handed rotations.

The gauge covariant derivative of Eqs. (2.3) and (2.4) is given in this form:

$$D_\mu = \partial_\mu + ig_3 G_\mu^A T^A + ig_2 W_\mu^a T^a + ig_1 B_\mu Y \tag{2.17}$$

with g_3, g_2, and g_1 being gauge coupling constants of $SU(3)$, $SU(2)$, and $U(1)$, and T^A, T^a, and Y are the $SU(3)$, $SU(2)$, and $U(1)$ generators, respectively. In Eq. (2.5), $g_{u,d,e}^{ij}$ are Yukawa couplings where $i, j = 1, 2, 3$ represent generation indices.

The field strenth tensors are [23]:

$$G_{\mu\nu}^A = \partial_\mu G_\nu^A - \partial_\nu G_\mu^A - g f_{BC}^A G_\mu^B G_\nu^C \tag{2.18}$$

$$W_{\mu\nu}^a = \partial_\mu W_\nu^a - \partial_\nu W_\mu^a - g_2 f_{bc}^a W_\mu^b W_\nu^c \tag{2.19}$$

$$B_{\mu\nu} = \partial_\mu B_\nu - \partial_\nu B_\mu \tag{2.20}$$

with f_{BC}^A and f_{bc}^a being structure constants of the gauge groups $SU(3)$ and $SU(2)$, respectively.

2.3 Open questions and challenges

Standard Model proved to be the best theory to describe the symbiotic world of particles and interactions, and its viability has been confirmed with every new elementary particle being discovered. This has culminated with the discovery of Higgs boson [24, 25] which was the last missing part of the Standard Model. Nonetheless, there are some open questions and challenges that portrait the Standard Model as an incomplete theory. Here are some of the questions and inputs for research in the fields beyond the

Standard Model physics:

- **Neutrino masses**

  Within the Standard Model, neutrinos are massless particles, even though the experiments have confirmed that at least two out of three must have a mass [26, 27, 28].

- **Dark matter**

  Building blocks of the Standard Model do not explain the origin nor the nature of the Dark Matter [29, 30].

- **Gravity**

  Standard Model unifies three out of four fundamental forces, omitting the force of gravity. Hence the hypothesized carrier of the gravitational force, i.e., graviton, is not a member of particle content of the Standard Model [31, 32].

- **Hierarchy problem**

  Hierarchy problem is usually related to the discrepancy between Higgs mass and other scales such as Planck scale M_{Planck} [33]. Specifically, if the cutoff of the theory is assumed to be Planck scale — the scale associated with weakness of gravity — the quantum corrections δm_H^2 to Higgs mass m_H^2, that at loop level come from self interactions, gauge loops, and fermion loops, are much greater than the observed mass, i.e., $\delta m_H^2 \gg m_H^2$ [34].

  For example, the one-loop correction to the dimension-2 Higgs mass parameter, due to the top quark loops, is [35]:

  $$\delta m_H^2 = -\frac{N_C y_t^2}{8\pi^2}\Lambda^2 + ... \tag{2.21}$$

  where Λ is ultra-violet cutoff for the loop momentum, N_C is number of colors and y_t is top quark Yukawa coupling. The disparity between δm_H and m_H is self-evident if one sets $\Lambda = M_{\text{Planck}} \approx 10^{18}$ GeV while $m_H \approx 10^2$ GeV.

- **CP violation**

  CP refers to charge conjugation parity symmetry, where C stands for charge symmetry and P for parity symmetry. Charge-conjugation symmetry and parity symmetry state that interchange between charge particle and its anti-particle as well as swapping left and right-handed particles should make no change in physical laws. The issue of CP violation within the Standard Model is related to the question of matter and anti-matter ratio, where experiments witness extreme disparity. If everything started at balance, at Big Bang, how did the world end up with so much matter and so little anti-matter? One possible explanation is violation of CP symmetry. And, in the Standard Model, there are three sources of CP violation. First comes from CKM matrix (quark sector), second comes from strong interaction and third comes from PMNS matrix (lepton

sector). Sources of CP violation in the Standard Model contribute in not so significant measure to matter-antimatter symmetry. Hence, in order to explain this phenomena, one must go beyond the Standard Model and look for answers elsewhere.

Chapter 3

Beyond Standard Model

Supposing a new era begins after the big crunch, will the number of protons (or baryons) be the same in the next cycle? Will the protons retain a memory of their previous life in the earlier epoch of the universe when deciding to decay or not to decay? Will there be subsequent cycles of big bangs and big crunches? If so, will proton decay affect the cycles of the far future? There exist no answers to such questions at present.

Jamal Nazrul Islam
"The Ultimate Fate Of The Universe"

Motivation to go beyond the Standard Model stems out of questions we have mentioned in previous chapter. We will in next few sections briefly describe some of the issues of the Standard Model and directions one takes to address them.

3.1   Fermionic mass hierarchy and flavor problem

There is a visible mass hiararchy problem in fermionic sector of the Standard Model. Namely, there is an observed hierarchy between masses of quarks and charged leptons that is not understood within the

framework of the Standard Model [35, 36]. The masses in question read:

$$m_u^{\text{diag}} = \begin{pmatrix} m_u & 0 & 0 \\ 0 & m_c & 0 \\ 0 & 0 & m_t \end{pmatrix} \sim \begin{pmatrix} 2.16\,\text{MeV} & 0 & 0 \\ 0 & 1.27\,\text{GeV} & 0 \\ 0 & 0 & 172.4\,\text{GeV} \end{pmatrix} \tag{3.1}$$

$$m_d^{\text{diag}} = \begin{pmatrix} m_d & 0 & 0 \\ 0 & m_s & 0 \\ 0 & 0 & m_b \end{pmatrix} \sim \begin{pmatrix} 4.67\,\text{MeV} & 0 & 0 \\ 0 & 0.093\,\text{GeV} & 0 \\ 0 & 0 & 4.18\,\text{GeV} \end{pmatrix} \tag{3.2}$$

$$m_e^{\text{diag}} = \begin{pmatrix} m_e & 0 & 0 \\ 0 & m_\mu & 0 \\ 0 & 0 & m_\tau \end{pmatrix} \sim \begin{pmatrix} 0.511\,\text{MeV} & 0 & 0 \\ 0 & 0.106\,\text{GeV} & 0 \\ 0 & 0 & 1.777\,\text{GeV} \end{pmatrix} \tag{3.3}$$

Clearly, there is a large disparity between masses of quarks and masses of charged leptons from different generations.

Neutrino sector currently exhibits two experimentally viable mass hierarchies. Normal hierarchy corresponds to $\triangle m_{23}^2 = m_2^2 - m_3^2 < 0$, where m_2 and m_3 are neutrino masses. Inverted hierarchy, on the other hand, features $\triangle m_{23}^2 > 0$. Experimental measurements currently yield:

$$\left| \triangle m_{12}^2 \right| = \left| m_1^2 - m_2^2 \right| = 7.37 \times 10^{-5} \text{eV}^2 \tag{3.4}$$

$$\left| \triangle m_{23}^2 \right| = \left| m_2^2 - m_3^2 \right| = 2.54 \times 10^{-3} \text{eV}^2 \tag{3.5}$$

Note that we do not know neutrino masses m_1, m_2, and m_3, but we do know corresponding mass-square differences. This leaves a space for a possibility that at least one of three neutrinos is a massless particle. It is also clear that neutrino masses are much lower in comparison with masses of other fermions:

$$\frac{m_{\nu_i}}{m_{l,q}} < 10^{-6} \tag{3.6}$$

There is also a hierarchy in CKM matrix entries for which we find no natural explanation. V_{CKM} looks almost diagonal. Namely, CKM matrix takes the following form, where we neglected CP violating phase, when presenting numerical values [37]:

$$
V_{\text{CKM}} = \begin{pmatrix} V_{ud} & V_{us} & V_{ub} \\ V_{cd} & V_{cs} & V_{cb} \\ V_{td} & V_{ts} & V_{tb} \end{pmatrix} \approx \begin{pmatrix} 0.974 & 0.225 & 0.0036 \\ 0.225 & 0.974 & 0.041 \\ 0.009 & 0.040 & 0.999 \end{pmatrix} \tag{3.7}
$$

The PMNS matrix elements also exhibits slight hierarchy that can be summarized as follows [38, 39]:

$$
U_{\text{PMNS}} \approx \begin{pmatrix} 0.803 - 0.845 & 0.514 - 0.578 & 0.142 - 0.155 \\ 0.233 - 0.505 & 0.460 - 0.693 & 0.630 - 0.779 \\ 0.262 - 0.525 & 0.473 - 0.702 & 0.610 - 0.762 \end{pmatrix} \tag{3.8}
$$

where we indicate allowed ranges for the matrix elements.

Flavor problem refers to relation between fermion masses and mixing patterns for quarks and leptons that we have shown above. Clearly, the flavor problem has its roots partly in dim-4 Yukawa couplings for quarks and leptons, and partly in dim-5 operators for neutrino masses.

3.2 Gauge coupling unification

Standard Model is a gauge theory represented by a gauge group $SU(3) \times SU(2) \times U(1)$, where each group has its own gauge coupling: g_s, g and g' respectively for strong, weak and hypercharge interactions in the Standard Model with $g_1 = \sqrt{\frac{5}{3}}g'$, $g_2 = g$, and $g_3 = g_s$. We can express their renormalization group equations (RGEs) at the one-loop level in the following way [40]:

$$
\frac{d\alpha_i}{d\ln\mu} = \beta(\alpha_i) = \frac{\alpha_i^2}{2\pi} a_i, \qquad i = 1, 2, 3 \tag{3.9}
$$

where $\alpha_i = g_i^2/(4\pi)$ while a_i are one-loop β-function coefficients $a_i = (\frac{41}{10}, -\frac{19}{6}, -7)$ of the Standard Model. Parameter μ represents a scale at which we measure relevant coupling. We will always use $\alpha_s(M_Z) = 0.1193 \pm 0.0016$, $\alpha^{-1}(M_Z) = 127.906 \pm 0.019$ and $\sin^2\theta_W = 0.23126 \pm 0.00005$ as input parameters [41].

Eq. (3.9), at the two-loop order, reads:

$$
\mu \frac{d\alpha_i}{d\mu} = a_i \frac{\alpha_i^3}{2\pi} + \sum_j \frac{b_{ij}\,\alpha_i^3}{8\pi^2}, \qquad i = 1, 2, 3 \tag{3.10}
$$

where b_{ij} are two-loop β-coefficients that read [42, 43]:

$$b = \begin{pmatrix} \frac{199}{50} & \frac{27}{10} & \frac{44}{5} \\\\ \frac{9}{10} & \frac{35}{6} & 12 \\\\ \frac{11}{10} & \frac{9}{2} & -26 \end{pmatrix} \tag{3.11}$$
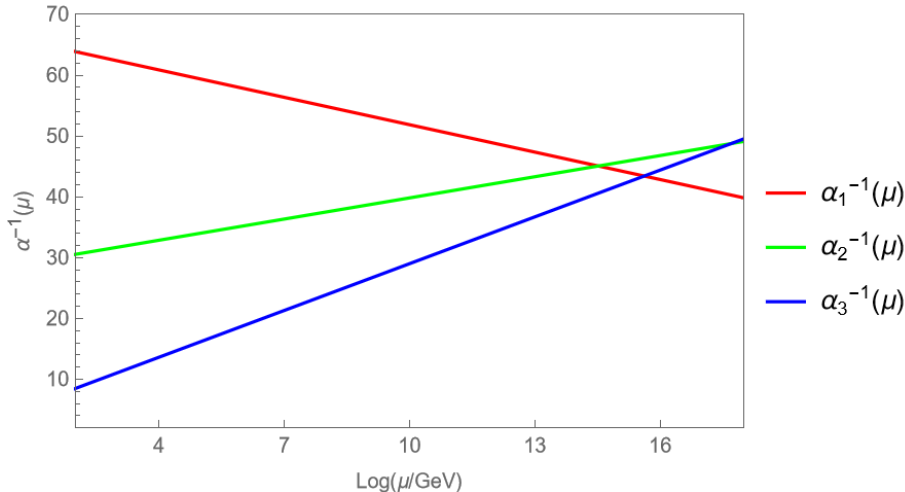
Figure 3.1: Standard Model gauge coupling constants

These three gauge couplings do not meet at any energy scale within the Standard Model framework [44, 45, 46] as it is presented in Fig. 3.1. We note that the successful unification of gauge couplings would imply common origin of the Standard Model interactions. There are currently several different approaches towards realisation of this desirable feature. In this work we will investigate non-supersymmetric approach towards gauge coupling unification within the context of Grand Unification. The most commonly used simple groups to discuss Grand Unification without supersymmetry [47] are $SU(5)$, $SO(10)$, and E_6. In this work, in the next few chapters, we will describe several prominent features of the $SU(5)$ group.

3.3 Baryon (B) and lepton (L) number violation

Baryon and Lepton number conservation is a consequence of accidental symmetry of the Standard Model and can be violated if one resorts to use of higher dimension operators. For example, neutrinos are massless in the Standard Model, where dim-4 operators are used. That situation corresponds to the conserved lepton number. But, since experiments argue differently, one can use dim-5 Weinberg operator in order to generate neutrino masses:

$$\mathcal{L}_{\text{dim}-5} = -\frac{c_{ij}}{M} \left(\bar{l}_i^c i \tau^2 H \right) \left(l_j i \tau^2 H \right) + \text{h.c.} \tag{3.12}$$

where c_{ij} represent matrix elements of the 3×3 symmetric complex matrix. This dim-5 operator violates

lepton number L by 2 units and it is the only dim-5 operator that we can write with the Standard Model particle content. Now, it follows that neutrinos are purely Majorana particles:

$$\mathcal{L}_\nu = -m_\nu \bar{\nu}^c \nu + \text{h.c.} \tag{3.13}$$

where requirement that $m_{\nu,ij} = \frac{c_{ij} v^2}{M} < 0.1\,\text{eV}$ gives an upper limit on new physics scale of $M \lesssim 10^{14}\,\text{GeV}$.

As for dim-6 operators, these can violate baryon number B. For example, operators of the form:

$$\mathcal{L}_{\text{dim}-6} = \frac{1}{M^2} \left(y_1^2 qqql + y_2^2 u^c e^c u^c d^c \right) + \frac{g^2}{M^2} \left(\bar{d}^c \bar{u}^c ql - \bar{e}^c \bar{u}^c qq \right), \tag{3.14}$$

violate both baryon and lepton numbers, where parameter M represents a scale of new physics. It can be derived, as it will be shown in next chapters, that the proton lifetime reads:

$$\tau(p \to e^+ \pi^0) \sim \frac{M^4}{g^4 m_p^5} > 2.4 \times 10^{34}\,\text{years}. \tag{3.15}$$

If we assume that g is of order 1, we see that experimental limit quoted on the right-hand side of Eq. (3.15) yields $M > 10^{15}\,\text{GeV}$. This implies that the energies associated with new physics that generates baryon number violation lie at much higher scales than any of the scales associated with the Standard Model.

Chapter 4

$SU(5)$

"One proton of faith, three electrons of humility, a neutron of compassion and a bond of honesty", Robert said, winking at his daughter. "What's that?" Cora frowned, confused. Maggie laughed. "That, according to your father, is the molecular structure of love."

Menna Van Praag

In the world of so many theories and specific explications and postulations, there has been a need and strive for a theory that could and would tell the whole story. Ever since James Clerk Maxwell, physicists have been trying to unite separate theories into a greater one to cover it all. Grand Unified Theory (GUT) is a term used to depict exactly the greater theory in physics. It is no longer a singular, due to the fact that there are more than one potentially viable GUT. Nonetheless, in this chapter, we will discuss one in particular — the theory based on the gauge group $SU(5)$.

There are certainly many interesting issues within the $SU(5)$ model building that one could discuss, but we will address the most pertinent ones, important for this thesis.

Recall, unification refers to the possibility that three different gauge coupling constants ($\alpha_s \equiv \alpha_3, \alpha_1$ and α_2) would unify at some energy scale to the same value. Again, these scale-dependent coupling constants are calculated using the RGEs:

$$\frac{1}{\alpha_i(\mu)} = \frac{1}{\alpha_i(m_{\mathrm{GUT}})} + \frac{\beta_i}{2\pi} \ln\left(\frac{\mu}{m_{\mathrm{GUT}}}\right) + ...$$

$$\begin{cases} \beta_1 = -\frac{1}{3}\left(4N_g + \frac{3}{10}\right) \\[2mm] \beta_2 = \frac{1}{3}\left(22 - 4N_g - \frac{1}{2}\right) \\[2mm] \beta_3 = \frac{1}{3}\left(33 - 4N_g\right) \end{cases} \tag{4.1}$$

where $\alpha_i = g_i^2/(4\pi)$ represents coupling constants of $SU(i)$ with $i = 2, 3$ and $\alpha_1 = \frac{5}{3}\frac{\alpha_{\mathrm{QED}}}{\cos^2\theta_W}$ represents coupling constant of $U(1)$ group; μ is the energy scale at which these constants are to be calculated, coefficients β_i are of the β-function coefficients $\beta_i = \mu\,\partial\alpha_i/\partial\mu$, and $N_g(=3)$ denotes the number of generations. These coefficients are derived under the assumption that the particle content of the theory is identical to the content of the Standard Model and should be reevaluated within any new physics model.

4.1 Georgi-Glashow model

Howard Georgi and Sheldon Glashow published in 1974 an article [3] with a bold introduction: "$SU(5)$ *is the gauge group of the world*". It was a fair assumption since the $SU(5)$ perfectly incorporates the first unification of $SU(2)$ and $U(1)$ with $SU(3)$. Rank of $SU(3) \times SU(2) \times U(1)$ is $2+1+1 = 4$ and hence the smallest possible rank of unification group must be 4. The following groups satisfy this requirement — $[SU(2)]^4$, $[SO(3)]^4$, $[SO(4)]^2$, $[SO(5)]^2$, $[S_p(4)]^2$, $SO(8)$, $SO(9)$, $S_p(8)$, $[G_2]^2$, F_4, $[SU(3)]^2$, and $SU(5)$ — but only two of them $(\mathrm{R}([SU(3)]^2) = [3-1]^2 = 4$ and $\mathrm{R}(SU(5)) = 5-1 = 4)$ have complex representations which is a prerequisite to incorporate the Standard Model fields. Due to the fact that the generator of the electric charge in $[SU(3)]^2$ is traceless and requires the sum of all quark charges to vanish [3], $SU(5)$ was indeed a unique candidate for GUT.

4.1.1 Fermion sector

In order to find the right representation to arrange and unify all the fermions, we organize their quantum numbers as shown in Table 4.1. Since one cannot have fermions of opposite chiralities within the same irreducible representation due to Lorentz symmetry, one needs to use charge conjugation operator to turn right-handed fields into left-handed fields. Hence the appearance of d_R^c, u_R^c, and e_R^c in Table 4.1. Clearly, there are 15 states in each generation of the Standard Model fermions. To relate hypercharge (Y), electric charge (Q), and weak isospin (T_3), we use $Q = T_3 + Y$, where Q is given in units of electric charge of positron.

The basic building block of $SU(5)$ is its 5-dimensional fundamental representation. There are thus

Table 4.1: Fermions' quantum numbers

States	$SU(3)$ irrep	$SU(2)$ irrep	$U(1)$ Hypercharge Y	Charge Q	Weak isospin T_3	Color
d^c_{Ri}	$\bar{3}$	1	$+\frac{1}{3}$	$+\frac{1}{3}$	0	$i=1,2,3$
u^c_{Ri}	$\bar{3}$	1	$-\frac{2}{3}$	$-\frac{2}{3}$	0	$i=1,2,3$
d_{Li}	3	2	$+\frac{1}{6}$	$-\frac{1}{3}$	$-\frac{1}{2}$	$i=1,2,3$
u_{Li}	3	2	$+\frac{1}{6}$	$+\frac{2}{3}$	$+\frac{1}{2}$	$i=1,2,3$
e^c_R	1	1	$+1$	$+1$	0	-
e_L	1	2	$-\frac{1}{2}$	-1	$-\frac{1}{2}$	-
ν_{eL}	1	2	$-\frac{1}{2}$	0	$+\frac{1}{2}$	-

only two options for construction of a multiplet with five states, if one consults the Table 4.1, and it needs simultaneously to include quarks and leptons:

$$\bar{5} = (d^c_{Ri}, e_L, \nu_{eL}) = (\bar{3}, 1, 1/3) \oplus (1, 2, -1/2) \tag{4.2}$$

$$\bar{5} = (u^c_{Ri}, e_L, \nu_{eL}) = (\bar{3}, 1, -2/3) \oplus (1, 2, -1/2) \tag{4.3}$$

We will consider electric charge operator Q to determine correct embedding:

$$Q = T_3 + Y \begin{cases} Q(d^c_{Ri}, e^-_L, \nu_{eL}) & = \sum_{a=1}^{5} Q_a = 3 \cdot Q(d^c_{Ri}) + Q(e^-_L) + Q(\nu_{eL}) \\ & = 3 \cdot 1/3 + (-1) + 0 = 0 \\ Q(u^c_{Ri}, e^-_L, \nu_{eL}) & = \sum_{a=1}^{5} Q_a = 3 \cdot Q(u^c_{Ri}) + Q(e^-_L) + Q(\nu_{eL}) \\ & = 3 \cdot (-2/3) + (-1) + 0 = -1 \end{cases} \tag{4.4}$$

It is clear that the correct option corresponds to the scenario with $Q = 0$. This is due to the fact that we will assign two of the $SU(5)$ generators to Y and T_3, and since both of them are traceless, the Q evaluated over full multiplet must be traceless as well. Again, it follows that the correct multiplet with both quarks and leptons looks like this:

$$\psi_\alpha = \bar{5} = \begin{pmatrix} d^c_{R1} \\ d^c_{R2} \\ d^c_{R3} \\ e_L \\ -\nu_{eL} \end{pmatrix} = (\bar{3}, 1, 1/3) \oplus (1, 2, -1/2) \tag{4.5}$$

Once we know $\bar{5}$, we can, by applying charge conjugation, find the fundamental representation to be $\psi^\alpha = 5 = (3, 1, -1/3) \oplus (1, 2, 1/2)$. We do that in order to find representation(s) comprising ten more missing states since in the Standard Model there are 15 Weyl fermions per generation, all in all.

Firstly, we will decompose direct product of two fundamental representations to find other irreducible representations of $SU(5)$:

$$5 \otimes 5 = 10 \oplus 15 \tag{4.6}$$

$$\square \otimes \square = \begin{array}{c}\square\\\square\end{array} \oplus \square\square \tag{4.7}$$

Under the exchange of two indices they carry (since fundamental ψ^α carries one), 10 is antisymmetric and 15 is symmetric representation. If we write direct product of Eq. (4.6) in terms of the Standard Model multiplets we obtain:

$$
\begin{aligned}
5 \otimes 5 &= \left(\left(3, 1, -\frac{1}{3}\right) \oplus \left(1, 2, \frac{1}{2}\right) \right) \otimes \left(\left(3, 1, -\frac{1}{3}\right) \oplus \left(1, 2, \frac{1}{2}\right) \right) \\
&= \left(3, 2, \frac{1}{6}\right) \oplus \left(\bar{3}, 1, -\frac{2}{3}\right) \oplus (1, 1, 1) \oplus \\
&\oplus \left(6, 1, -\frac{2}{3}\right) \oplus \left(3, 2, \frac{1}{6}\right) \oplus (1, 3, 1)
\end{aligned}
\tag{4.8}
$$

from where we can recognize that antisymmetric 10 is exactly the representation that contains ten remaining fields:

$$Q_L = \begin{pmatrix} u_i \\ d_i \end{pmatrix}_L \equiv \left(3, 2, \frac{1}{6}\right) \tag{4.9}$$

$$u_R^c = \left(\bar{3}, 1, -\frac{2}{3}\right) \tag{4.10}$$

$$e_R^c = (1, 1, 1) \tag{4.11}$$

Therefore, antisymmetric 10 would have this form:

$$
10 = \frac{1}{\sqrt{2}} \begin{pmatrix}
0 & u_3^c & -u_2^c & u_1 & d_1 \\
-u_3^c & 0 & u_1^c & u_2 & d_2 \\
u_2^c & -u_1^c & 0 & u_3 & d_3 \\
-u_1 & -u_2 & -u_3 & 0 & e^c \\
-d_1 & -d_2 & -d_3 & -e^c & 0
\end{pmatrix}, \tag{4.12}
$$

where multiplicative factor $2^{-\frac{1}{2}}$ comes from the need for appropriate normalization of kinetic terms as the number of states in 10 is doubled.

Table 4.2: Decomposition of direct product of representations within $SU(5)$ [48]

Direct product	Decomposition
$5 \otimes \bar{5}$	$1 \oplus 24$
$5 \otimes 5$	$10 \oplus 15$
$\bar{5} \otimes 10$	$5 \oplus 45$
$5 \otimes 10$	$40 \oplus \overline{10}$
$10 \otimes 10$	$\bar{5} \oplus \overline{45} \oplus 50$
$\overline{10} \otimes 10$	$1 \oplus 24 \oplus 75$

4.1.2   Gauge sector

After fundamental representation with one index, symmetric and antisymmetric representations of $SU(5)$ with two indices, the next one is adjoint representation. Table 4.2 summarizes the decomposition of direct products of lowest lying irreducible representations. The adjoint can be found using direct product $5 \otimes \bar{5}$ since

$$5 \otimes \bar{5} = 1 \oplus 24$$

$$\tag{4.13}$$

$$
\begin{aligned}
5 \otimes \bar{5} &= \left(\left(3, 1, -\frac{1}{3} \right) \oplus \left(1, 2, -\frac{1}{2} \right) \right) \otimes \left(\left(\bar{3}, 1, \frac{1}{3} \right) \oplus \left(1, 2, \frac{1}{2} \right) \right) \\
&= (1, 1, 0) \oplus \left((8, 1, 0) \oplus \left(\bar{3}, 2, \frac{5}{6} \right) \oplus \left(3, 2, -\frac{5}{6} \right) \oplus (1, 3, 0) \oplus (1, 1, 0) \right).
\end{aligned}
\tag{4.14}
$$

$SU(5)$ has 24 generators. Eight of these will be from $SU(3)$, three from $SU(2)$, and one corresponds to the hypercharge Y of $U(1)$ in the Standard Model. These twelve generators are of this form:

$$
L_1 = \begin{pmatrix} 0 & 1 & 0 & 0 & 0 \\ 1 & 0 & 0 & 0 & 0 \\ 0 & 0 & 0 & 0 & 0 \\ 0 & 0 & 0 & 0 & 0 \\ 0 & 0 & 0 & 0 & 0 \end{pmatrix}
L_2 = \begin{pmatrix} 0 & -i & 0 & 0 & 0 \\ i & 0 & 0 & 0 & 0 \\ 0 & 0 & 0 & 0 & 0 \\ 0 & 0 & 0 & 0 & 0 \\ 0 & 0 & 0 & 0 & 0 \end{pmatrix}
L_3 = \begin{pmatrix} 1 & 0 & 0 & 0 & 0 \\ 0 & -1 & 0 & 0 & 0 \\ 0 & 0 & 0 & 0 & 0 \\ 0 & 0 & 0 & 0 & 0 \\ 0 & 0 & 0 & 0 & 0 \end{pmatrix}
$$

$$L_4 = \begin{pmatrix} 0 & 0 & 1 & 0 & 0 \\ 0 & 0 & 0 & 0 & 0 \\ 1 & 0 & 0 & 0 & 0 \\ 0 & 0 & 0 & 0 & 0 \\ 0 & 0 & 0 & 0 & 0 \end{pmatrix} L_5 = \begin{pmatrix} 0 & 0 & -i & 0 & 0 \\ 0 & 0 & 0 & 0 & 0 \\ i & 0 & 0 & 0 & 0 \\ 0 & 0 & 0 & 0 & 0 \\ 0 & 0 & 0 & 0 & 0 \end{pmatrix} L_6 = \begin{pmatrix} 0 & 0 & 0 & 0 & 0 \\ 0 & 0 & 1 & 0 & 0 \\ 0 & 1 & 0 & 0 & 0 \\ 0 & 0 & 0 & 0 & 0 \\ 0 & 0 & 0 & 0 & 0 \end{pmatrix}$$

$$L_7 = \begin{pmatrix} 0 & 0 & 0 & 0 & 0 \\ 0 & 0 & -i & 0 & 0 \\ 0 & i & 0 & 0 & 0 \\ 0 & 0 & 0 & 0 & 0 \\ 0 & 0 & 0 & 0 & 0 \end{pmatrix} L_8 = \frac{1}{\sqrt{3}} \begin{pmatrix} 1 & 0 & 0 & 0 & 0 \\ 0 & 1 & 0 & 0 & 0 \\ 0 & 0 & -2 & 0 & 0 \\ 0 & 0 & 0 & 0 & 0 \\ 0 & 0 & 0 & 0 & 0 \end{pmatrix} \quad SU(3)$$

$$L_9 = \begin{pmatrix} 0 & 0 & 0 & 0 & 0 \\ 0 & 0 & 0 & 0 & 0 \\ 0 & 0 & 0 & 0 & 0 \\ 0 & 0 & 0 & 0 & 1 \\ 0 & 0 & 0 & 1 & 0 \end{pmatrix} L_{10} = \begin{pmatrix} 0 & 0 & 0 & 0 & 0 \\ 0 & 0 & 0 & 0 & 0 \\ 0 & 0 & 0 & 0 & 0 \\ 0 & 0 & 0 & 0 & -i \\ 0 & 0 & 0 & i & 0 \end{pmatrix} L_{11} = \begin{pmatrix} 0 & 0 & 0 & 0 & 0 \\ 0 & 0 & 0 & 0 & 0 \\ 0 & 0 & 0 & 0 & 0 \\ 0 & 0 & 0 & 1 & 0 \\ 0 & 0 & 0 & 0 & -1 \end{pmatrix} \quad SU(2)$$

$$L_{12} = \frac{1}{\sqrt{15}} \begin{pmatrix} -2 & 0 & 0 & 0 & 0 \\ 0 & -2 & 0 & 0 & 0 \\ 0 & 0 & -2 & 0 & 0 \\ 0 & 0 & 0 & 3 & 0 \\ 0 & 0 & 0 & 0 & 3 \end{pmatrix} \quad U(1)$$

Since rank of $SU(5)$ is 4, the four diagonal generators will be $T_3 \equiv L_{11}$ from $SU(2)$, $Y \equiv L_{12}$ from $U(1)$ and L_3 and L_8.

The remaining 12 generators are:

$$L_{13} = \begin{pmatrix} 0 & 0 & 0 & 1 & 0 \\ 0 & 0 & 0 & 0 & 0 \\ 0 & 0 & 0 & 0 & 0 \\ 1 & 0 & 0 & 0 & 0 \\ 0 & 0 & 0 & 0 & 0 \end{pmatrix} L_{14} = \begin{pmatrix} 0 & 0 & 0 & i & 0 \\ 0 & 0 & 0 & 0 & 0 \\ 0 & 0 & 0 & 0 & 0 \\ -i & 0 & 0 & 0 & 0 \\ 0 & 0 & 0 & 0 & 0 \end{pmatrix} L_{15} = \begin{pmatrix} 0 & 0 & 0 & 0 & 1 \\ 0 & 0 & 0 & 0 & 0 \\ 0 & 0 & 0 & 0 & 0 \\ 0 & 0 & 0 & 0 & 0 \\ 1 & 0 & 0 & 0 & 0 \end{pmatrix} L_{16} = \begin{pmatrix} 0 & 0 & 0 & 0 & i \\ 0 & 0 & 0 & 0 & 0 \\ 0 & 0 & 0 & 0 & 0 \\ 0 & 0 & 0 & 0 & 0 \\ -i & 0 & 0 & 0 & 0 \end{pmatrix}$$

$$L_{17} = \begin{pmatrix} 0 & 0 & 0 & 0 & 0 \\ 0 & 0 & 0 & 1 & 0 \\ 0 & 0 & 0 & 0 & 0 \\ 0 & 1 & 0 & 0 & 0 \\ 0 & 0 & 0 & 0 & 0 \end{pmatrix} L_{18} = \begin{pmatrix} 0 & 0 & 0 & 0 & 0 \\ 0 & 0 & 0 & i & 0 \\ 0 & 0 & 0 & 0 & 0 \\ 0 & -i & 0 & 0 & 0 \\ 0 & 0 & 0 & 0 & 0 \end{pmatrix} L_{19} = \begin{pmatrix} 0 & 0 & 0 & 0 & 0 \\ 0 & 0 & 0 & 0 & 1 \\ 0 & 0 & 0 & 0 & 0 \\ 0 & 0 & 0 & 0 & 0 \\ 0 & 1 & 0 & 0 & 0 \end{pmatrix} L_{20} = \begin{pmatrix} 0 & 0 & 0 & 0 & 0 \\ 0 & 0 & 0 & 0 & i \\ 0 & 0 & 0 & 0 & 0 \\ 0 & 0 & 0 & 0 & 0 \\ 0 & -i & 0 & 0 & 0 \end{pmatrix}$$

$$L_{21} = \begin{pmatrix} 0 & 0 & 0 & 0 & 0 \\ 0 & 0 & 0 & 0 & 0 \\ 0 & 0 & 0 & 1 & 0 \\ 0 & 0 & 1 & 0 & 0 \\ 0 & 0 & 0 & 0 & 0 \end{pmatrix} L_{22} = \begin{pmatrix} 0 & 0 & 0 & 0 & 0 \\ 0 & 0 & 0 & 0 & 0 \\ 0 & 0 & 0 & i & 0 \\ 0 & 0 & -i & 0 & 0 \\ 0 & 0 & 0 & 0 & 0 \end{pmatrix} L_{23} = \begin{pmatrix} 0 & 0 & 0 & 0 & 0 \\ 0 & 0 & 0 & 0 & 0 \\ 0 & 0 & 0 & 0 & 1 \\ 0 & 0 & 0 & 0 & 0 \\ 0 & 0 & 1 & 0 & 0 \end{pmatrix} L_{24} = \begin{pmatrix} 0 & 0 & 0 & 0 & 0 \\ 0 & 0 & 0 & 0 & 0 \\ 0 & 0 & 0 & 0 & i \\ 0 & 0 & 0 & 0 & 0 \\ 0 & 0 & -i & 0 & 0 \end{pmatrix}$$

It is clear that these twelve generators act simultaneously with the $SU(3)$ and $SU(2)$ spaces. The gauge boson of 24 can be expressed in the following way [49]:

$$V_\mu = \begin{pmatrix} G_1^1 - \frac{2B}{\sqrt{30}} & G_2^1 & G_3^1 & X_1 & Y_1 \\ G_1^2 & G_2^2 - \frac{2B}{\sqrt{30}} & G_3^2 & X_2 & Y_2 \\ G_1^3 & G_2^3 & G_3^3 - \frac{2B}{\sqrt{30}} & X_3 & Y_3 \\ \bar{X}_1 & \bar{X}_2 & \bar{X}_3 & \frac{W^0}{\sqrt{2}} + \frac{3B}{\sqrt{30}} & W^+ \\ \bar{Y}_1 & \bar{Y}_2 & \bar{Y}_3 & W^- & -\frac{W^0}{\sqrt{2}} + \frac{3B}{\sqrt{30}} \end{pmatrix} \tag{4.15}$$

where

$$G_2^1 = \frac{(g_1 - ig_2)}{\sqrt{2}} \qquad G_1^2 = \frac{(g_1 + ig_2)}{\sqrt{2}}$$

$$G_3^1 = \frac{(g_4 - ig_5)}{\sqrt{2}} \qquad G_1^3 = \frac{(g_4 + ig_5)}{\sqrt{2}}$$

$$G_3^2 = \frac{(g_6 - ig_7)}{\sqrt{2}} \qquad G_2^3 = \frac{(g_6 + ig_7)}{\sqrt{2}} \tag{4.16}$$

$$G_1^1 = \frac{g_3}{\sqrt{2}} + \frac{g_8}{\sqrt{6}} \quad G_2^2 = -\frac{g_3}{\sqrt{2}} + \frac{g_8}{\sqrt{6}} \quad G_3^3 = -\sqrt{\frac{2}{2}} g_8$$

and $g_i (i = 1...8)$ represent eight gluons, while X and Y are vector gauge bosons — mediators of the proton decay — whose mass is associated with the new energy scale of unification of three gauge coupling constants. These new bosons convert quarks into leptons and vice versa. They can be expressed in terms of pairs of fermions that they interact with:

$$X \sim (e_L)^c d_L^c \text{ or } u_R u_L$$

$$Y \sim (\nu_L)^c d_L^c \text{ or } u_R d_L \tag{4.17}$$

It follows that they form an isospin doublet that carries color:

$$X(SU(3), SU(2), U(1), Q, T_3) = (3, 2, -5/6, -4/3, -1/2) \tag{4.18}$$

$$Y(SU(3), SU(2), U(1), Q, T_3) = (3, 2, -5/6, -1/3, 1/2) \tag{4.19}$$

Since they turn leptons to quarks and vice versa, they are sometimes referred to as leptoquarks.

4.1.3 Scalar sector and symmetry breaking

The $SU(5)$ symmetry can be broken to $SU(3) \times SU(2) \times U(1)$ by either 24-dimensional [3] or 75-dimensional scalar multiplet [50, 51]. The 12 new vector bosons (X, Y) become massive after the first stage of spontaneous symmetry breaking of $SU(5)$ since the Standard Model has 12 gauge bosons and $SU(5)$ 24. This first stage needs to happen at mass scale $\mu \simeq M_{\text{GUT}} \geq 10^{15}$ GeV [49, 52] due to constraints from proton decay experiments. As we already mentioned, X and Y vector bosons reside at that scale.

The second stage of breaking is needed to go from $SU(3) \times SU(2) \times U(1)$ down to $SU(3) \times U(1)_{\text{em}}$ and it is accomplished by the field that transforms as the Standard Model Higgs field. The breaking takes place at the electroweak scale $\mu \simeq 250$ GeV when $W^{\pm}$ and Z acquire their masses, and, in the process, charged fermions of the Standard Model also become massive.

We will use, for the first stage of symmetry breaking, 24-dimensional scalar field Φ. Since $5 \otimes \bar{5} = 24 \oplus 1$, it follows that scalar field Φ can be represented by a traceless 5×5 matrix. The idea is to have a scalar field to give masses to X and Y gauge bosons and not to other gauge bosons. This field is Hermitian and it will transform as:

$$\Phi \rightarrow U\Phi U^\dagger \tag{4.20}$$

under the $SU(5)$ transformations. It is well known that Hermitian matrix can be put in diagonal form using the proper unitary matrix U:

$$U\Phi U^\dagger = \Phi^{\text{diag}} \tag{4.21}$$

Knowing that matrix Φ^{diag} is also traceless, there are several options:

$$\text{diag}\,(a, a, a, b, -3a - b) \tag{4.22}$$

$$\text{diag}\,(a, a, b, b, -2a - 2b) \tag{4.23}$$

$$\text{diag}\,(a, a, a, -3a/2, -3a/2) \tag{4.24}$$

$$\text{diag}\,(a, a, a, a, -4a) \tag{4.25}$$

$$\text{diag}\,(0, 0, 0, 0, 0) \tag{4.26}$$

which read:

$$\text{diag}\,(1, -1, 0, 0, 0) \tag{4.27}$$

$$\text{diag}\,(1, 1, -1, -1, 0) \tag{4.28}$$

$$\text{diag}\,(2, 2, 2, -3, -3) \tag{4.29}$$

$$\text{diag}\,(1, 1, 1, 1, -4) \tag{4.30}$$

$$\text{diag}\,(0, 0, 0, 0, 0) \tag{4.31}$$

The only realistic option here is a structure given in Eq. (4.29). Hence the form of VEV for scalar field Φ is:

$$\langle \Phi \rangle = \langle 24_H \rangle = \begin{pmatrix} 2 & & & & \\ & 2 & & & \\ & & 2 & & \\ & & & -3 & \\ & & & & -3 \end{pmatrix} V \tag{4.32}$$

where $V = v_{\text{GUT}}/\sqrt{30}$. It is clear that the upper 3×3 block is reserved for $SU(3)$ group, lower 2×2 block is reserved for $SU(2)$ group and the fact that it is diagonal is associated with $U(1)$ group of the Standard Model. However, this scalar field cannot induce the second phase of $SU(5)$ symmetry breaking that would simultaneously give masses to $W^{\pm}$ and Z. This is because Φ does not have a color singlet and an isospin doublet necessary to generate masses of $W^{\pm}$ and Z. Beside this, Φ cannot couple and give mass to fermions since fermions reside in either $\bar{5}$ or 10 and the only possible contractions correspond to combinations $10\,10$, $10\,\bar{5}$, and $\bar{5}\,\bar{5}$. Group theory, as already specified in Table 4.2, stipulates that:

$$\bar{5} \otimes \bar{5} = \overline{10} \oplus \overline{15} \tag{4.33}$$

$$\bar{5} \otimes 10 = 5 \oplus 45 \tag{4.34}$$

$$10 \otimes 10 = \bar{5} \oplus \overline{45} \oplus 50 \tag{4.35}$$

Clearly, fermion masses can potentialy come from the representations on the right hand side of Eqs. (4.33) through (4.35). It turns out that the only two representations that contain a field that transforms as the Standard Model Higgs boson H are 5-dimensional and 45-dimensional representations. The simplest version is to have Higgs to be in 5. We know that 5 would contain an additional color triplet scalar T:

$$5_H \equiv \begin{bmatrix} T \\ H \end{bmatrix} \tag{4.36}$$

in agreement with the transformation properties presented in Eq. (4.5). Since 5_H now can give mass to fermions, the mass giving Yukava interaction would be of this schematic form:

$$[10] \times [10] \times [5_H] \rightarrow m_u \tag{4.37}$$

$$[\bar{5}] \times [10] \times [5_H^*] \rightarrow m_d \tag{4.38}$$

$$[\bar{5}] \times [10] \times [5_H^*] \rightarrow m_e. \tag{4.39}$$

The explicit form of Yukawa Lagrangian reads:

$$\mathcal{L}_{\text{Y}} = Y_{5ij}\,10_i^{\alpha\beta}\,\bar{5}_{\alpha j}\,5_{H\beta}^* + \epsilon_{\alpha\beta\gamma\delta\eta}Y_{10\,ij}10_i^{\alpha\beta\,c}10_j^{\gamma\delta}5_H^{\eta} \tag{4.40}$$

where Y_5 and Y_{10} are 3×3 matrices in generation space and $\epsilon_{\alpha\beta\gamma\delta\eta}$ is 5-dimensional Levi-Civita tensor used here to contract all upper indices. For properties of Levi-Civita tensor, see Appendix A.

To summarize, the minimal $SU(5)$ of Georgi-Glashow has two scalar multiplets. One (24_H) is used for spontaneous symmetry breaking of $SU(5)$ and the other one (5_H) is responsible for breaking of $SU(3) \times SU(2) \times U(1)$ down to $SU(3) \times U(1)_{\text{em}}$. 24_H provides masses for X and Y gauge bosons whereas

5_H generates masses of the Standard Model particles.

4.1.4 Mass hierarchy problem

The starting point of the Georgi-Glashow [3] $SU(5)$ model is the mass generating part of the Lagrangian of the following form:

$$\mathcal{L}_{\text{Yukawa}} = g_u \epsilon_{ijklm} \overline{\psi}_{10}^{c\,ij} \psi_{10}^{kl} 5_H^m + g_d \overline{\psi}_{5a} \psi_{10}^{ab} 5_{Hb}^* + \text{h.c.} \tag{4.41}$$

Using the simplest Higgs in the second stage of symmetry breaking, transforming like fundamental representation of $SU(5)$, and substituting into Eq. (4.41), we have:

$$\mathcal{L} = -\frac{g_d v}{\sqrt{2}} [\overline{d}_R d_L + \overline{e_R^c} e_L^c + \text{h.c.}] \tag{4.42}$$

where sum over both flavor and color indices is understood. This leads to degeneracy in mass for down-type quarks and charged leptons. Namely, due to the fact that g_d is a common Yukawa coupling matrix for down quarks and charged leptons, we conclude [3, 53]:

$$m_d = m_e \quad m_s = m_\mu \quad m_b = m_\tau \,. \tag{4.43}$$

In Georgi-Glashow model, neutrinos are massless particles. This obviously contradicts experimental observations. Since these predictions of the model do not agree with the experimental results, it was clear that there was a problem in the mass sector, and only extensions or modifications of the original $SU(5)$ proposal could potentially resolve this issue.

Chapter 6 introduces a simple extension of Georgi-Glashow model that addresses both of these problems. Before we do that, we will discuss seminal prediction of GUTs which is proton decay.

Chapter 5

Proton Decay

The flash would prove that
proton decay really happens. The
flash would mean that the matter
of the proton - the solid stuff -
had turned into the energy of the
flash. Totally. Nothing left
behind. No ash. No smoke. No
smell. Nada. One moment it's
there, the next moment - pffft -
gone. What would it mean? Only
this: Nothing lasts. Nothing.
Because everything that exists is
made of protons.

Jerry Spinelli
"Smiles to Go"

5.1   Historical background and introduction

Proton decay is one of the most intriguing predictions of Grand Unified Theories [54, 55].

It was the Nobel Prize Laureate Andrei Sakharov who was the first to propose such a captivating and provocative possibility [56]. His paper addressed the baryon asymmetry problem of our universe. It was Paul Dirac who predicted [57] in his equation, where he combined quantum mechanics and special relativity to describe motion of an electron, that for every particle exists a corresponding antiparticle. However, we do not observe nor detect equal amounts of matter and antimatter in the universe. In order to explain this asymmetry, Andrei Sakharov formulated three requirements for this to happen,

know as *Sakharov conditions*: baryon number (B) violation, C-symmetry and CP-symmetry violation, and interactions out of thermal equilibrium. For proton to decay, baryon number needs to be violated. Nonetheless, Sakharov's ideas remained in hidden corner in the next few years, until the Grand Unification was brought to daylight in 1974 [4].

Proton has proven to be one of the most stable particles and so far, no proton decay has been observed. The possibility that the proton decay is detected would provide window into scales that cannot be reached with conventional collider technologies. For example, the Georgi-Glashow model [3] predicts proton lifetime to be

$$\tau \propto \frac{M_{X,Y}^4}{m_p^5} \, , \tag{5.1}$$

where m_p is proton mass and $M_{X,Y}$ is the mass of a heavy mediator. If one takes the latest experimental limits, one naively obtains $M_{X,Y} \gtrsim 2 \times 10^{15}$ GeV [4].

The Georgi-Glashow model is called *minimal $SU(5)$* due to the fact that it has fewest number of "adjustable parameters", even though it isn't realistic for aforementioned reasons. One of the nicer features of the model is that the mass $M_{X,Y}$ corresponds to the energy scale at which three out of four fundamental forces in nature come together and become indistinguishable. In other words, $SU(5)$ should be able to predict scale associated with proton decay.

5.2   Operators of dimension 6

GUTs have as a typical prediction appearance of nucleon (proton and neutron) decay operators. These operators are of higher dimensions ($d \geq 6$) since operators of lower dimensions in the Standard Model do not violate baryon number. The apparent conservation of baryon and lepton numbers [58] is referred to as an accidental symmetry of the Standard Model. The main reason that GUTs imply proton decay lies in a fact that different Standard Model representations reside in the same multiplets, as it is shown in Eq. (4.5), which makes quarks and leptons indistinguishable when it comes to interactions. Hence the violation of baryon and lepton numbers.

Proton decay, in conventional GUTs, can be mediated via two types of particles — gauge bosons and scalar leptoquarks. The representative diagrams for the gauge boson and scalar leptoquark mediations of proton decay are presented in Figs. 5.1 and 5.2, respectively.

It turns out that these two types of mediation of the two-body proton decays conserve $B - L$. Baryon number (B) and lepton number (L) are not conserved separately, but the difference of the two is. We show this in Table 5.1 for each two-body proton decay under consideration in this thesis. One of the upshots of $B - L$ conservation is that proton always decays into antileptons. Clearly, we can distinguish eight two-body proton decay channels, where it is understood that some possibilities are kinematically forbiden such as $p \to \pi^0 \tau^+$.
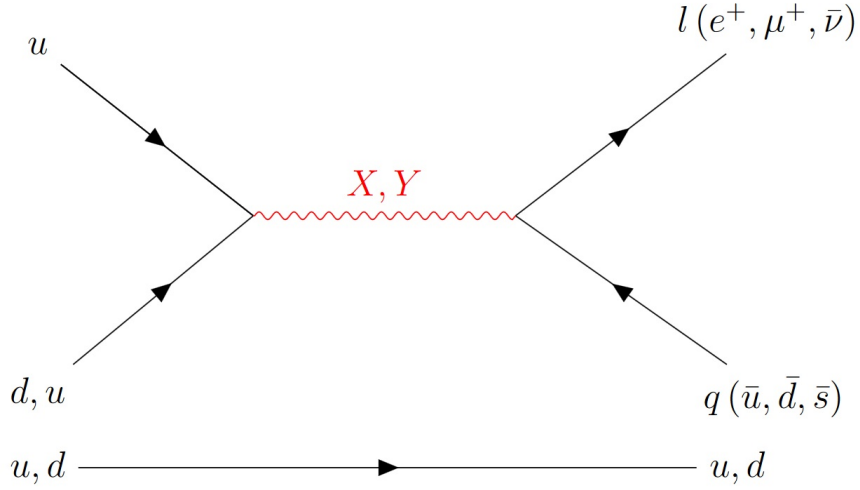
Figure 5.1: Proton decay via the gauge boson mediation
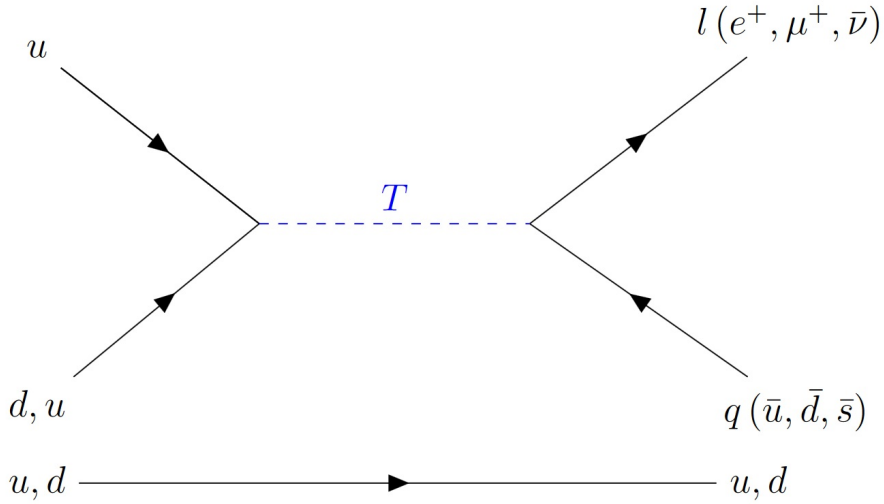
Figure 5.2: Proton decay via the scalar leptoquark mediation

We are interested in finding the dominant channels in both proton decay through gauge bosons and through scalar leptoquark within a well-defined GUT model. The idea is to calculate the decay width for each of eight channels for both types of mediation and to perform correlation study. In order to do so, we will analyze separately proton decay through gauge bosons and through scalar leptoquark and apply these analyses within a specific model.

5.2.1 Proton decay induced by gauge bosons

Baryon and lepton numbers are violated in proton decay mediated by gauge bosons, but their combination $B - L$ is conserved. Therefore, the only decays allowed are the ones involving $L = -1$ particles $(e^+, \mu^+, \bar{\nu}_i)$.

There are 59 [59, 60] operators at the $d = 6$ level if one uses Standard Model particle content that preserve baryon number and only 4 that violate it. Again, we are interested in the latter.

Table 5.1: Conservation of $B - L$ in two-body proton decays

decay channel	baryon number B	lepton number L	$B - L$
$p \to \pi^0 e^+$	$1 \neq 0 + 0$	$0 \neq -1 + 0$	$1 = 0 - (-1)$
$p \to \pi^0 \mu^+$	$1 \neq 0 + 0$	$0 \neq 0 + (-1)$	$1 = 0 - (-1)$
$p \to \eta^0 e^+$	$1 \neq 0 + 0$	$0 \neq 0 + (-1)$	$1 = 0 - (-1)$
$p \to \eta^0 \mu^+$	$1 \neq 0 + 0$	$0 \neq 0 + (-1)$	$1 = 0 - (-1)$
$p \to K^0 e^+$	$1 \neq 0 + 0$	$0 \neq 0 + (-1)$	$1 = 0 - (-1)$
$p \to K^0 \mu^+$	$1 \neq 0 + 0$	$0 \neq 0 + (-1)$	$1 = 0 - (-1)$
$p \to \pi^+ \bar{\nu}$	$1 \neq 0 + 0$	$0 \neq 0 + (-1)$	$1 = 0 - (-1)$
$p \to K^+ \bar{\nu}$	$1 \neq 0 + 0$	$0 \neq 0 + (-1)$	$1 = 0 - (-1)$

Proton decay process involves four fermions (plus spectator quark) and if we start with left-handed fermions $\psi \in \{l, e^c, q, u^c, d^c\}$, rulling out combinations $\psi\psi\psi\bar{\psi}$ and $\psi\bar{\psi}\bar{\psi}\bar{\psi}$ due to Lorentz non-invariance [60], it can be shown that these four $B-$violating combinations are:

$$(qqql), \quad (d^c u^c u^c e^c), \quad (qq\bar{u}^c \bar{e}^c), \quad (ql\bar{u}^c \bar{d}^c). \tag{5.2}$$

Knowing that there can be four possible combinations with left-handed and right-handed states:

$$(\psi_R \psi_R)(\psi_L \psi_L) \tag{5.3}$$

$$(\psi_L \psi_L)(\psi_R \psi_R) \tag{5.4}$$

$$(\psi_L \psi_L)(\psi_L \psi_L) \tag{5.5}$$

$$(\psi_R \psi_R)(\psi_R \psi_R) \tag{5.6}$$

the relevant operators can be written [61], using $SU(3) \times SU(2) \times U(1)$ symmetry, as:

$$O^1_{abcd} = (d_{\alpha a R} u_{\beta b R})(q_{i\gamma cL} l_{jdL}) \, \epsilon_{\alpha\beta\gamma} \epsilon_{ij} \tag{5.7}$$

$$O^2_{abcd} = (q_{i\alpha a L} q_{j\beta b L})(u_{\gamma cR} l_{dR}) \, \epsilon_{\alpha\beta\gamma} \epsilon_{ij} \tag{5.8}$$

$$O^3_{abcd} = (q_{i\alpha a L} q_{j\beta b L})(q_{k\gamma cL} l_{ldL}) \, \epsilon_{\alpha\beta\gamma} \epsilon_{il} \epsilon_{jk} \tag{5.9}$$

$$O^4_{abcd} = (d_{\alpha a R} u_{\beta b R})(u_{\gamma cR} l_{dR}) \, \epsilon_{\alpha\beta\gamma} \tag{5.10}$$

where α, β, γ are color $SU(3)$ indices, i, j, k, l are $SU(2)$ indices and a, b, c, d are generation or family indices.

The former operators for non-supersymmetric model can be expressed as $SU(3) \times SU(2) \times U(1)$

invariants [62, 63, 64] like [65]:

$$O_I^{B-L} = k^2 \, \epsilon_{ijk} \, \epsilon_{\alpha\beta} \, \overline{u_{i,a}^C} \gamma^\mu q_{j\alpha a} \, \overline{e_b^C} \, \gamma_\mu \, q_{k\beta b} \tag{5.11}$$

$$O_{II}^{B-L} = k^2 \, \epsilon_{ijk} \, \epsilon_{\alpha\beta} \, \overline{u_{i,a}^C} \gamma^\mu \, q_{j\alpha a} \, \overline{d_{kb}^C} \, \gamma_\mu \, l_{\beta b} \tag{5.12}$$

where $k = g_{\mathrm{GUT}}/M_{X,Y}$, $M_{X,Y} \sim M_{\mathrm{GUT}}$, $q = (u, d)$, $l = (\nu, e)$ and i, j and k are the color indices, a and b are family indices (only first two family should be taken into account) and α, $\beta = 1, 2$ are $SU(2)$ indices. Note the appearance of g_{GUT} and mass of X and Y bosons in Eqs. (5.11) and (5.12). The scaling with respect to these parameters is self-evident from Fig. 5.1.

However, operators in Eqs. (5.11) and (5.12) are still not in physical mass eigenstate basis for fermions. In order to rewrite them in physical basis, we look at final states knowing that only first two families in the charged lepton and down-type quark sectors should be considered. Also, all three neutrino flavors are relevant even though proton decay experiments do not distinguish between neutrino flavors. Now Eqs. (5.11) and (5.12) can be written as three effective operators, where last two come from Eq. (5.12):

$$O(e_\alpha^C, d_\beta) = c(e_\alpha^C, d_\beta) \, \epsilon_{ijk} \, \overline{u_i^C} \, \gamma^\mu \, u_j \, \overline{e_\alpha^C} \, \gamma_\mu \, d_{k\beta} \tag{5.13}$$

$$O(e_\alpha, d_\beta^C) = c(e_\alpha, d_\beta^C) \, \epsilon_{ijk} \, \overline{u_i^C} \, \gamma^\mu \, u_j \, \overline{d_{k\beta}^C} \, \gamma_\mu \, e_\alpha \tag{5.14}$$

$$O(\nu_l, d_\alpha, d_\beta^C) = c(\nu_l, d_\alpha, d_\beta^C) \, \epsilon_{ijk} \, \overline{u_i^C} \, \gamma^\mu \, d_{j\alpha} \, \overline{d_{k\beta}^C} \, \gamma_\mu \, \nu_l \tag{5.15}$$

We will demonstrate the procedure of going from flavor basis to mass eigenstate basis for both O_I^{B-L} and O_{II}^{B-L}. This procedure explicitly determines coefficients in Eqs. (5.13) through (5.15). We will be temporarily using the convention adopted from Ref. [66] for unitary transformations of quarks and leptons. These are defined via:

$$M_U^{\mathrm{diag}} = U_C^T M_U U$$

$$M_D^{\mathrm{diag}} = D_C^T M_D D$$

$$M_E^{\mathrm{diag}} = E_C^T M_E E$$

$$M_N^{\mathrm{diag}} = N^T M_N N \tag{5.16}$$

where relevant mixing matrices are defined as:

$$V_1 = U_C^\dagger U \qquad V_2 = E_C^\dagger D \qquad V_3 = D_C^\dagger E \qquad V_{UD} = U^\dagger D \qquad V_{EN} = E^\dagger N \tag{5.17}$$

For quark mixing we have:

$$V_{UD} = U^\dagger D = K_1 V_{\mathrm{CKM}} K_2 \tag{5.18}$$

where K_1 and K_2 are diagonal matrices containing three and two phases, respectively. For leptonic mixing we have:

$$V_{EN} = K_3 V_l^M \tag{5.19}$$

where V_l^M is the leptonic mixing matrix at low energy for the neutrino Majorana case and K_3 is a diagonal unitary matrix.

For O_I^{B-L} we have:

$$
\begin{aligned}
O_I^{B-L} &= k^2\, \epsilon_{ijk}\, \epsilon_{\alpha\beta}\, \overline{u_{ia}^C} \gamma^\mu q_{j\alpha a}\, \overline{e_b^C}\, \gamma_\mu\, q_{k\beta b} \\
&= k^2\, \epsilon_{ijk}\, \left[\overline{u_{ia}^C} \gamma^\mu u_{ja}\, \overline{e_b^C}\, \gamma_\mu\, d_{kb} - \overline{u_{ia}^C} \gamma^\mu d_{ja}\, \overline{e_b^C}\, \gamma_\mu\, u_{kb} \right] \\
&= k^2\, \epsilon_{ijk}\, \left[\overline{u_{ic}^C} (U_C^\dagger)_{ca} \gamma^\mu (U)_{ad}\, u_{jd}\, \overline{e_e^C}\, (E_C^\dagger)_{eb}\, \gamma_\mu\, (D)_{bf}\, d_{kf} - \right. \\
&\qquad \left. - \overline{u_{ic}^C} (U_C^\dagger)_{ca}\, \gamma^\mu\, (D)_{ad}\, d_{jd}\, \overline{e_e^C}\, (E_C^\dagger)_{eb}\, \gamma_\mu\, (U)_{bf} u_{kf} \right] \\
&= k^2\, \epsilon_{ijk}\, \left[\overline{u_{ic}^C} (U_C^\dagger U)_{cd}\, \gamma^\mu\, u_{jd}\, \overline{e_e^C}\, (E_C^\dagger D)_{ef}\, \gamma_\mu\, d_{kf} - \right. \\
&\qquad \left. - \overline{u_{ic}^C} (U_C^\dagger D)_{cd}\, \gamma^\mu\, d_{jd}\, \overline{e_e^C}\, (E_C^\dagger U)_{ef}\, \gamma_\mu\, u_{kf} \right] \\
&= k^2\, \epsilon_{ijk}\, \left[V_1^{cd} \overline{u_{ic}^C} \gamma^\mu\, u_{jd}\, V_2^{ef}\, \overline{e_e^C}\, \gamma_\mu\, d_{kf} - \left(U_C^\dagger U U^\dagger D \right)_{cd} \overline{u_{ic}^C} \gamma^\mu\, d_{jd}\, \overline{e_e^C}\, \left(E_C^\dagger D D^\dagger U \right)_{ef}\, \gamma_\mu\, u_{kf} \right] \\
&= k^2\, \epsilon_{ijk}\, \left[V_1^{cd} V_2^{ef}\, \overline{u_{ic}^C} \gamma^\mu\, u_{jd}\, \overline{e_e^C}\, \gamma_\mu\, d_{kf} - (V_1 V_{UD})^{cd}\, \left(V_2 V_{UD}^\dagger \right)^{ef}\, \overline{u_{ic}^C} \gamma^\mu\, d_{jd}\, \overline{e_e^C}\, \gamma_\mu\, u_{kf} \right] \\
&= k^2\, \epsilon_{ijk}\, \left[V_1^{cd} V_2^{ef}\, \overline{u_{ic}^C} \gamma^\mu\, u_{jd}\, \overline{e_e^C}\, \gamma_\mu\, d_{kf} + (V_1 V_{UD})^{cd}\, \left(V_2 V_{UD}^\dagger \right)^{ef}\, \overline{u_{ic}^C} \gamma^\mu\, u_{jd}\, \overline{e_e^C}\, \gamma_\mu\, d_{kf} \right] \\
&= k^2\, \epsilon_{ijk}\, \left[V_1^{cd} V_2^{ef} + (V_1 V_{UD})^{cf}\, \left(V_2 V_{UD}^\dagger \right)^{ed} \right] \overline{u_{ic}^C} \gamma^\mu\, u_{jd}\, \overline{e_e^C}\, \gamma_\mu\, d_{kf} \tag{5.20}
\end{aligned}
$$

Note that in the third line we make a transition from flavor eigenstate notation to the mass eigenstate notation. From sixth to seventh row with equality sign in front, we perform Fierz transformation and hence the change in sign and indices in the second part. To read off the coefficients $c(e_\alpha^C, d_\beta)$, one needs to perform the following identification: $c = d = 1$, $e = 1, 2 \equiv \alpha$, and $f = 1, 2 \equiv \beta$.

Now, for O_{II}^{B-L} we follow the same steps:

$$
\begin{aligned}
O_{II}^{B-L} &= k^2\, \epsilon_{ijk}\, \epsilon_{\alpha\beta}\, \overline{u_{ia}^C}\, \gamma^\mu\, q_{j\alpha a}\, \overline{d_{kb}^C}\, \gamma_\mu\, l_{\beta b} \\
&= k^2\, \epsilon_{ijk}\, \left[\overline{u_{ia}^C}\, \gamma^\mu\, u_{ja}\, \overline{d_{kb}^C}\, \gamma_\mu\, e_b + \overline{u_{ia}^C}\, \gamma^\mu\, d_{ja}\, \overline{d_{kb}^C}\, \gamma_\mu\, \nu_b \right] \\
&= k^2\, \epsilon_{ijk}\, \left[\overline{u_{ic}^C} (U_C^\dagger)_{ca} \gamma^\mu (U)_{ad}\, u_{jd}\, \overline{d_{ke}^C}\, (D_C^\dagger)_{eb}\, \gamma_\mu\, (E)_{bf}\, e_f + \overline{u_{ic}^C} (U_C^\dagger)_{ca}\, \gamma^\mu\, (D)_{ad}\, d_{jd}\, \overline{d_{ke}^C}\, (D_C^\dagger)_{eb}\, \gamma_\mu\, (N)_{bf}\, \nu_f \right] \\
&= k^2\, \epsilon_{ijk}\, \left[\overline{u_{ic}^C} (U_C^\dagger U)_{cd} \gamma^\mu\, u_{jd}\, \overline{d_{ke}^C}\, (D_C^\dagger E)_{ef}\, \gamma_\mu\, e_f + \overline{u_{ic}^C} (U_C^\dagger D)_{cd}\, \gamma^\mu\, d_{jd}\, \overline{d_{ke}^C}\, (D_C^\dagger N)_{ef}\, \gamma_\mu\, \nu_f \right] \\
&= k^2\, \epsilon_{ijk}\, \left[V_1^{cd} \overline{u_{ic}^C} \gamma^\mu\, u_{jd}\, V_3^{ef}\, \overline{d_{ke}^C}\, \gamma_\mu\, e_f + (U_C^\dagger U U^\dagger D)_{cd}\, \overline{u_{ic}^C} \gamma^\mu\, d_{jd} (D_C^\dagger E E^\dagger N)_{ef} \overline{d_{ke}^C}\, \gamma_\mu\, \nu_f \right] \\
&= k^2\, \epsilon_{ijk}\, \left[V_1^{cd} \overline{u_{ic}^C} \gamma^\mu\, u_{jd}\, V_3^{ef} \overline{d_{ke}^C}\, \gamma_\mu\, e_f + (V_1 V_{UD})^{cd}\, (V_3 V_{EN})^{ef}\, \overline{u_{ic}^C} \gamma^\mu\, d_{jd}\, \overline{d_{ke}^C}\, \gamma_\mu\, \nu_f \right] \\
&= k^2\, \epsilon_{ijk}\, \left[V_1^{cd} V_3^{ef} \overline{u_{ic}^C} \gamma^\mu\, u_{jd}\, \overline{d_{ke}^C}\, \gamma_\mu\, e_f + (V_1 V_{UD})^{cd}\, (V_3 V_{EN})^{ef}\, \overline{u_{ic}^C} \gamma^\mu\, d_{jd}\, \overline{d_{ke}^C}\, \gamma_\mu\, \nu_f \right] \tag{5.21}
\end{aligned}
$$

from where we can distinguish two operators, one for charged leptons and the other for neutrinos. Consequently, we have:

$$O(e_\alpha, d_\beta^C) = k^2 \, V_1^{11} V_3^{\beta\alpha} \epsilon_{ijk} \overline{u_i^C} \, \gamma^\mu \, u_j \, \overline{d_{k\beta}^C} \, \gamma_\mu \, e_\alpha \tag{5.22}$$

$$O(\nu_l, d_\alpha, d_\beta^C) = k^2 \, (V_1 V_{UD})^{1\alpha} \, (V_3 V_{EN})^{\beta l} \, \epsilon_{ijk} \overline{u_i^C} \, \gamma^\mu \, d_{j\alpha} \, \overline{d_{k\beta}^C} \, \gamma_\mu \, \nu_l \tag{5.23}$$

Relevant coefficients in these equations can thus be expressed in this way [65, 66]:

$$c(e_\alpha^C, d_\beta) = k^2 \, V_1^{11} V_2^{\alpha\beta} + k^2 \, (V_1 V_{UD})^{1\beta} (V_2 V_{UD}^\dagger)^{\alpha 1} \tag{5.24}$$

$$c(e_\alpha, d_\beta^C) = k^2 V_1^{11} V_3^{\beta\alpha} \tag{5.25}$$

$$c(\nu_l, d_\alpha, d_\beta^C) = k^2 (V_1 V_{UD})^{1\alpha} (V_3 V_{EN})^{\beta l} \tag{5.26}$$

We will show in next few lines what happens when we perform summation over neutrino flavors. We do this because neutrino flavor is not an observable when it comes to proton decay experiments. The explicit summation reads:

$$
\begin{aligned}
c(\nu_l, d_\alpha, d_\beta^C) \cdot c^*(\nu_l, d_\gamma, d_\delta^C) &= k^4 \left[(V_1 V_{UD})^{1\alpha} \, (V_3 V_{EN})^{\beta l} \right] \left[(V_1 V_{UD})^{1\gamma} \, (V_3 V_{EN})^{\delta l} \right]^* \\
&= k^4 \left[(V_1 V_{UD})^{1\alpha} \, (V_3 V_{EN})^{\beta l} \right] \left[(V_3 V_{EN})^{\dagger \, l\delta} \, (V_1 V_{UD})^{\dagger \, \gamma 1} \right] \\
&= k^4 \left[\left(U_C^\dagger U \right)^{1\alpha} \left(D_C^\dagger N \right)^{\beta l} \right] \left[\left(D_C^\dagger N \right)^{\dagger \, l\delta} \left(U_C^\dagger U \right)^{\dagger \, \gamma 1} \right] \\
&= k^4 \left[\left(U_C^\dagger U \right)^{1\alpha} \left(D_C^\dagger N \right)^{\beta l} \right] \left[\left(N^\dagger D_C \right)^{l\delta} \left(U^\dagger U_C \right)^{\gamma 1} \right] \\
&= k^4 \left[\left(U_C^\dagger U \right)^{1\alpha} \left(D_C^\dagger N \right)^{\beta l} \cdot \left(N^\dagger D_C \right)^{l\delta} \left(U^\dagger U_C \right)^{\gamma 1} \right] \\
&= k^4 \left[\left(U_C^\dagger U \right)^{1\alpha} \left(D_C^\dagger N N^\dagger D_C \right)^{\beta\delta} \left(U^\dagger U_C \right)^{\gamma 1} \right] \\
&= k^4 \left[\left(U_C^\dagger U \right)^{1\alpha} \left(D_C^\dagger D_C \right)^{\beta\delta} \left(U^\dagger U_C \right)^{\gamma 1} \right] \tag{5.27}
\end{aligned}
$$

Eq. (5.27) shows that with summation over neutrino flavors, any information associated with neutrino mixing vanishes from proton decay signatures even though it is present at the amplitude level. Note, however, that both left- and right-handed rotations enter proton decay signature predictions.

In order to calculate decay widths for different proton decay channels, we need hadronic matrix elements $\langle PS | O^{B-L} | P \rangle$, where P stands for proton in the initial state and PS stands for pseudoscalar mesons π, K, and η in the final state. In this work, we are not interested in the explicit calculation of hadronic matrix elements as this is the task of lattice QCD. We will simply use relevant results in order to calculate proton decay widths. We refer readers interested in this subject to Refs. [67, 68, 69, 70, 71, 72].

Matrix elements we need, are of the form:

$$\langle PS \,|\, \epsilon_{ijk} \left(\psi_1^{iT} \, C P_{R,L} \, \psi_2^{j} \right) P_L \, \psi_3^{k} \,|\, P \rangle \tag{5.28}$$

where $\psi_{1,2,3}$ denotes three quarks in the process, C is the charge conjugation matrix $(\overline{\psi^c} = \psi^T C, \, C = \gamma_4 \gamma_2)$, and:

$$P_L = \frac{1 - \gamma_5}{2} \tag{5.29}$$

$$P_R = \frac{1 + \gamma_5}{2} \tag{5.30}$$

Now, Eq. (5.28) can be written in a simple form:

$$\langle PS \,|\, (\psi_1 \, \psi_2)_{R,L} \, \psi_{3L} \,|\, P \rangle \tag{5.31}$$

Decay width can be evaluated, in general case of two body decay, using this formula:

$$\Gamma = \frac{S|\vec{p}|}{8\pi m_i} |\mathcal{M}|^2 \tag{5.32}$$

that comes from expression for decay width in general case of n-body decay

$$d\Gamma = |\mathcal{M}|^2 \frac{S}{2m_i} \left(\prod_{k=1}^{n} \frac{d^3 \vec{p}_k}{(2\pi)^3 2E_k} \right) \times (2\pi)^4 \delta^4 \left(p_i - \sum_{k=1}^{n} p_k \right) \tag{5.33}$$

where p_k is the 4-momentum of the kth particle, S is a product of statistical factors, $|\vec{p}|$ is the magnitude of the momentum of either outgoing particle in the parent's rest frame, $\mathcal{M}$ is matrix element, and m_i is the mass of initial particle. Knowing that, we can write decay widths for each of the channels [66]:

$$\Gamma(p \to \pi^0 e_\beta^+) = \frac{m_p}{8\pi} \cdot \left(1 - \left(\frac{m_\pi}{m_p} \right)^2 \right)^2 \cdot A_L^2 \cdot \frac{|\alpha|^2}{2f_\pi^2} (1 + D + F)^2 \left\{ |c(e_\beta, d^C)|^2 + |c(e_\beta^C, d)|^2 \right\}$$

$$= \frac{m_p}{16\pi f_\pi^2} \cdot \left(1 - \left(\frac{m_\pi}{m_p} \right)^2 \right)^2 \cdot A_L^2 \cdot |\alpha|^2 \, (1 + D + F)^2 \, \cdot k^4. \tag{5.34}$$

$$\cdot \left\{ \left| V_1^{11} V_3^{1\beta} \right|^2 + \left| V_1^{11} V_2^{\beta 1} + (V_1 V_{UD})^{11} (V_2 V_{UD}^{\dagger})^{\beta 1} \right|^2 \right\}$$

$$\Gamma(p \to \pi^+ \bar{\nu}) = \frac{m_p}{8\pi} \cdot \left(1 - \left(\frac{m_\pi}{m_p} \right)^2 \right)^2 \cdot A_L^2 \cdot \frac{|\alpha|^2}{f_\pi^2} (1 + D + F)^2 \cdot \sum_{i=1}^{3} |c(\nu_i, d, d^C)|^2$$

$$= \frac{m_p}{8\pi f_\pi^2} \cdot \left(1 - \left(\frac{m_\pi}{m_p} \right)^2 \right)^2 \cdot A_L^2 \cdot |\alpha|^2 \, (1 + D + F)^2 \, \cdot k^4 \cdot \sum_{i=1}^{3} \left| (V_1 V_{UD})^{11} (V_3 V_{EN})^{1i} \right|^2 \tag{5.35}$$

$$\Gamma(p \to K^0 e_\beta^+) = \frac{m_p}{8\pi} \cdot \left(1 - \left(\frac{m_K}{m_p}\right)^2\right)^2 \cdot A_L^2 \cdot \frac{|\alpha|^2}{f_\pi^2} \left(1 + (D - F)\frac{m_p}{m_B}\right)^2 \left\{ |c(e_\beta, s^C)|^2 + |c(e_\beta^C, s)|^2 \right\}$$

$$= \frac{m_p}{8\pi f_\pi^2} \cdot \left(1 - \left(\frac{m_K}{m_p}\right)^2\right)^2 \cdot A_L^2 \cdot |\alpha|^2 \left(1 + (D - F)\frac{m_p}{m_B}\right)^2 \cdot k^4 \cdot$$

$$\cdot \left\{ \left|V_1^{11} V_3^{2\beta}\right|^2 + \left|V_1^{11} V_2^{\beta 2} + (V_1 V_{UD})^{12}(V_2 V_{UD}^\dagger)^{\beta 1}\right|^2 \right\}$$

$$(5.36)$$

$$\Gamma(p \to K^+ \bar\nu) = \frac{m_p}{8\pi} \cdot \left(1 - \left(\frac{m_K}{m_p}\right)^2\right)^2 \cdot A_L^2 \cdot \frac{|\alpha|^2}{f_\pi^2} \sum_{i=1}^3 \left| \frac{2D}{3} \frac{m_p}{m_B} c(\nu_i, d, s^C) + \left[1 + (\frac{D}{3} + F)\frac{m_p}{m_B}\right] c(\nu_i, s, d^C) \right|^2$$

$$= \frac{m_p}{8\pi f_\pi^2} \cdot \left(1 - \left(\frac{m_K}{m_p}\right)^2\right)^2 \cdot A_L^2 \cdot |\alpha|^2 \cdot k^4 \cdot$$

$$\cdot \sum_{i=1}^3 \left| \frac{2D}{3} \frac{m_p}{m_B}(V_1 V_{UD})^{11}(V_3 V_{EN})^{2i} + \left[1 + (\frac{D}{3} + F)\frac{m_p}{m_B}\right] (V_1 V_{UD})^{12}(V_3 V_{EN})^{1i} \right|^2$$

$$(5.37)$$

$$\Gamma(p \to \eta e_\beta^+) = \frac{m_p}{8\pi} \cdot \left(1 - \left(\frac{m_\eta}{m_p}\right)^2\right)^2 \cdot A_L^2 \cdot \frac{|\alpha|^2}{6 f_\pi^2}(1 + D - 3F)^2 \left\{ |c(e_\beta, d^C)|^2 + |c(e_\beta^C, d)|^2 \right\}$$

$$= \frac{m_p}{48\pi f_\pi^2} \cdot \left(1 - \left(\frac{m_\eta}{m_p}\right)^2\right)^2 \cdot A_L^2 \cdot |\alpha|^2 (1 + D - 3F)^2 \cdot k^4 \cdot \qquad (5.38)$$

$$\cdot \left\{ \left|V_1^{11} V_3^{1\beta}\right|^2 + \left|V_1^{11} V_2^{\beta 1} + (V_1 V_{UD})^{11}(V_2 V_{UD}^\dagger)^{\beta 1}\right|^2 \right\},$$

where we explicitly specify flavor dependence of these decay modes.

To introduce matrix elements, we use following identities provided by baryon chiral perturbation theory (BChPT) [61, 71],

$$\langle \pi^0 | (ud)_R u_L | p \rangle = \frac{\alpha}{\sqrt{2}f}(1 + D + F) \qquad (5.39)$$

$$\langle \pi^0 | (ud)_L u_L | p \rangle = \frac{\beta}{\sqrt{2}f}(1 + D + F) \qquad (5.40)$$

$$\langle \pi^+ | (ud)_R d_L | p \rangle = \frac{\alpha}{f}(1 + D + F) \qquad (5.41)$$

$$\langle \pi^+|(ud)_L d_L|p\rangle = \frac{\beta}{f}\left(1 + D + F\right) \tag{5.42}$$

$$\langle K^0|(us)_L u_L|p\rangle = \frac{\beta}{f}\left(1 - (D - F)\frac{m_N}{m_B}\right) \tag{5.43}$$

$$\langle K^0|(us)_R u_L|p\rangle = -\frac{\alpha}{f}\left(1 + (D - F)\frac{m_N}{m_B}\right) \tag{5.44}$$

$$\langle K^+|(us)_R d_L|p\rangle = \frac{\alpha}{f}\frac{2D}{3}\frac{m_N}{m_B} \tag{5.45}$$

$$\langle K^+|(us)_L d_L|p\rangle = \frac{\beta}{f}\frac{2D}{3}\frac{m_N}{m_B} \tag{5.46}$$

$$\langle K^+|(ud)_R s_L|p\rangle = \frac{\alpha}{f}\left(1 + (\frac{D}{3} + F)\frac{m_N}{m_B}\right) \tag{5.47}$$

$$\langle K^+|(ud)_L s_L|p\rangle = \frac{\beta}{f}\left(1 + (\frac{D}{3} + F)\frac{m_N}{m_B}\right) \tag{5.48}$$

$$\langle K^+|(ds)_R u_L|p\rangle = \frac{\alpha}{f}\left(1 + (\frac{D}{3} - F)\frac{m_N}{m_B}\right) \tag{5.49}$$

$$\langle K^+|(ds)_L u_L|p\rangle = -\frac{\beta}{f}\left(1 - (\frac{D}{3} - F)\frac{m_N}{m_B}\right) \tag{5.50}$$

$$\langle \eta|(ud)_R u_L|p\rangle = -\frac{\alpha}{\sqrt{6}f}\left(1 + D - 3F\right) \tag{5.51}$$

$$\langle \eta|(ud)_L u_L|p\rangle = \frac{\beta}{\sqrt{6}f}\left(3 - D + 3F\right) \tag{5.52}$$

where $D = 0.80$ and $F = 0.47$ are low-energy parameters, $m_N = 0.96\,\text{GeV}$, $m_B = 1.15\,\text{GeV}$, and $A_\text{L} = 1.2$ is long-distance coefficient that captures RGE running of relevant operators from electroweak scale to $1\,\text{GeV}$ [71, 73]. It is these equalities and parameters that we will use in our calculations.

Outline of numerical analysis for proton decay induced by gauge bosons

For numerical analysis, we are using a software system Wolfram Mathematica 13.1, where we implement the following expressions for each channel:

- $p \to \pi^0 e_\beta^+$

$$\Gamma(p \to \pi^0 e_\beta^+) = \frac{m_p}{8\pi} \cdot \left(1 - \left(\frac{m_\pi}{m_p}\right)^2\right)^2 \cdot A_L^2 \cdot \frac{\alpha_{\mathrm{GUT}}^2 \, 4\pi^2}{M_{\mathrm{GUT}}^4} \cdot$$
$$\cdot \left\{ \left| A_{SR} \langle \pi^0 | (ud)_R u_L | p \rangle \, c(e_\beta, d^C) \right|^2 + \left| A_{SL} \langle \pi^0 | (ud)_L u_L | p \rangle \, c(e_\beta^C, d) \right|^2 \right\} \tag{5.53}$$

where A_{SR} and A_{SL} are short distance coefficients that capture the running between GUT scale and electroweak scale. These are evaluated using procedure specified in Ref. [74]. The coefficients have the form:

$$c(e_\beta, d^C) = (U_R^\dagger U_L^*)^{11} (D_R^\dagger E_L^*)^{1\beta} \tag{5.54}$$

$$c(e_\beta^C, d) = (U_R^\dagger U_L^*)^{11} (E_R^\dagger D_L^*)^{\beta 1} + (U_R^\dagger D_L^*)^{11} (E_R^\dagger U_L^*)^{\beta 1} \tag{5.55}$$

as explained in detail in Chapter 7. Here we switch to our convention that is defined via:

$$M_U^{\mathrm{diag}} = U_L^\dagger M_U U_R = U_R^T M_U^T U_L^*$$
$$M_D^{\mathrm{diag}} = D_L^\dagger M_D D_R = D_R^T M_D^T D_L^*$$
$$M_E^{\mathrm{diag}} = E_L^\dagger M_E E_R = E_R^T M_E^T E_L^*$$
$$M_N^{\mathrm{diag}} = N^\dagger M_N N^*$$
$$V_{UD} = U_L^T D_L^*$$
$$V_{EN} = N^* \tag{5.56}$$

In our model, we furthermore have that:

$$U_L = D_L \mathrm{diag}(1, e^{i\eta_1}, e^{i\eta_2}) V_{\mathrm{CKM}}^T \mathrm{diag}(e^{i\kappa_1}, e^{i\kappa_2}, e^{i\kappa_3}) = D_L D(\eta) V_{\mathrm{CKM}}^T D(\kappa) \tag{5.57}$$

$$U_R = U_L^* \mathrm{diag}(e^{i\xi_1}, e^{i\xi_2}, e^{i\xi_3}) = U_L^* D(\xi) \tag{5.58}$$

$$E_L = \mathbb{1} \tag{5.59}$$

$$E_R = \mathbb{1} \tag{5.60}$$

$$N = \mathrm{diag}(e^{i\gamma_1}, e^{i\gamma_2}, e^{i\gamma_3}) V_{PMNS}^* \tag{5.61}$$

We will later on explain the origin of these expressions. Hence we can write:

$$U_R^\dagger U_L = (U_L^* D(\xi))^\dagger U_L = D(-\xi) \tag{5.62}$$

$$D_L^\dagger U_L = D(\eta) V_{\mathrm{CKM}}^T D(\kappa) \tag{5.63}$$

$$U_R^\dagger D_L^* = D(-\xi + \kappa) V_{\mathrm{CKM}} D(\eta) \tag{5.64}$$

Now, coefficients $c(e_\beta, d^C)$ and $c(e_\beta^C, d)$ are:

$$c(e_\beta, d^C) = e^{-i\xi_1}(D_R^\dagger)^{1\beta} \tag{5.65}$$

$$c(e_\beta^C, d) = e^{-i\xi_1}(D_L^*)^{\beta 1} + e^{-i\xi_1 + i\kappa_1}(V_{\text{CKM}})^{11}(U_L^*)^{\beta 1} \tag{5.66}$$

where:

$$(U_L^*)^{\beta 1} = (D_L^* D(-\eta)V_{\text{CKM}}^\dagger D(-\kappa))^{\beta 1} \tag{5.67}$$

$$= (D_L^* D(-\eta)V_{\text{CKM}}^\dagger)^{\beta 1}e^{-i\kappa_1} \tag{5.68}$$

These manipulations finally yield:

$$c(e_\beta, d^C) = e^{-i\xi_1}(D_R^\dagger)^{1\beta} \tag{5.69}$$

$$c(e_\beta^C, d) = e^{-i\xi_1}\left[(D_L^*)^{\beta 1} + (V_{\text{CKM}})^{11} \cdot (D_L^* D(-\eta)V_{\text{CKM}}^\dagger)^{\beta 1}\right] \tag{5.70}$$

- $p \to \pi^+ \bar{\nu}$

$$\Gamma(p \to \pi^+ \bar{\nu}) = \frac{m_p}{8\pi} \cdot \left(1 - \left(\frac{m_\pi}{m_p}\right)^2\right)^2 \cdot A_L^2 \cdot \frac{\alpha_{\text{GUT}}^2 \, 4\pi^2}{M_{\text{GUT}}^4} \cdot$$
$$\cdot A_{SR}^2 \, |\langle \pi^+|(ud)_R d_L|p\rangle|^2 \cdot \sum_{i=1}^{3} |\, c(\nu_i, d, d^C)\,|^2 \tag{5.71}$$

where coefficient is of form:

$$\sum_{i=1}^{3} |\, c(\nu_i, d, d^C)\,|^2 = \left|(D(-\xi + \kappa)V_{\text{CKM}}D(\eta))^{11}\right|^2 = \left|(V_{\text{CKM}})^{11}\right|^2 \tag{5.72}$$

- $p \to K^0 e_\beta^+$

$$\Gamma(p \to K^0 e_\beta^+) = \frac{m_p}{8\pi} \cdot \left(1 - \left(\frac{m_K}{m_p}\right)^2\right)^2 \cdot A_L^2 \cdot \frac{\alpha_{\text{GUT}}^2 \, 4\pi^2}{M_{\text{GUT}}^4} \cdot$$
$$\cdot \left\{ \left|A_{SR}\langle K^0|(us)_R u_L|p\rangle \, c(e_\beta, s^C)\right|^2 + \left|A_{SL}\langle K^0|(us)_L u_L|p\rangle \, c(e_\beta^C, s)\right|^2 \right\} \tag{5.73}$$

with coefficients:

$$c(e_\beta, s^C) = e^{-i\xi_1}(D_R^\dagger)^{2\beta} \tag{5.74}$$

$$c(e_\beta^C, s) = e^{-i\xi_1}(D_L^*)^{\beta 2} + (U_R^\dagger D_L^*)^{12} \cdot (E_R^\dagger U_L^*)^{\beta 1} \cdot (D_L^* D(-\eta)V_{\text{CKM}}^\dagger)^{\beta 1}e^{-i\kappa_1}$$

$$= e^{-i\xi_1}\left[(D_L^*)^{\beta 2} + e^{i\eta_1}(V_{\text{CKM}})^{12} \cdot (D_L^* D(-\eta)V_{\text{CKM}}^\dagger)^{\beta 1}\right] \tag{5.75}$$

- $p \to K^+ \bar{\nu}$

$$\Gamma(p \to K^+ \bar{\nu}) = \frac{m_p}{8\pi} \cdot \left(1 - \left(\frac{m_K}{m_p} \right)^2 \right)^2 \cdot A_L^2 \cdot \frac{\alpha_{\mathrm{GUT}}^2 \, 4\pi^2}{M_{\mathrm{GUT}}^4} \cdot$$

$$\cdot \left\{ A_{SR}^2 \left| \langle K^+ | (us)_R d_L | p \rangle \right|^2 \sum_{i=1}^3 \left| c(\nu_i, d, s^C) \right|^2 + A_{SL}^2 \left| \langle K^+ | (ud)_R s_L | p \rangle \right|^2 \sum_{i=1}^3 \left| c(\nu_i, s, d^C) \right|^2 \right\} \tag{5.76}$$

with coefficients:

$$\sum_{i=1}^3 \left| c(\nu_i, d, s^C) \right|^2 = \left| (D(-\xi + \kappa) V_{\mathrm{CKM}} D(\eta))^{11} \right|^2 = \left| (V_{\mathrm{CKM}})^{11} \right|^2 \tag{5.77}$$

$$\sum_{i=1}^3 \left| c(\nu_i, s, d^C) \right|^2 = \left| (V_{\mathrm{CKM}})^{12} \right|^2 \tag{5.78}$$

- $p \to \eta e_\beta^+$

$$\Gamma(p \to \eta e_\beta^+) = \frac{m_p}{8\pi} \cdot \left(1 - \left(\frac{m_\eta}{m_p} \right)^2 \right)^2 \cdot A_L^2 \cdot \frac{\alpha_{\mathrm{GUT}}^2 \, 4\pi^2}{M_{\mathrm{GUT}}^4} \cdot$$

$$\cdot \left\{ \left| A_{SR} \langle \eta | (ud)_R u_L | p \rangle \, c(e_\beta, d^C) \right|^2 + \left| A_{SL} \langle \eta | (ud)_L u_L | p \rangle \, c(e_\beta^C, d) \right|^2 \right\} \tag{5.79}$$

with coefficients:

$$c(e_\beta, d^C) = e^{i\xi_1} (D_R^\dagger)^{1\beta} \tag{5.80}$$

$$c(e_\beta^C, d) = e^{i\xi_1} \left[(D_L^*)^{1\beta} + (V_{\mathrm{CKM}})^{11} \cdot (D_L^* D(-\eta) V_{\mathrm{CKM}}^\dagger)^{\beta 1} \right] \tag{5.81}$$

In the above written expressions, the following common parameters are used: $A_L = 1.2$ [75], $m_p = 0.938272\,\mathrm{GeV}$ [76], $m_K = 0.493677\,\mathrm{GeV}$ [77], $m_{\eta^0} = 0.547862\,\mathrm{GeV}$ [41], $m_{\pi^0} = 0.13497\,\mathrm{GeV}$ [41], $m_{\pi^\pm} = 0.13957\,\mathrm{GeV}$ [41]. For simplicity we use central values for all the parameters.

All other parameters such as $A_{SL}, A_{SR}, \alpha_{\mathrm{GUT}}, M_{\mathrm{GUT}}$ and matrix elements of U_L, U_R, E_L, E_R, N, D_L, and D_R unitary transformations will be taken from the model that we will use to accomplish this correlation study. In addition to this, we will also need Yukawa couplings that will also be taken from our model. Results of this numerical analysis will be presented in Chapter 8.

5.2.2 Proton decay induced by scalar leptoquark

Another possibility for proton to decay is through scalar leptoquarks. The two-body decay processes mediated by scalar leptoquarks are schematically depicted in Fig. 5.2. Scalar leptoquarks can be categorized into singlets, doublets and triplets of $SU(2)$ as they need to simultaneously couple to quarks and leptons. They are clearly always triplets of color for that same reason. Table 5.2 gives all possible quantum numbers for scalar leptoquarks [78].

Table 5.2: Scalar leptoquarks' quantum numbers

LQ	Spin	$SU(3)$	$SU(2)$	$U(1)$	Allowed Coupling
S_1	0	3	1	$-1/3$	$\bar{q}_L^C l_L$ & $\bar{u}_R^C e_R$ & $\bar{q}_L^C q_L$ & $\bar{u}_R^C d_R$
$\tilde{S}_1$	0	3	1	$-4/3$	$\bar{d}_R^C e_R$ & $\bar{u}_R^C u_R$
S_3	0	$\bar{3}$	3	$1/3$	$\bar{q}_L^C l_L$ & $\bar{q}_L^C q_L$
R_2	0	3	2	$7/6$	$\bar{q}_L e_R$ & $\bar{u}_R l_L$
$\tilde{R}_2$	0	3	2	$1/6$	$\bar{d}_R l_L$

As it is previously mentioned, there is only one scalar leptoquark that mediates proton decay in the model that we plan to consider. This state is found in 5-dimensional scalar representation and corresponds to S_1 from Table 5.2. We will refer to it as Λ_3 in what follows.

The specific operators for proton decay through scalar leptoquark can be written as follows [65, 66]:

$$O_H(d_\alpha, e_\beta) = a(d_\alpha, e_\beta)\, u^T L\, C^{-1}\, d_\alpha\, u^T L\, C^{-1}\, e_\beta \tag{5.82}$$

$$O_H(d_\alpha, e_\beta^C) = a(d_\alpha, e_\beta^C)\, u^T L\, C^{-1}\, d_\alpha\, e_\beta^{C\dagger} L\, C^{-1}\, u^{C*} \tag{5.83}$$

$$O_H(d_\alpha^C, e_\beta) = a(d_\alpha^C, e_\beta)\, d_\alpha^{C\dagger} L\, C^{-1}\, u^{C*}\, u^T L\, C^{-1}\, e_\beta \tag{5.84}$$

$$O_H(d_\alpha^C, e_\beta^C) = a(d_\alpha^C, e_\beta^C)\, d_\alpha^{C\dagger} L\, C^{-1}\, u^{C*}\, e_\beta^{C\dagger} L\, C^{-1}\, u^{C*} \tag{5.85}$$

$$O_H(d_\alpha, d_\beta, \nu_i) = a(d_\alpha, d_\beta, \nu_i)\, u^T L\, C^{-1}\, d_\alpha\, d_\beta^T L\, C^{-1}\, \nu_i \tag{5.86}$$

$$O_H(d_\alpha, d_\beta^C, \nu_i) = a(d_\alpha, d_\beta^C, \nu_i)\, d_\beta^{C\dagger} L\, C^{-1}\, u^{C*}\, d_\alpha^T L\, C^{-1}\, \nu_i \tag{5.87}$$

where C is charge conjugation operator and $L = (1 - \gamma_5)/2$. Coefficients in aforementioned operators are:

$$a(d_\alpha, e_\beta) = \frac{1}{M_{\Lambda_3}^2}(U^T(\underline{A} + \underline{A}^T)D)_{1\alpha}(U^T\underline{C}E)_{1\beta} \tag{5.88}$$

$$a(d_\alpha, e_\beta^C) = \frac{1}{M_{\Lambda_3}^2}(U^T(\underline{A} + \underline{A}^T)D)_{1\alpha}(E_C^\dagger\underline{B}^\dagger U_C^*)_{\beta 1} \tag{5.89}$$

$$a(d_\alpha^C, e_\beta) = \frac{1}{M_{\Lambda_3}^2}(D_C^\dagger\underline{D}^\dagger U_C^*)_{\alpha 1}(U^T\underline{C}E)_{1\beta} \tag{5.90}$$

$$a(d_\alpha^C, e_\beta^C) = \frac{1}{M_{\Lambda_3}^2}(D_C^\dagger\underline{D}^\dagger U_C^*)_{\alpha 1}(E_C^\dagger\underline{B}^\dagger U_C^*)_{\beta 1} \tag{5.91}$$

$$a(d_\alpha, d_\beta, \nu_i) = \frac{1}{M_{\Lambda_3}^2}(U^T(\underline{A} + \underline{A}^T)D)_{1\alpha}(D^T\underline{C}N)_{\beta i} \tag{5.92}$$

$$a(d_\alpha, d_\beta^C, \nu_i) = \frac{1}{M_{\Lambda_3}^2}(D_C^\dagger\underline{D}^\dagger U_C^*)_{\beta 1}(D^T\underline{C}N)_{\alpha i} \tag{5.93}$$

where M_{Λ_3} is the mass of scalar leptoquark, indices α and β are flavor indices that can take values of 1 and 2, as well as $i = 1, 2, 3$. Capital letters represent specific matrices, where $\underline{A}$, $\underline{B}$, $\underline{C}$, and $\underline{D}$ are linear combinations of the Yukawa couplings, while U, U_C, D, D_C, E, E_C, and N are unitary matrices [66]. In

our model, we have:

$$\underline{A} = \underline{B} \to Y^u = \frac{M_U}{8v_5} \tag{5.94}$$

$$\underline{C} = \underline{D} \to \frac{1}{\sqrt{2}} Y^d = \frac{M_E}{\sqrt{2}v_5} \tag{5.95}$$

$$U \to U_L^* \tag{5.96}$$

$$E \to E_L^* = \mathbb{1} \tag{5.97}$$

$$E_C \to E_R = \mathbb{1} \tag{5.98}$$

$$D \to D_L^* \tag{5.99}$$

$$N \to N^* \tag{5.100}$$

$$D_C \to D_R \tag{5.101}$$

$$U_C \to U_R \tag{5.102}$$

$$\tag{5.103}$$

We will furthermore use the following expressions from previous subsection:

$$D_L^\dagger U_L = D(\eta) V_{\text{CKM}}^T D(\kappa) \tag{5.104}$$

$$D(\eta) = \text{diag}(1, e^{i\eta_1}, e^{i\eta_2}) \tag{5.105}$$

$$U_R^* D_L^* = D(-\xi + \kappa) V_{\text{CKM}} D(\eta) \tag{5.106}$$

$$U_L = D_L D(\eta) V_{\text{CKM}}^T D(\kappa) \tag{5.107}$$

All these expressions are needed to extract proton decay widths for our numerical analyses.

- $a(d_\alpha, e_\beta)$

$$
\begin{aligned}
a(d_\alpha, e_\beta) &= \frac{1}{M_{\Lambda_3}^2} (U^T(\underline{A} + \underline{A}^T)D)_{1\alpha} (U^T \underline{C} E)_{1\beta} = \frac{1}{M_{\Lambda_3}^2} \left[U_L^\dagger \frac{M_U}{2v_5} D_L^* \right]_{1\alpha} \left[U_L^\dagger \frac{M_E}{\sqrt{2}v_5} E_L^* \right]_{1\beta} \\
&= \frac{m_\beta^E}{M_{\Lambda_3}^2 2^{\frac{3}{2}} v_5^2} \cdot \left[M_U^{diag} U_R^\dagger D_L^* \right]_{1\alpha} \left[U_L^\dagger \right]_{1\beta} = \frac{m_1^U m_\beta^E}{M_{\Lambda_3}^2 2^{\frac{3}{2}} v_5^2} \cdot \left[U_R^\dagger D_L^* \right]_{1\alpha} \left[U_L^\dagger \right]_{1\beta} \\
&= \frac{m_1^U m_\beta^E}{M_{\Lambda_3}^2 2^{\frac{3}{2}} v_5^2} \cdot [D(-\xi + \kappa) V_{\text{CKM}} D(\eta)]_{1\alpha} \left[U_L^\dagger \right]_{1\beta} \\
&= \frac{m_1^U m_\beta^E}{M_{\Lambda_3}^2 2^{\frac{3}{2}} v_5^2} \cdot [D(-\xi + \kappa) V_{\text{CKM}} D(\eta)]_{1\alpha} \left[D(-\kappa) V_{\text{CKM}}^* D(-\eta) D_L^\dagger \right]_{1\beta} \\
&= \frac{m_1^U m_\beta^E}{M_{\Lambda_3}^2 2^{\frac{3}{2}} v_5^2} \cdot e^{-i\xi_1} \cdot [V_{\text{CKM}} D(\eta)]_{1\alpha} \left[V_{\text{CKM}}^* D(-\eta) D_L^\dagger \right]_{1\beta}
\end{aligned}
\tag{5.108}
$$

- $a(d_\alpha, e_\beta^C)$

73

$$a(d_\alpha, e_\beta^C) = \frac{1}{M_{\Lambda_3}^2}(U^T(\underline{A} + \underline{A}^T)D)_{1\alpha}(E_C^\dagger \underline{B}^\dagger U_C^*)_{\beta 1}$$

$$= \frac{1}{M_{\Lambda_3}^2}\left[U_L^\dagger \frac{M_U}{2v_5}D_L^*\right]_{1\alpha}\left[E_R^\dagger \frac{M_U^\dagger}{4v_5}U_C^*\right]_{\beta 1}$$

$$= \frac{1}{M_{\Lambda_3}^2 2^3 v_5^2}\left[M_U^{diag}U_R^\dagger D_L^*\right]_{1\alpha}\left[M_U^\dagger U_R^*\right]_{\beta 1}$$

$$= \frac{1}{M_{\Lambda_3}^2 2^3 v_5^2}\left[M_U^{diag}U_R^\dagger D_L^*\right]_{1\alpha}[M_U^* U_R^*]_{\beta 1}$$

$$= \frac{m_1^U}{M_{\Lambda_3}^2 2^3 v_5^2}\left[U_R^\dagger D_L^*\right]_{1\alpha}\left[U_L^* M_U^{diag}U_R U_R^*\right]_{\beta 1}$$

$$= \frac{m_1^U}{M_{\Lambda_3}^2 2^3 v_5^2}\left[U_R^\dagger D_L^*\right]_{1\alpha}\left[U_L^* M_U^{diag}\right]_{1\beta}$$

$$= \frac{m_1^{U^2}}{M_{\Lambda_3}^2 2^3 v_5^2}\left[U_R^\dagger D_L^*\right]_{1\alpha}\left[U_L^*\right]_{1\beta}$$

$$= \frac{m_1^U}{m_\beta^E}\cdot\frac{a(d_\alpha, e_\beta)}{2^{3/2}} \tag{5.109}$$

The useful and insightful result here is the relation between the two coefficients in Eqs. (5.108) and (5.109) that reads:

$$a(d_\alpha, e_\beta^C) = \frac{m_1^U}{m_\beta^E}\cdot\frac{a(d_\alpha, e_\beta)}{2^{3/2}} \tag{5.110}$$

- $a(d_\alpha^C, e_\beta)$

$$a(d_\alpha^C, e_\beta) = \frac{1}{M_{\Lambda_3}^2}(D_C^\dagger \underline{D}^\dagger U_C^*)_{\alpha 1}(U^T \underline{C} E)_{1\beta}$$

$$= \frac{1}{M_{\Lambda_3}^2}\left[D_C^\dagger \frac{M_E}{\sqrt{2}v_5}U_C^*\right]_{\alpha 1}\left[U_L^\dagger \frac{M_E}{\sqrt{2}v_5}E_L^*\right]_{1\beta}$$

$$= \frac{m_\beta^E}{M_{\Lambda_3}^2 \sqrt{2}v_5}\left[D_R^\dagger \frac{M_E}{\sqrt{2}v_5}U_R^*\right]_{\alpha 1}\left[U_L^\dagger\right]_{\beta 1}$$

$$= \frac{m_\beta^E}{M_{\Lambda_3}^2 \sqrt{2}v_5}\left[D_R^\dagger \frac{M_E}{\sqrt{2}v_5}D_L D(\eta)V_{\text{CKM}}^T D(\kappa - \xi)\right]_{\alpha 1}\left[U_L^\dagger\right]_{1\beta}$$

$$= \frac{m_\beta^E}{M_{\Lambda_3}^2 2v_5^2}\left[D_R^\dagger M_E D_L D(\eta)V_{\text{CKM}}^T D(\kappa - \xi)\right]_{\alpha 1}\left[U_L^\dagger\right]_{1\beta}$$

$$= \frac{m_\beta^E}{M_{\Lambda_3}^2 2v_5^2}\cdot e^{-i\xi_1}\left[D_R^\dagger M_E D_L D(\eta)V_{\text{CKM}}^T\right]_{\alpha 1}\left[V_{\text{CKM}}^* D(-\eta)D_L^\dagger\right]_{1\beta} \tag{5.111}$$

from where we can see that this $a(d_\alpha^C, e_\beta)$ coefficient does not depend on $D(\kappa)$.

- $a(d_\alpha^C, e_\beta^C)$

$$a(d_\alpha^C, e_\beta^C) = \frac{1}{M_{\Lambda_3}^2}(D_C^\dagger \underline{D}^\dagger U_C^*)_{\alpha 1}(E_C^\dagger \underline{B}^\dagger U_C^*)_{\beta 1}$$

$$= \frac{m_1^U e^{i(\kappa_1-\xi_1)}}{M_{\Lambda_3}^2 2^{5/2} v_5^2}\left[D_R^\dagger M_E D_L D(\eta)V_{CKM}^T\right]_{\alpha 1}\left[U_L^\dagger\right]_{1\beta}$$

$$= \frac{m_1^U e^{-i\xi_1}}{M_{\Lambda_3}^2 2^{5/2} v_5^2}\left[D_R^\dagger M_E D_L D(\eta)V_{CKM}^T\right]_{\alpha 1}\left[V_{CKM}^* D(-\eta)D_L^\dagger\right]_{1\beta}$$

$$(5.112)$$

from where we can see that this $a(d_\alpha^C, e_\beta^C)$ coefficient does not depend on $D(\kappa)$. And, again, the important and insightful result here is the relation between the two coefficients:

$$a(d_\alpha^C, e_\beta^C) = \frac{m_1^U}{m_\beta^E} \cdot \frac{a(d_\alpha^C, e_\beta)}{2^{3/2}} \tag{5.113}$$

- $a(d_\alpha, d_\beta, \nu_i)$

$$a(d_\alpha, d_\beta, \nu_i) = \frac{1}{M_{\Lambda_3}^2}(U^T(\underline{A}+\underline{A}^T)D)_{1\alpha}(D^T\underline{C}N)_{\beta i} = \frac{1}{M_{\Lambda_3}^2}\left[U_L^\dagger \frac{M_U}{2v_5}D_L^*\right]_{1\alpha}\left[D^T\frac{M_E}{\sqrt{2}v_5}N\right]_{\beta i}$$

$$= \frac{1}{M_{\Lambda_3}^2 2^{3/2} v_5^2}\left[M_U^{diag}U_R^\dagger D_L^*\right]_{1\alpha}\left[D_L^\dagger M_E N^*\right]_{\beta i}$$

$$= \frac{m_1^U e^{-i\xi_1+i\kappa_1}}{M_{\Lambda_3}^2 2^{3/2} v_5^2}\left[V_{CKM}D(\eta)\right]_{1\alpha}\left[D_L^\dagger M_E N^*\right]_{\beta i} \tag{5.114}$$

and the last one:

- $a(d_\alpha, d_\beta^C, \nu_i)$

$$a(d_\alpha, d_\beta^C, \nu_i) = \frac{1}{M_{\Lambda_3}^2}(D_C^\dagger \underline{D}^\dagger U_C^*)_{\beta 1}(D^T\underline{C}N)_{\alpha i} = \frac{e^{i\kappa_1-i\xi_1}}{M_{\Lambda_3}^2 2 v_5^2}\left[D_R^\dagger M_E D_L D(\eta)V_{CKM}^T\right]_{\beta 1}\left[D_L^\dagger M_E N^*\right]_{\alpha i}$$

$$(5.115)$$

In order to find decay width, for some decay channels we will need:

$$\sum_i a(d_\alpha, d_\beta, \nu_i)a^*(d_\gamma, d_\delta, \nu_i) = \frac{m_1^{U2}}{M_{\Lambda_3}^4 2^3 v_5^4} \cdot \left[V_{CKM}D(\eta)\right]_{1\alpha} \cdot$$

$$\cdot \left[V_{CKM}^* D(-\eta)\right]_{1\gamma}\left[D_L^\dagger M_E^2 D_L\right]_{\beta\delta} \tag{5.116}$$

$$\sum_i a(d_\alpha, d_\beta^C, \nu_i)a^*(d_\gamma, d_\delta^C, \nu_i) = \frac{1}{M_{\Lambda_3}^4 2^2 v_5^4} \cdot \left[D_R^\dagger M_E D_L D(\eta)V_{CKM}^T\right]_{\beta 1} \cdot$$

$$\cdot \left[D_R^T M_E D_L^* D(-\eta)V_{CKM}^\dagger\right]_{\delta 1}\left[D_L^\dagger M_E^2 D_L\right]_{\alpha\gamma} \tag{5.117}$$

$$\sum_i a(d_\alpha, d_\beta, \nu_i)a^*(d_\gamma, d_\delta^C, \nu_i) = \frac{m_1^U}{M_{\Lambda_3}^4 2^{5/2} v_5^4} \cdot \left[D_L^\dagger M_E^2 D_L\right]_{\beta\gamma} \cdot$$

$$\cdot \left[V_{CKM}D(\eta)\right]_{1\alpha}\left[D_R^T M_E D_L^* D(-\eta)V_{CKM}^\dagger\right]_{\delta 1} \tag{5.118}$$

After derivation of all the coefficients needed for expressions for decay widths, we can provide decay widths formulae for each channel:

- $p \to \pi^+ \bar\nu$

$$\Gamma(p \to \pi^+ \bar\nu_i) = \frac{(m_p^2 - m_{\pi^+}^2)^2}{32\pi m_p^3} \cdot A_L^2 \cdot \left| A_{SR} C_{RL}^{\nu_i} \langle \pi^+ | (du)_R d_L | p \rangle + A_{SL} C_{LL}^{\nu_i} \langle \pi^+ | (du)_L d_L | p \rangle \right|^2 \quad (5.119)$$

where, again, A_L is a parameter for renormalization from electroweak scale to $1\,\mathrm{GeV}$. We furthermore use the following notation $C_{RL}^{\nu_i} = a(d, d^C, \nu_i) \equiv a(d_1, d_1^C, \nu_i)$ and $C_{LL}^{\nu_i} = a(d, d, \nu_i) \equiv a(d_1, d_1, \nu_i)$ and rely on the identity:

$$\langle \pi^+ | (du)_\Gamma d_L | p \rangle = \sqrt{2} \langle \pi^0 | (du)_\Gamma u_L | p \rangle \text{ with } \Gamma = L, R \text{ [71]} \quad (5.120)$$

In Eqs. (5.116) through (5.118) we have given the most general expressions for products of different coefficients. We will also need the following specific contractions with $\alpha = \beta = \gamma = \delta = 1$ when we discuss proton decays with anti-neutrinos in the final state:

$$\sum_i a(d_1, d_1, \nu_i) a^*(d_1, d_1, \nu_i) = \frac{m_1^{U^2}}{M_{\Lambda_3}^4 2^3 v_5^4} \cdot \left| [V_{\mathrm{CKM}}]_{11} \right|^2 \left[D_L^\dagger M_E^2 D_L \right]_{11}$$

$$\sum_i a(d_1, d_1^C, \nu_i) a^*(d_1, d_1^C, \nu_i) = \frac{1}{M_{\Lambda_3}^4 2^2 v_5^4} \cdot \left| \left[D_R^\dagger M_E D_L D(\eta) V_{\mathrm{CKM}}^\dagger \right]_{11} \right|^2 \cdot \left[D_L^\dagger M_E^2 D_L \right]_{11}$$

$$\sum_i a(d_1, d_1, \nu_i) a^*(d_1, d_1^C, \nu_i) = \frac{m_1^U}{M_{\Lambda_3}^4 2^{5/2} v_5^4} \cdot \left[D_L^\dagger M_E^2 D_L \right]_{11} \cdot \left[V_{\mathrm{CKM}} \right]_{11} \left[D_R^T M_E D_L^* D(-\eta) V_{\mathrm{CKM}}^\dagger \right]_{11}$$

Common matrix element for all three above written expressions is $\left[D_L^\dagger M_E^2 D_L \right]_{11}$. It can be developed in the following manner:

$$\left[D_L^\dagger M_E^2 D_L \right]_{11} = [D_L^\dagger]_{1i} m_i^{E^2} [D_L]_{i1} = m_i^{E^2} \left| [D_L]_{i1} \right|^2 = m_e^2 \left| [D_L]_{11} \right|^2 + m_\mu^2 \left| [D_L]_{21} \right|^2 + m_\tau^2 \left| [D_L]_{31} \right|^2 \quad (5.121)$$

Now the final expression for decay width $p \to \pi^+ \bar\nu$ is of this form:

$$\Gamma(p \to \pi^+ \bar\nu) = \frac{(m_p^2 - m_{\pi^+}^2)^2}{32\pi m_p^3} \cdot A_L^2 \cdot \frac{\left[D_L^\dagger M_E^2 D_L \right]_{11}}{M_{\Lambda_3}^4 2^2 v_5^4} \cdot$$

$$\cdot \left\{ A_{SR}^2 \langle \pi^+ | (du)_R d_L | p \rangle^2 \cdot \left| \left[D_R^\dagger M_E D_L D(\eta) V_{\mathrm{CKM}}^\dagger \right]_{11} \right|^2 + \right.$$

$$+ A_{SL}^2 \langle \pi^+ | (du)_L d_L | p \rangle^2 \cdot \frac{m_1^{U^2}}{2} \left| [V_{\mathrm{CKM}}]_{11} \right|^2 + A_{SR} A_{SL} \langle \pi^+ | (du)_R d_L | p \rangle \langle \pi^+ | (du)_L d_L | p \rangle \cdot \frac{m_1^U}{\sqrt{2}} \cdot$$

$$\left. \cdot 2 \, \mathbb{Re} \left(\left[V_{\mathrm{CKM}} \right]_{11} \left[D_R^T M_E D_L^* D(-\eta) V_{\mathrm{CKM}}^\dagger \right]_{11} \right) \right\} \quad (5.122)$$

We will not write explicit expression for decay width of $p \to K^+ \bar\nu$ because it is quite lengthy. Since it

relies on Eqs. (5.116)–(5.118) it is analogous to the form of $\Gamma(p \to \pi^+ \overline{\nu})$.

- $p \to \pi^0 e_i^+$

For this channel, we need the following matrix elements:

$$\langle \pi^0 | (du)_R u_L | p \rangle = \frac{\alpha}{\sqrt{2}f} \left(1 + D + F \right) \tag{5.123}$$

$$\langle \pi^0 | (du)_L d_L | p \rangle = \frac{\beta}{\sqrt{2}f} \left(1 + D + F \right) \tag{5.124}$$

where D, F, α and β are, once again, parameters in chiral Lagrangian [79, 71, 69].

Relevant Lagrangian for this process is [66]:

$$\mathcal{L} \propto C_{RL}^{e_i} O_{RL}^{ei} + C_{LR}^{e_i} O_{LR}^{e_i} + C_{LL}^{e_i} O_{LL}^{e_i} + C_{RR}^{e_i} O_{RR}^{e_i} \tag{5.125}$$

where operators are [66]:

$$O_{RL}^{e_i} = \varepsilon_{abc} \overline{(d_{Ra})^C} \, u_{Rb} \, \overline{(u_{Lc})^C} \, e_{iL} \tag{5.126}$$

$$O_{LR}^{e_i} = \varepsilon_{abc} \overline{(d_{La})^C} \, u_{Lb} \, \overline{(u_{Rc})^C} \, e_{iR} \tag{5.127}$$

$$O_{LL}^{e_i} = \varepsilon_{abc} \overline{(d_{La})^C} \, u_{Lb} \, \overline{(u_{Lc})^C} \, e_{iL} \tag{5.128}$$

$$O_{RR}^{e_i} = \varepsilon_{abc} \overline{(d_{Ra})^C} \, u_{Rb} \, \overline{(u_{Rc})^C} \, e_{iR} \tag{5.129}$$

and coefficients [66] can be expressed with chiral Lagrangian parameters:

$$C_{RL}^{'e_i} = \alpha C_{RL}^{e_i} \tag{5.130}$$

$$C_{LL}^{'e_i} = \beta C_{LL}^{e_i} \tag{5.131}$$

$$C_{LR}^{'e_i} = \alpha C_{LR}^{e_i} \tag{5.132}$$

$$C_{RR}^{'e_i} = \beta C_{RR}^{e_i} \tag{5.133}$$

Now, we will make a relation in notation between our coefficients and the ones above mentioned:

$$a(d_\alpha^C, e_\beta)\Big|_{\alpha=1} = C_{RL}^{e_\beta} \tag{5.134}$$

$$a(d_\alpha, e_\beta^C)\Big|_{\alpha=1} = C_{LR}^{e_\beta} \tag{5.135}$$

$$a(d_\alpha, e_\beta)\Big|_{\alpha=1} = C_{LL}^{e_\beta} \tag{5.136}$$

$$a(d_\alpha^C, e_\beta^C)\Big|_{\alpha=1} = C_{RR}^{e_\beta} \tag{5.137}$$

Previously, we have derived the relation between these coefficients in Eqs. (5.110) and (5.113):

$$a(d_\alpha^C, e_\beta^C) = H_\beta a(d_\alpha^C, e_\beta) \tag{5.138}$$

$$a(d_\alpha, e_\beta^C) = H_\beta a(d_\alpha, e_\beta) \tag{5.139}$$

$$H_\beta = \frac{m_1^U}{m_\beta^E} \cdot \frac{1}{2^{3/2}} \tag{5.140}$$

The decay width for this process now can be derived in the following way:

$$
\Gamma(p \to e_\beta^+ \pi^0) = \frac{(m_p^2 - m_{\pi^0}^2)^2}{32\pi m_p^3} \cdot \frac{1}{2f^2} \cdot \left\{ \left| \alpha\, a(d^C, e_\beta) + \beta\, a(d, e_\beta) \right|^2 + \right.
$$

$$
+ \left| \alpha\, a(d, e_\beta^C) + \beta\, a(d^C, e_\beta^C) \right|^2 \cdot (1 + D + F)^2
$$

$$
= \frac{(m_p^2 - m_{\pi^0}^2)^2}{32\pi m_p^3} \cdot A_L^2 \cdot \left\{ \left| a(d^C, e_\beta) A_{SR} \langle \pi^0 | (du)_R u_L | p \rangle + \right. \right.
$$

$$
+\ a(d, e_\beta) A_{SL} \langle \pi^0 | (du)_L u_L | p \rangle \Big|^2 + \Big| a(d, e_\beta^C) A_{SL} \langle \pi^0 | (du)_L u_L | p \rangle +
$$

$$
\left. \left. +\ a(d^C, e_\beta^C) A_{SR} \langle \pi^0 | (du)_R u_L | p \rangle \Big|^2 \right\} \right. \tag{5.141}
$$

- $p \to \eta^0 e_i^+$

$$
\Gamma(p \to \eta^0 e_i^+) = \frac{(m_p^2 - m_{\eta^0}^2)^2}{32\pi f^2 m_p^3} \cdot \frac{3}{2} \cdot \left\{ \left| C_{LL}^{'e_i}(1 - \frac{D}{3} + F) + C_{RL}^{'e_i}(-\frac{1}{3} - \frac{D}{3} + F) \right|^2 + \right.
$$

$$
\left. + \left| C_{RR}^{'e_i}(1 - \frac{D}{3} + F) + C_{LR}^{'e_i}(-\frac{1}{3} - \frac{D}{3} + F) \right|^2 \right\}
$$

$$
= \frac{(m_p^2 - m_{\eta^0}^2)^2}{32\pi f^2 m_p^3} \cdot \frac{3}{2} \cdot
$$

$$
\cdot \left\{ \left| \beta C_{LL}^{'e_i}(3 - D + 3F) \cdot \frac{1}{3} + \alpha C_{RL}^{'e_i}(1 + D - 3F) \cdot (-\frac{1}{3}) \right|^2 + \right.
$$

$$
\left. + \left| \beta C_{RR}^{'e_i}(3 - D + 3F) \cdot \frac{1}{3} + \alpha C_{LR}^{'e_i}(1 + D - 3F) \cdot (-\frac{1}{3}) \right|^2 \right\}
$$

$$
= \frac{(m_p^2 - m_{\eta^0}^2)^2}{32\pi m_p^3} \cdot \left\{ \left| C_{LL}^{e_i} \langle \eta | (ud)_L u_L | p \rangle + C_{RL}^{e_i} \langle \eta | (ud)_R u_L | p \rangle \right|^2 + \right.
$$

$$
\left. + \left| C_{RR}^{e_i} \langle \eta | (ud)_L u_L | p \rangle + C_{LR}^{e_i} \langle \eta | (ud)_R u_L | p \rangle \right|^2 \right\} \tag{5.142}
$$

We have used relations for matrix elements:

$$
\langle \eta | (ud)_R u_L | p \rangle = -\frac{\alpha}{\sqrt{2}f}(1 + D - 3F) \quad \text{and} \quad \langle \eta | (ud)_L u_L | p \rangle = \frac{\beta}{\sqrt{2}f}(3 - D + 3F) \tag{5.143}
$$

- $p \to K^0 e_i^+$

$$\Gamma(p \to K^0 e_i^+) = \frac{(m_p^2 - m_K^2)^2}{32\pi f^2 m_p^3} \cdot \left\{ \frac{1}{2} \left| -\tilde{C}_{RL}^{\prime e_i} + \tilde{C}_{LL}^{\prime e_i} + \tilde{C}_{LR}^{\prime e_i} - \tilde{C}_{RR}^{\prime e_i} - \right. \right.$$

$$\left. - \frac{m_p}{m_B}(\tilde{C}_{RL}^{\prime e_i} + \tilde{C}_{LL}^{\prime e_i} - \tilde{C}_{LR}^{\prime e_i} - \tilde{C}_{RR}^{\prime e_i})(D-F) \right|^2 +$$

$$\left. + \frac{1}{2} \left| -\tilde{C}_{RL}^{\prime e_i} + \tilde{C}_{LL}^{\prime e_i} - \tilde{C}_{LR}^{\prime e_i} + \tilde{C}_{RR}^{\prime e_i} - \frac{m_p}{m_B}(\tilde{C}_{RL}^{\prime e_i} + \tilde{C}_{LL}^{\prime e_i} + \tilde{C}_{LR}^{\prime e_i} + \tilde{C}_{RR}^{\prime e_i})(D-F) \right|^2 \right\}$$

$$= \frac{(m_p^2 - m_K^2)^2}{32\pi f^2 m_p^3} \cdot \left\{ \frac{1}{2} \left| \tilde{C}_{RL}^{\prime e_i} \left[-1 - \frac{m_p}{m_B}(D-F) \right] + \right. \right.$$

$$+ \tilde{C}_{LL}^{\prime e_i} \left[1 - \frac{m_p}{m_B}(D-F) \right] + \tilde{C}_{LR}^{\prime e_i} \left[1 + \frac{m_p}{m_B}(D-F) \right] +$$

$$\left. + \tilde{C}_{RR}^{\prime e_i} \left[-1 + \frac{m_p}{m_B}(D-F) \right] \right|^2 + \frac{1}{2} \left| \tilde{C}_{RL}^{\prime e_i} \left[-1 - \frac{m_p}{m_B}(D-F) \right] + \right.$$

$$+ \tilde{C}_{LL}^{\prime e_i} \left[1 - \frac{m_p}{m_B}(D-F) \right] + \tilde{C}_{LR}^{\prime e_i} \left[-1 - \frac{m_p}{m_B}(D-F) \right] +$$

$$\left. \left. + \tilde{C}_{RR}^{\prime e_i} \left[1 - \frac{m_p}{m_B}(D-F) \right] \right|^2 \right\} \tag{5.144}$$

Knowing relations between coefficients [66] and chiral Lagrangian parameters α and β:

$$C_{RL}^{\prime e_i} = \alpha C_{RL}^{e_i} \tag{5.145}$$

$$C_{LL}^{\prime e_i} = \beta C_{LL}^{e_i} \tag{5.146}$$

$$C_{LR}^{\prime e_i} = \alpha C_{LR}^{e_i} \tag{5.147}$$

$$C_{RR}^{\prime e_i} = \beta C_{RR}^{e_i} \tag{5.148}$$

we can now write:

$$\Gamma(p \to K^0 e_i^+) = \frac{(m_p^2 - m_K^2)^2}{32\pi f^2 m_p^3} \cdot \left\{ \frac{1}{2} \left| \alpha \tilde{C}_{RL}^{e_i} \left[-1 - \frac{m_p}{m_B}(D-F) \right] + \right. \right.$$

$$+ \beta \tilde{C}_{LL}^{e_i} \left[1 - \frac{m_p}{m_B}(D-F) \right] + \alpha \tilde{C}_{LR}^{e_i} \left[1 + \frac{m_p}{m_B}(D-F) \right] +$$

$$\left. + \beta \tilde{C}_{RR}^{e_i} \left[-1 + \frac{m_p}{m_B}(D-F) \right] \right|^2 + \frac{1}{2} \left| \alpha \tilde{C}_{RL}^{e_i} \left[-1 - \frac{m_p}{m_B}(D-F) \right] + \right.$$

$$+ \beta \tilde{C}_{LL}^{e_i} \left[1 - \frac{m_p}{m_B}(D-F) \right] + \alpha \tilde{C}_{LR}^{e_i} \left[-1 - \frac{m_p}{m_B}(D-F) \right] +$$

$$\left. \left. + \beta \tilde{C}_{RR}^{e_i} \left[1 - \frac{m_p}{m_B}(D-F) \right] \right|^2 \right\} \tag{5.149}$$

Having for matrix elements the following relations:

$$\langle K^0 | (us)_R u_L | p \rangle = -\frac{\alpha}{f} \left(1 + (D-F)\frac{m_p}{m_B} \right) \tag{5.150}$$

$$\langle K^0 | (us)_L u_L | p \rangle = \frac{\beta}{f} \left(1 - (D-F)\frac{m_p}{m_B} \right) \tag{5.151}$$

we can write:

$$
\begin{aligned}
\Gamma(p \to K^0 e_i^+) = \frac{(m_p^2 - m_K^2)^2}{64\pi f^2 m_p^3} \cdot &\left\{ \left| \tilde{C}_{RL}^{e_i} \langle K^0|(us)_R\, u_L|p\rangle + \tilde{C}_{LL}^{e_i} \langle K^0|(us)_L\, u_L|p\rangle + \right. \right. \\
& \left. + (-1)\tilde{C}_{LR}^{e_i} \langle K^0|(us)_R\, u_L|p\rangle + (-1)\tilde{C}_{RR}^{e_i} \langle K^0|(us)_L\, u_L|p\rangle \right|^2 + \\
& + \left| \tilde{C}_{RL}^{e_i} \langle K^0|(us)_R\, u_L|p\rangle + \tilde{C}_{LL}^{e_i} \langle K^0|(us)_L\, u_L|p\rangle + \right. \\
& \left. \left. + \tilde{C}_{LR}^{e_i} \langle K^0|(us)_R\, u_L|p\rangle + \tilde{C}_{RR}^{e_i} \langle K^0|(us)_L\, u_L|p\rangle \right|^2 \right\}
\end{aligned}
\tag{5.152}
$$

Before we conclude this section, we stress that all the relevant parameters that appear in decay widths for two-body proton decays via gauge and scalar mediation are known within the model that will be considered in Chapter 7 except for two particular phases.

Chapter 6

Experiments

> You're never given a dream
> without also being given the
> power to make it true.

<div align="right">

Richard Bach
</div>

In previous chapters, we have discussed proton decay within a specific grand unified model that is based on $SU(5)$ gauge group. The two-body decay processes in question occur with the exchange of either scalar leptoquark or gauge bosons via dim-6 operators. The associated proton lifetime for gauge mediation can be easily estimated on dimensional grounds to be:

$$\tau_P \propto \frac{M_G^4}{\alpha_G^2 m_p^5} \tag{6.1}$$

where M_G is mass of gauge boson, α_G is gauge coupling constant at that scale and m_p is proton mass. The scalar mediated proton decay, on the other hand, is estimated to be:

$$\tau_P \propto \frac{M_T^4}{Y^4 m_p^5} \tag{6.2}$$

where M_T is mass of scalar leptoquark and Y is a generic coupling constant at that scale. Again, this can be deduced from the diagrams presented in Figs. 5.1 and 5.2.

Within a well define GUT theory, partial proton lifetimes should be, in principle, completely calculable. This implies that M_G, M_T, α_G, and Y could be indirectly observed through these rare processes. It is expected that M_G and M_T are associated with very high energy scales that cannot be accessed with conventional methods. The only hope to probe these scales is with dedicated proton decay experiments. Experimental searches for these illusive processes have started decades ago with projects and experiments such as Kolar Gold Mine [80], NUSEX [81], Homestake [82], Frejus [83], Soudan [84], IMB [85] etc. Nice feature of these experiments is their direct connection to neutrino physics. Nowdays, the experiment with

greatest capacity to detect nucleon decay is Super-Kamiokande.

6.1   What do experiments look for?

The search for proton decay is primarily based on theoretical and numerical predictions about channel dominance, because proton can hypothetically decay into two, three or more particles in different, kinematically allowed, ways. So, instead of looking and analyzing all potential decays such as $p \to K^+ \overline{\nu}$, $p \to K^0 e^+$, $p \to \eta^0 e^+$, $p \to \pi^+ \overline{\nu}$, $p \to \pi^0 \mu^+$, $p \to e^+ e^+ e^-$ etc., experimental searches are in practice focused on specific decays, the ones with best statistical chance to be detected with implemented detector technology. For example, in minimal $SU(5)$ GUT model [86], the dominant channel is $p \to \pi^0 e^+$ and ring imaging water Cherenkov detectors such as Super-Kamiokande have very high efficiency in identifying both e^+ and π^0. The experimental signal would be manifestation of three rings of Cherenkov light, one from positron and two from γ rays to which π^0 would decay as shown in Fig. 6.1.
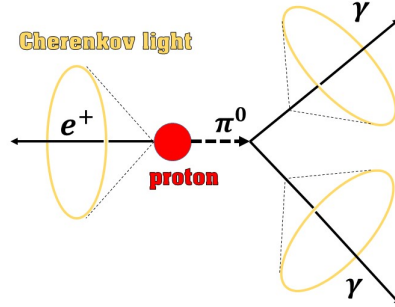
Figure 6.1: Experimental signature of $p \to \pi^0 e^+$ decay process

Most of the models in literature list two dominant two-body decay channels that are $p \to \pi^0 e^+$ and $p \to K^+ \overline{\nu}$. These two have been accordingly searched for and analyzed in recent years within Super-Kamiokande for different values of exposures λ_i, signal efficiencies $\hat{\epsilon}_i \pm \triangle_{\epsilon_i}$, total backgrounds $\hat{b}_i \pm \triangle_{b_i}$ etc [87, 9]. Based on these results, proton partial decay widths have been calculated for different confidence levels (95 %, 90 % C.L. etc.) [88]. Even though Super-Kamiokande can search for proton decay via both channels, it shows less sensitivity for $p \to K^+ \overline{\nu}$ mode. It is a water-based Cherenkov detector with a fiducial mass greater than 20 ktons. However, K^+ particle is produced below its Cherenkov threshold in water, therefore it can be detected only indirectly via its decay particles.

Current lower limits of Super-Kamiokande of proton partial lifetimes for these two channels are [88]:

$$
\tau_p/Br(p \to K^+\overline{\nu}) >
\begin{cases}
5.1 \times 10^{33} & \text{years at } 95\,\%\,\text{C.L.,} \\
6.6 \times 10^{33} & \text{years at } 90\,\%\,\text{C.L.,} \\
1.3 \times 10^{34} & \text{years at } 68\,\%\,\text{C.L.,} \\
2.2 \times 10^{34} & \text{years at } 50\,\%\,\text{C.L.,}
\end{cases}
\tag{6.3}
$$

and

$$
\tau_p/Br(p \to \pi^0 e^+) >
\begin{cases}
1.9 \times 10^{34} & \text{years at } 95\,\%\ \text{C.L.,} \\
2.4 \times 10^{34} & \text{years at } 90\,\%\ \text{C.L.,} \\
4.9 \times 10^{34} & \text{years at } 68\,\%\ \text{C.L.,} \\
8.1 \times 10^{34} & \text{years at } 50\,\%\ \text{C.L..}
\end{cases}
\tag{6.4}
$$

There are eight ways that proton can decay into mesons and anti-leptons and we will analyze all of these eight channels utilizing experimental limits presented in Table 6.1 whenever we conduct numerical analysis in this thesis.

Table 6.1: Experimental lower bounds on partial proton decay lifetimes at $90\,\%$ C.L.

PROTON DECAY CHANNELS	Proton lifetime bound at 90% C.L.
$p \to \pi^0 e^+$	2.4×10^{34} years [9]
$p \to \pi^0 \mu^+$	1.6×10^{34} years [9]
$p \to \pi^+ \overline{\nu}$	3.9×10^{32} years [89]
$p \to \eta^0 e^+$	1.0×10^{34} years [90]
$p \to \eta^0 \mu^+$	4.7×10^{33} years [90]
$p \to K^0 e^+$	1.1×10^{33} years [90]
$p \to K^0 \mu^+$	3.5×10^{33} years [13]
$p \to K^+ \overline{\nu}$	6.6×10^{33} years [89]

6.2 Future experiments

There are four major planned experiments [91] that are highly promising when it comes to improving limits on proton lifetimes:

- DUNE - 68 kton liquid argon detector located in llinois and South Dakota, USA;

- ESSnuSB - 0.5 Mton water-Cherenkov detector in Sweden;

- Hyper-Kamiokande - 188 kton water-Cherenkov detector in Gifu, Japan;

- JUNO - 20 kton liquid scintillator detector located in Jiangmen, China.

6.2.1 DUNE [92, 93]

DUNE stands for Deep Underground Neutrino Experiment. It is located in USA, at two locations: Fermilab, near Chicago, and SURF, in South Dakota. This is a project aiming to study in detail neutrino oscillations including CP violation in neutrino sector, neutrino mass hierarchy, but it will also look for a proton decay processes. It is expected to start in 2026 and to collect data in next decade or more. There are two detectors that will be positioned on the path of neutrino beam provided by the Long-Baseline Neutrino Facility. This experiment is specific due to use of liquid argon technology (LAr). With this technology, it will be possible to reconstruct events and particle types with great precision and accuracy in time-projection chambers (TPCs). However, this type of construction and technology would not be able to compete with water-based Cherenkov detector experiments when it comes to $p \to \pi^0 e^+$ decay mode. Maximum detection efficiency is expected to be 40% to 45%. On the other hand, there is 97% efficiency for decay mode $p \to K^+ \overline{\nu}$. This is due to specific analysis of energy loss profile of K^+ particles.

6.2.2 ESSnuSB [94, 95, 96]

ESSnuSB stands for European Spallation Source Neutrino Super Beam. It is based on the European Spallation Source (ESS) currently under construction at Lund in Sweden. Construction of the facility and commissioning should take place in the period 2027–2034. In 2035 data taking should begin.

It is focused on lepton sector, namely on the precise measurements of CP violation parameters. It will investigate the difference in the neutrino oscillation probabilities. Both neutrino and anti-neutrino oscillations will be analyzed, muon neutrino to electron neutrino and electron anti-neutrino to muon anti-neutrino. ESS linear accelerator is responsible for production of very intense neutrino beam that reduces systematic errors. This would be possible thanks to the observation of the neutrino oscillations at the second oscillation maximum. The linac pulse frequency would be doubled from 14 Hz to 28 Hz,

once finished. Beside this, there are two detectors in construction plan. One would be near-detector, close to the ESS accelerator and other would be far-detector, many kilometers away from linac.

The neutrino beam will be sent to the water-Cherenkov detector. This technology would take a step forward into investigating open questions in leptonic sector such as the mass ordering and the matter/antimatter asymmetry. Beside this, there will be complementary research conducted in a domain of fundamental physics, in particular proton decay.

6.2.3 Hyper-Kamiokande [97, 98]

Hyper-Kamiokande is an experiment that is to surpass Super-Kamiokande with its resources, research capabilities and expectations. It can be considered as a successor to Super-Kamiokande. It will be located, once built, on the site of the Kamioka Observatory, near Kamioka, in Japan. There will be a far detector with a long baseline neutrino experiment for the J-PARC neutrino beam. This experiment will be using ultra pure water, billions of litres, with volume 20 times larger than one currently used in Super-Kamiokande. Beside its main purpose of investigation — CP violation — other physics questions will be analyzed and researched for answers such as proton decay, atmospheric neutrinos, as well as neutrinos from astronomical sources. When it comes to proton decay, Super-Kamiokande had set lower limit for proton lifetime to be around 10^{34} years, and Hyper-Kamiokande is aiming to set lower limit to be around 10^{35} years.

6.2.4 JUNO [99, 100, 101]

JUNO stands for Jiangmen Underground Neutrino Observatory. It is located in China, and represents an enormous experiment with vast variety of goals. Mainly, it is aiming to detect anti-neutrinos from reactors. The purpose is to investigate and analyze neutrino oscillations. It is based on dual-calorimetry technique. This is something relatively new in experimental and applied physics, with the two independent photosensor systems. Beside focus on research on neutrino mass hierarchy, this experiment will be looking into proton decay, astroparticle sources, and rare processes.

6.3 Future expectations

With more investments in experimental development, upgrades in detector technologies, resources, and experimental facilities, it will be possible to achieve better sensitivity and produce more stringent constraints on proton partial lifetimes. We present current bounds on partial proton lifetimes and future

Table 6.2: Future expectations for a ten-year period of data taking

decay channel	current bound τ_p [years]	future sensitivity τ_p [years]
$p \to \pi^0 e^+$	2.4×10^{34} [9]	7.8×10^{34} [10]
$p \to \pi^0 \mu^+$	1.6×10^{34} [9]	7.7×10^{34} [10]
$p \to \eta^0 e^+$	1.0×10^{34} [11]	4.3×10^{34} [10]
$p \to \eta^0 \mu^+$	4.7×10^{33} [11]	4.9×10^{34} [10]
$p \to K^0 e^+$	1.1×10^{33} [12]	-
$p \to K^0 \mu^+$	3.6×10^{33} [13]	-
$p \to \pi^+ \overline{\nu}$	3.9×10^{32} [14]	-
$p \to K^+ \overline{\nu}$	6.6×10^{33} [15]	9.6×10^{33} [16] & 3.2×10^{34} [10]

sensitivities where available, in Table 6.2 [90].

Part III

Results

Chapter 7

Specific $SU(5)$ Model

All matter originates and exists only by virtue of a force which brings the particle of an atom to vibration and holds this most minute solar system of the atom together. We must assume behind this force the existence of a conscious and intelligent mind. This mind is the matrix of all matter.

Max Planck

In Chapter 4 we have presented beautiful features and issues emerging from Georgi-Glashow $SU(5)$ model. The most prominent difficulties of Georgi-Glashow model are mass degeneracy problem, lack of neutrino masses, and an inability to unify gauge couplings. Since it is the simplest gauge group that could have explained the unification, particle physicists often tend to recur to its origins, if not for solution, then for an inspiration.

In this thesis, we want to present a new and somewhat specific and indeed unique $SU(5)$ [7, 74] model that eliminates problems encountered in Georgi-Glashow model. The predictivity of this novel proposal has been discussed in Ref. [7] whereas the viability of parameter space of the model has been studied in Ref. [74].

7.1 The model description

7.1.1 Particle content and notation

The model is built on eight representations: 5_H, 24_H, 35_H, $\bar{5}_{Fi}$, 10_{Fi}, 15_F, $\overline{15}_F$, and 24_V. The subscripts stand for scalars (H), fermions (F) and gauge bosons (V), while index i stands for number of generations ($i = 1, 2, 3$). The particle content of the model, except for the gauge fields from 24_V, is summarized in Table 7.1.

Table 7.1: Particle content of a specific $SU(5)$ model and associated β-function coefficients

Type of representations	$SU(5)$ state	Standard Model $(SU(3),\ SU(2),\ U(1))$	β-function coefficients (b_3, b_2, b_1)
scalar	$5_H \equiv \Lambda$	$\Lambda_1 \left(1, 2, \frac{1}{2}\right)$	$\left(0, \frac{1}{6}, \frac{1}{10}\right)$
		$\Lambda_3 \left(3, 1 - \frac{1}{3}\right)$	$\left(\frac{1}{6}, 0, \frac{1}{15}\right)$
	$24_H \equiv \phi$	$\phi_0 \left(0, 0, 0\right)$	$\left(0, 0, 0\right)$
		$\phi_1 \left(1, 3, 0\right)$	$\left(0, \frac{1}{3}, 0\right)$
		$\phi_3 \left(3, 2, -\frac{5}{6}\right)$	$\left(\frac{1}{6}, \frac{1}{4}, \frac{5}{12}\right)$
		$\phi_{\bar{3}} \left(\bar{3}, 2, \frac{5}{6}\right)$	$\left(\frac{1}{6}, \frac{1}{4}, \frac{5}{12}\right)$
		$\phi_8 \left(8, 1, 0\right)$	$\left(\frac{1}{2}, 0, 0\right)$
	$35_H \equiv \Phi$	$\Phi_1 \left(1, 4, -\frac{3}{2}\right)$	$\left(0, \frac{5}{3}, \frac{9}{5}\right)$
		$\Phi_3 \left(\bar{3}, 3, -\frac{2}{3}\right)$	$\left(\frac{1}{2}, 2, \frac{4}{5}\right)$
		$\Phi_6 \left(\bar{6}, 2, \frac{1}{6}\right)$	$\left(\frac{5}{3}, 1, \frac{1}{15}\right)$
		$\Phi_{10} \left(\overline{10}, 1, 1\right)$	$\left(\frac{5}{2}, 0, 2\right)$
fermion	$\bar{5}_{Fi} \equiv F_i$	$L_i \left(1, 2, -\frac{1}{2}\right)$	$\left(0, 1, \frac{3}{5}\right)$
		$d_i^C \left(\bar{3}, 1, \frac{1}{3}\right)$	$\left(1, 0, \frac{2}{5}\right)$
	$10_{Fi} \equiv T_i$	$Q_i \left(3, 2, \frac{1}{6}\right)$	$\left(2, 3, \frac{1}{5}\right)$
		$u_i^C \left(\bar{3}, 1, -\frac{2}{3}\right)$	$\left(1, 0, \frac{8}{5}\right)$
		$e_i^C \left(1, 1, 1\right)$	$\left(0, 0, \frac{6}{5}\right)$
	$15_F \equiv \Sigma$	$\Sigma_1 \left(1, 3, 1\right)$	$\left(0, \frac{4}{3}, \frac{6}{5}\right)$
		$\Sigma_3 \left(3, 2, \frac{1}{6}\right)$	$\left(\frac{2}{3}, 1, \frac{1}{15}\right)$
		$\Sigma_6 \left(6, 1, -\frac{2}{3}\right)$	$\left(\frac{5}{3}, 0, \frac{16}{15}\right)$
	$\overline{15}_F \equiv \bar{\Sigma}$	$\bar{\Sigma}_1 \left(1, 3, -1\right)$	$\left(0, \frac{4}{3}, \frac{6}{5}\right)$
		$\bar{\Sigma}_3 \left(\bar{3}, 2, -\frac{1}{6}\right)$	$\left(\frac{2}{3}, 1, \frac{1}{15}\right)$
		$\bar{\Sigma}_6 \left(\bar{6}, 1, \frac{2}{3}\right)$	$\left(\frac{5}{3}, 0, \frac{16}{15}\right)$

There are couple of specific predictions of this model. Neutrinos are Majorana particles with mass ordering corresponding to the normal hierarchy. And, one of the neutrinos is massless particle. Also, the model provides firm predictions for partial proton decay lifetimes thus establishing the link between experimental bounds on matter stability and a lower bound on the associated mass scales of new physics. This will be explained in detail later on.

The Lagrangian of the model, with the exception of kinetic terms, is:

$$
\begin{aligned}
\mathcal{L} \supset \Bigg\{ &+ Y_{ij}^u \, T_i^{\alpha\beta} T_j^{\gamma\delta} \Lambda^{\rho}_{\epsilon_{\alpha\beta\gamma\delta\rho}} + Y_{ij}^d \, T_i^{\alpha\beta} F_{\alpha j} \Lambda^*_\beta + Y_i^a \Sigma^{\alpha\beta} F_{\alpha i} \Lambda^*_\beta + Y_i^b \overline{\Sigma}_{\beta\gamma} F_{\alpha i} \Phi^{*\alpha\beta\gamma} \\
&+ Y_i^c \, T_i^{\alpha\beta} \overline{\Sigma}_{\beta\gamma} \phi_\alpha^\gamma + \text{h.c.} \Bigg\} + M_\Sigma \overline{\Sigma}_{\alpha\beta} \Sigma^{\alpha\beta} + y \overline{\Sigma}_{\alpha\beta} \Sigma^{\beta\gamma} \phi_\gamma^\alpha - \\
&- \mu_\Lambda^2 (\Lambda_\alpha^* \Lambda^\alpha) + \lambda_0^\Lambda (\Lambda_\alpha^* \Lambda^\alpha)^2 + \mu_1 \Lambda_\alpha^* \Lambda^\beta \phi_\beta^\alpha + \lambda_1^\Lambda (\Lambda_\alpha^* \Lambda^\alpha)(\phi_\gamma^\beta \phi_\beta^\gamma) + \lambda_2^\Lambda \Lambda_\alpha^* \Lambda^\beta \phi_\beta^\gamma \phi_\gamma^\alpha - \\
&- \mu_\phi^2 (\phi_\gamma^\beta \phi_\beta^\gamma) + \mu_2 \phi_\beta^\alpha \phi_\gamma^\beta \phi_\alpha^\gamma + \lambda_0^\phi (\phi_\gamma^\beta \phi_\beta^\gamma)^2 + \lambda_1^\phi \phi_\beta^\alpha \phi_\gamma^\beta \phi_\delta^\gamma \phi_\alpha^\delta + \mu_\Phi^2 (\Phi^{*\alpha\beta\gamma} \Phi_{\alpha\beta\gamma}) + \\
&+ \lambda_0^\Phi \Phi^{*\alpha\beta\gamma} \Phi_{\alpha\beta\gamma}(\Lambda_\rho^* \Lambda^\rho) + \lambda_0^{''} \Phi^{*\alpha\beta\gamma} \Phi_{\beta\gamma\delta} \Lambda^\delta \Lambda_\alpha^* + \mu_3 \Phi^{*\alpha\beta\gamma} \Phi_{\beta\gamma\delta} \phi_\alpha^\delta + \\
&+ \lambda_1 \Phi^{*\alpha\beta\gamma} \Phi_{\alpha\delta\rho} \phi_\beta^\delta \phi_\gamma^\rho + \lambda_2 \Phi^{*\alpha\beta\rho} \Phi_{\alpha\beta\delta} \phi_\rho^\gamma \phi_\gamma^\delta + \Big\{ \lambda^{'} \Lambda^\alpha \Lambda^\beta \Lambda^\gamma \Phi_{\alpha\beta\gamma} + \text{h.c.} \Big\}
\end{aligned}
\tag{7.1}
$$

In comparison with the original Georgi-Glashow model, this model is extended with one additional scalar representation 35_H and an additional vector-like fermion generation represented with 15_F and $\overline{15}_F$. These additions are important in order to create an experimentally observed mismatch between the masses of the down-type quarks and charged leptons, generate realistic neutrino masses, and provide gauge coupling unification.

7.1.2   Symmetry breaking and unification

Since this proposal is an extension of Georgi-Glashow model, the symmetry breaking happens in the same way: $SU(5) \rightarrow SU(3) \times SU(2) \times U(1) \rightarrow SU(3) \times U(1)_{\text{em}}$. The relevant VEVs are:

$$
\langle 24_H \rangle = \frac{v_{24}}{\sqrt{15}}
\begin{pmatrix}
1 & & & & \\
& 1 & & & \\
& & 1 & & \\
& & & -\frac{3}{2} & \\
& & & & -\frac{3}{2}
\end{pmatrix}
\tag{7.2}
$$

and

$$\langle 5_H \rangle = \begin{pmatrix} 0 \\ 0 \\ 0 \\ 0 \\ v_5 \end{pmatrix} \tag{7.3}$$

where $v_5 = 174.104 \, \text{GeV}$ is the Standard Model VEV.

Since there are two stages in symmetry breaking process, we have two VEVs at two different energy scales. However, before we explicitly break $SU(5)$ symmetry, associated representations can be freely rotated. We do that to make adequate choice of basis for parameter counting and subsequent numerical analysis. In particular, we go into basis where Y^d is a diagonal matrix.

Particle content is specified in Table 7.1 from where we can outline some states that are *a priori* not known, and by unknown, we mean their masses, that are crucial part of the gauge coupling unification analysis of this specific model. Those are Φ_1, Φ_3, Φ_6, $\Phi_{10} \in 35_H$, Σ_1, Σ_3, $\Sigma_6 \in 15_F$, ϕ_1, $\phi_8 \in 24_H$, and $\Lambda_3 \in 5_H$.

In the process of $SU(5)$ symmetry breaking, scalar fields ϕ_3 and $\phi_{\bar{3}}$ play a key role because they yield necessary degrees of freedom to the proton mediating gauge bosons in 24_V. Another information that comes out of symmetry breaking is information on mass relations. In subsection 7.1.1 we have introduced vector-like fermions 15_F and $\overline{15}_F$. The relevant Standard Model multiplets in 15_F and $\overline{15}_F$ are denoted with Σ_1, Σ_3, and Σ_6. The masses of these multiplets are generated by the last two terms in the second line of Eq. (7.1) from where we get the following mass relation:

$$M_{\Sigma_6} = 2M_{\Sigma_3} - M_{\Sigma_1} \tag{7.4}$$

Similar situation happens with states in 35_H. There are four Standard Model multiplets in this representation, but only three linearly independent contractions in Eq. (7.1) that generate their masses from where one can deduce that:

$$M_{\Phi_{10}}^2 = M_{\Phi_1}^2 - 3M_{\Phi_3}^2 + 3M_{\Phi_6}^2 \tag{7.5}$$

The gauge coupling analysis shows that Φ_1 needs to be very heavy ($M_{\Phi_1} \gg v_5$). Other two states Φ_3 and Φ_6 tend to be light when the unification scale M_{GUT} is large enough to be compatible with proton

decay constraints. This implies, using Eq. (7.5), that Φ_{10} and Φ_1 are both heavy and of the same mass, from where it follows that the states Φ_3 and Φ_6 are both light and mass degenerate in a viable parameter space. Now, having initially started with four different states in Eq. (7.5), we finally have only two mass scales in 35_H. Following this analysis, we come to one more degeneracy among masses. Namely, the fields Σ_1, Σ_3 and Σ_6 turn out to be mass degenerate with masses $M_{\Sigma_1}, M_{\Sigma_3}, M_{\Sigma_6} \gg v_5$. This happens in this model where neutrinos have masses and unification is achievable. As with the previous set of fields, we again reduce mass scales from three to one in case of vector-like fermions in 15_F and $\overline{15}_F$. Consequently, a single mass scale in vector like fermions' sector does not affect M_{GUT} but rather the value of α_{GUT}.
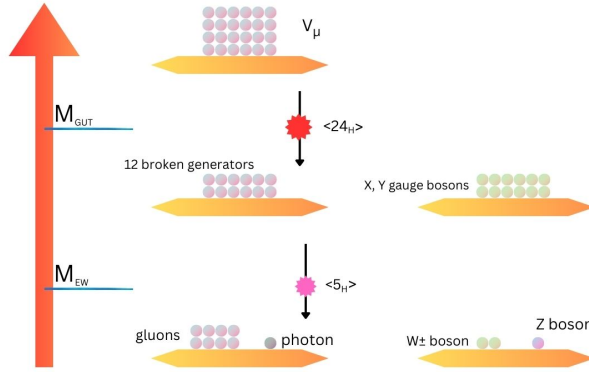
Figure 7.1: Simplified graphical representation of spontaneous symmetry breaking in $SU(5)$

Finally, we have six relevant mass scales governing the gauge coupling unification: one originates from 5_H (Λ_3), two from 24_H (ϕ_1 and ϕ_8), two from 35_H, and one from 15_F and $\overline{15}_F$. It is important to stress that mass of Λ_3 needs to be quite large, $M_{\Lambda_3} \geq 3 \times 10^{11}$ GeV, so that proton does not decay rapidly via scalar leptoquark mediation [102].

7.1.3 Mass generation mechanism

Neutrino masses

Neutrinos can either be Majorana or Dirac particles [103]. However, in our model, neutrinos are purely Majorana particles. Since neutrinos reside in $\overline{5}_{Fi}$ of $SU(5)$, or, more precisely, in doublet L_i when represented in terms of the Standard Model multiplets, the leading order contribution for generating their mass via dim-5 operator at the one-loop level [104, 105] is shown in Fig. 7.2 [74].

It is clear that the state $\Lambda_1(1, 2, 1/2)$ as well as its VEV $\langle 5_H \rangle \equiv \langle \Lambda_1(1, 2, 1/2) \rangle$ are necessary for the process of neutrino mass generation. Since we have quartic scalar coupling vertex with three Λ states and
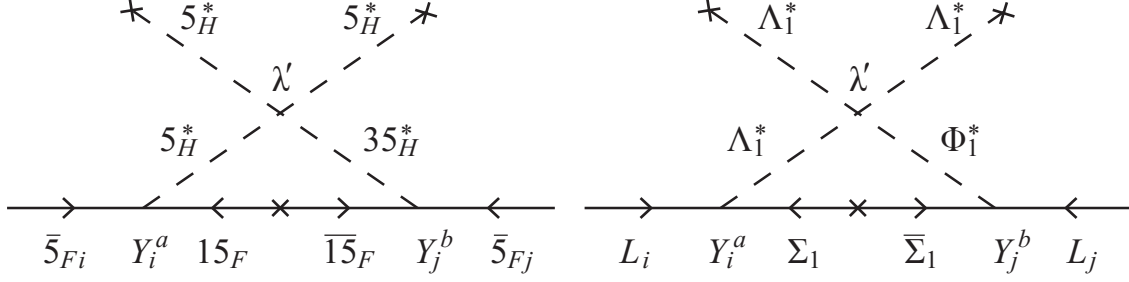
Figure 7.2: The Feynman diagrams of the leading order contribution towards Majorana neutrino masses at the $SU(5)$ (left panel) and the Standard Model (right panel) levels.

one Φ state, it follows that the relevant contraction here is the last term $\lambda' \Lambda^\alpha \Lambda^\beta \Lambda^\gamma \Phi_{\alpha\beta\gamma}$ in Eq. (7.1).

Due to the experimentally observed mismatch between the charged leptons and down-type quarks, we need vector-like fermions in 15_F and $\overline{15}_F$ to address this issue. It is a physical mixing between the vector-like fermions and ordinary fermions from 10_{F_i} that yields the mismatch. The consequences for the charged fermion masses of this particular type of mixing have been previously analyzed within the grand unified model based on $SU(5)$ and supersymmetry [106]. One can notice from Table 7.1 that quark doublets $Q_i \in 10_{F_i}$ and a multiplet $\Sigma_3 \in 15_F$ transform in the same manner under the Standard Model. This is the reason why these states interact at the $SU(5)$ symmetry breaking level. We can again recognize the relevant mixing term from Eq. (7.1) with specific coefficient values:

$$\mathcal{L} \supset \frac{1}{4}\sqrt{\frac{10}{3}}\, v_{24}\, Y_i^C\, Q_i\, \overline{\Sigma}_3 \tag{7.6}$$

where v_{24} is VEV defined in Eq. (7.2). It is precisely this VEV of 24_H that helps create the mismatch between the masses of the charged leptons and the down-type quarks.

The neutrino mass matrix elements, when $M_{\Sigma_1}, M_{\Phi_1} \gg v_5$, would be:

$$(M_N)_{ij} \approx \frac{\lambda' v_5^2}{8\pi^2}(Y_i^a Y_j^b + Y_i^b Y_j^a)\frac{M_{\Sigma_1}}{M_{\Sigma_1}^2 - M_{\Phi_1}^2}\ln\left(\frac{M_{\Sigma_1}^2}{M_{\Phi_1}^2}\right) = m_0(Y_i^a Y_j^b + Y_i^b Y_j^a). \tag{7.7}$$

The neutrino mass matrix M_N is composed out of two matrices with elements $Y_i^a Y_j^b$ and $Y_i^b Y_j^a$. Other contributions for M_N are proportional to sum of $Y_i^a Y_j^b$ and $Y_i^b Y_j^a$ as well. Nonetheless, it is important to say that these additional contributions are suppressed and therefore irrelevant. Now, based on this information, it is certain that one of the neutrinos must be massless. There is a requirement for neutrino mass scale:

$$m_0 \geq \frac{\sqrt{\Delta m_{31}^2}}{2} \tag{7.8}$$

where Δm_{31}^2 is the largest among two neutrino mass squared differences that are known from experiment [107, 108, 109].

Since in our model one of neutrinos is massless we can set $m_1 = 0$ and hence the neutrino matrix eleements are:

$$(M_N)_{ij} = m_0 \left(Y_i^a Y_j^b + Y_i^b Y_j^a \right) = \left(N \, \text{diag}(0, m_2, m_3) \, N^T \right)_{ij}, \tag{7.9}$$

where N is unitary matrix and m_2 and m_3 are neutrino mass eigenstates. Unitary matrix N reads:

$$N = \begin{pmatrix} e^{i\gamma_1} & 0 & \\ 0 & e^{i\gamma_2} & 0 \\ 0 & 0 & e^{i\gamma_3} \end{pmatrix} V_{\text{PMNS}}^*, \tag{7.10}$$

due to the fact that we are in the basis with charged leptons being in mass eigenstate basis. Here V_{PMNS} is the Pontecorvo-Maki-Nakagawa-Sakata unitary mixing matrix with three mixing angles, two Majorana phases, and one CP violating Dirac phase. With inversion of Eq. (7.9) in order to start from the generalized master formula for Majorana neutrinos:

$$f(y_1^T M y_2 + y_2^T M^T y_1) = U^T m U \tag{7.11}$$

and using results in Refs. [110, 111], one can obtain from the normal ordering the following expressions for Y^{aT} and Y^{bT}:

$$Y^{aT} = \frac{1}{\rho\sqrt{2}} \begin{pmatrix} i\, r_2 \, N_{12} + r_3 \, N_{13} \\ i\, r_2 \, N_{22} + r_3 \, N_{23} \\ i\, r_2 \, N_{32} + r_3 \, N_{33} \end{pmatrix}, \quad Y^{bT} = \frac{\rho}{\sqrt{2}} \begin{pmatrix} -i\, r_2 \, N_{12} + r_3 \, N_{13} \\ -i\, r_2 \, N_{22} + r_3 \, N_{23} \\ -i\, r_2 \, N_{32} + r_3 \, N_{33} \end{pmatrix}, \tag{7.12}$$

where $r_2 = \sqrt{m_2/m_0}$ and $r_3 = \sqrt{m_3/m_0}$. Note that there is an unknown parameter ρ in Eq. (7.12) that accounts for the fact that the matrix elements of Y^a and Y^b are always featured as products in Eq. (7.9). Since V_{PMNS} has three phases (one CP violation Dirac phase and two Majorana phases), N matrix has overall six phases. Besides three from V_{PMNS} there are three more from Eq. (7.10) γ_1, γ_2, and γ_3. Hence in Eq. (7.12) we have six arbitrary phases. This is consistent with the process of trading the six real parameters from Y^a and Y^b for three PMNS angles and three neutrino masses in procedure of inversion.

Charged fermion masses

We have already mentioned that in order to produce experimentally observed difference between masses of charged leptons and the down-type quarks, we need vector-like fermions in 15_F and $\overline{15}_F$. It is the physical mixing between the vector-like fermions and ordinary fermions from 10_{F_i} that yields the required mismatch. The mixing is allowed since quark doublets $Q_i \in 10_{F_i}$ and a multiplet $\Sigma_3 \in 15_F$ transform in

the same manner under the Standard Model as one can notice from Table 7.1. Again, the consequences for the charged fermion masses of this particular type of mixing have been previously analyzed within the grand unified model based on supersymmetric $SU(5)$ [106].

Since symmetry breaking happens at two scales, first one taking place at M_{GUT} and second one at electroweak scale, there are additional mixing terms at the electroweak level between the vector-like fermions 15_F and $\overline{15}_F$, and other fermions in $\overline{5}_{F_i}$ and 10_{F_i}. This occurs every time when these different fermions transform the same way under $SU(3) \times U(1)_{\text{em}}$ with induced terms being proportional to v_5.

Table 7.2: Decomposition of $SU(5)$ states under $SU(3) \times U(1)_{\text{em}}$

$SU(5)$ states	decomposition	$SU(3)$	$U(1)_{\text{em}}$
Q_i	u_i	3	$\frac{2}{3}$
	d_i	3	$-\frac{1}{3}$
L_i	e_i	1	-1
	ν_i	1	0
Σ_3	Σ^u	3	$\frac{2}{3}$
	Σ^d	3	$-\frac{1}{3}$
Σ_1	Σ^ν	1	0
	Σ^{e^C}	1	1
	$\Sigma^{e^C e^C}$	1	2

The states from $SU(5)$ that emerge with same transformation under $SU(3) \times U(1)_{\text{em}}$ are given in Table 7.2. From this second stage of symmetry breaking we have the following mass terms for charged fermions:

$$\mathcal{L} \supset \begin{pmatrix} u_i & \Sigma^u \end{pmatrix} \begin{pmatrix} 4v_5(Y_{ij}^u + Y_{ji}^u) & \frac{1}{4}\sqrt{\frac{10}{3}} v_{24} Y_i^c \\ 0 & M_{\Sigma_3} \end{pmatrix} \begin{pmatrix} u_j^C \\ \overline{\Sigma}^u \end{pmatrix} \tag{7.13}$$

$$+ \begin{pmatrix} d_i & \Sigma^d \end{pmatrix} \begin{pmatrix} v_5 Y_{ij}^d & \frac{1}{4}\sqrt{\frac{10}{3}} v_{24} Y_i^c \\ v_5 Y_j^a & M_{\Sigma_3} \end{pmatrix} \begin{pmatrix} d_j^C \\ \overline{\Sigma}^d \end{pmatrix} + \begin{pmatrix} e_i & \overline{\Sigma}^{e^C} \end{pmatrix} \begin{pmatrix} v_5 Y_{ji}^d & v_5 Y_i^a \\ 0 & M_{\Sigma_1} \end{pmatrix} \begin{pmatrix} e_j^C \\ \Sigma^{e^C} \end{pmatrix}.$$

In order to generate neutrino masses along with the gauge coupling unification, we find some limits and requirements for certain states. Namely, states Σ^{u,d,e^C} need to be very heavy with the limit that $v_{24} Y^c, M_{\Sigma_1}, M_{\Sigma_3} \gg v_5$. Now, the mass matrices for charged fermions are:

$$M_U = \left(\mathbb{1} + \delta'^2 \, Y^c Y^{c\dagger}\right)^{-\frac{1}{2}} 4v_5 (Y^u + Y^{u\,T}), \tag{7.14}$$

$$M_D = \left(\mathbb{1} + \delta'^2 \, Y^c Y^{c\dagger}\right)^{-\frac{1}{2}} v_5 \left(Y^d + \delta' \, Y^c Y^a\right), \tag{7.15}$$

$$M_E = v_5 Y^{d\,T}, \tag{7.16}$$

where M_U, M_D, and M_E stand for up-type quarks, down-type quarks and charged leptons, respectively. Parameter $\delta' \equiv \sqrt{10/3}\, v_{24}/(4M_{\Sigma_3})$ is a dimensionless parameter and $\mathbb{1}$ is the 3×3 identity matrix. In our model, in our specific space we analyze, contributions proportional to $\delta'^2 \, Y^c Y^{c\dagger}$ are completely negligible and Eqs. (7.14), (7.15), and (7.16) become:

$$M_U = 4v_5 (Y^u + Y^{u\,T}), \tag{7.17}$$

$$M_D = v_5 \left(Y^d + \delta' \, Y^c Y^a\right), \tag{7.18}$$

$$M_E = v_5 Y^{d\,T}. \tag{7.19}$$

Masses of vector-like fermions are not changed in interaction with the Standard Model fermions and they are:

$$M_{\Sigma^u} = M_{\Sigma^d} = M_{\Sigma_3} \left(1 + \delta'^2 \, Y^{c\dagger} Y^c\right)^{\frac{1}{2}} \approx M_{\Sigma_3}, \; M_{\Sigma^{e^C}} = M_{\Sigma^{e^C} e^C} = M_{\Sigma^\nu} = M_{\Sigma_1}. \tag{7.20}$$

To summarize, the extension of Georgi-Glashow $SU(5)$ model with one vector-like set of fermions in 15_F and $\overline{15}_F$ and one scalar representation 35_H accomplishes the following:

- generates two neutrino masses;

- creates viable mismatch between the down-type quark and charged lepton masses;

- provides gauge coupling unification.

Chapter 8

Correlation between proton decay signatures

> Science cannot solve the ultimate
> mystery of nature. And that is
> because, in the last analysis, we
> ourselves are a part of the
> mystery that we are trying to
> solve.
>
> *Max Planck*

In previous chapters, we have laid down the theoretical groundwork for our specific $SU(5)$ model. We have introduced the model and explored it in detail – the particle content, symmetry breaking procedure, the process of generating fermion and scalar masses etc. Now, it is time to check the validity of our model and present the correlation between proton decay signatures via gauge boson and scalar leptoquark mediations. We will conduct the numerical analysis in four stages. We will first generate viable gauge coupling unification points. We will follow this up with running of Yukawa couplings at the one-loop level for those points. These two steps will be subsequently followed by numerical fit of fermion masses, and, finally, extraction of proton decay signatures that we are after.

8.1 Numerical Analysis

8.1.1 Gauge coupling unification generation

In Chapter 7, in Section 7.1.1, we have outlined that some states, with *a priori* unknown masses, are crucial for the gauge coupling unification analysis in our $SU(5)$ model. Those states are Φ_1, Φ_3, Φ_6,

$\Phi_{10} \in 35_H$, Σ_1, Σ_3, $\Sigma_6 \in 15_F$, ϕ_1, $\phi_8 \in 24_H$, and $\Lambda_3 \in 5_H$. Since the neutrino mass scale depends only on masses of two fields — Σ_1 and Φ_1 — we will present viable parameter space in the M_{Φ_1}-M_{Σ_1} plane. It is important to stress that in order for Yukawa couplings Y_i^a and Y_i^b to remain perturbative, m_0 parameter that appears as a prefactor in neutrino mass relation given in Eq. (7.7) needs to exceed certain value. This value practically corresponds to the mass of the heaviest neutrino in the normal hierarchy case since our model predicts one neutrino to be massless. Once gauge coupling unification is achieved, the mass spectra of all the abovementioned fields are known, including the masses of proton decay mediating gauge bosons as well as the parameters M_{GUT} and α_{GUT}. These mass spectra will be used to run Yukawa couplings of the Standard Model charged fermions to M_{GUT}, where the numerical fermion mass fit will be performed and extraction of unitary matrices that take fermions from flavor into mass eigenstate basis accomplished.

During this first stage of numerical analysis, we need to implement several constraints discussed in Chapter 7 such as mass relations between states in 35_H and 15_F. Another constraint would be to impose a lower mass limit for triplet Λ_3 from 5_H to be approximately 10^{12} GeV [102]. Our analysis of proton decay signatures will eventually yield correct bound on M_{Λ_3}.

Our aim here is to find the maximum possible unification scale M_{GUT} for fixed M_{Φ_1} and M_{Σ_1} values and associated mass spectra of all other fields. To accomplish maximization, we set a lower limit on the masses of new physics' states. We do this by introducing a scale $M \equiv \min(M_J)$, that represents the lowest possible mass in the theory of the fields beyond the Standard Model content, where $J = \Phi_1, \Phi_3, \Phi_6, \Phi_{10}, \Sigma_1, \Sigma_3, \Sigma_6, \phi_1, \phi_8, \Lambda_3$. We will consider three distinct cases for which we will present and discuss the results. These are scenarios with $M \geq 1$ TeV, $M \geq 10$ TeV, and $M \geq 100$ TeV.

Three gauge coupling constants are α_1, α_2, and α_3, where first two are associated with electroweak interactions and the third with strong force. The one-loop level running can be summarized as:

$$\alpha_i(M_{\text{GUT}}) = \alpha_i(M_Z) + b_i \ln \frac{M_{\text{GUT}}}{M_Z} \tag{8.1}$$

where b_i, in this case, would be coefficients of the Standard Model particle content. However, if we go, as we will do, from M_Z to M_{GUT} through several intermediate mass scales or, in other words, through M_J's, we can write:

$$\alpha_i(M_{\text{GUT}}) = \alpha_i(M_Z) + \sum_J b_i^J \ln \frac{M_{\text{GUT}}}{M_J} . \tag{8.2}$$

Now, for each of three gauge coupling constants we can write:

$$\alpha_1(M_{\text{GUT}}) = \alpha_1(M_Z) + \sum_J b_1^J \ln \frac{M_{\text{GUT}}}{M_J} , \tag{8.3}$$

$$\alpha_2(M_{\mathrm{GUT}}) = \alpha_2(M_Z) + \sum_J b_2^J \ln \frac{M_{\mathrm{GUT}}}{M_J} , \qquad (8.4)$$

$$\alpha_3(M_{\mathrm{GUT}}) = \alpha_3(M_Z) + \sum_J b_3^J \ln \frac{M_{\mathrm{GUT}}}{M_J} . \qquad (8.5)$$

With the assumption that these three couplings will meet at the GUT scale, meaning that all three at that energy scale have the same value, we can subtract one from other in order to get the difference between the two at M_Z scale. For example, if we do this for Eqs. (8.4) and (8.5), we obtain:

$$0 = \alpha_3(M_Z) - \alpha_2(M_Z) + \sum_J (b_3^J - b_2^J) \ln \frac{M_{\mathrm{GUT}}}{M_J}$$

$$\alpha_3(M_Z) - \alpha_2(M_Z) = \sum_J (b_2^J - b_3^J) \ln \frac{M_{\mathrm{GUT}}}{M_J}$$

$$\left(\alpha_3(M_Z) - \alpha_2(M_Z)\right) \ln \frac{M_Z}{M_{\mathrm{GUT}}} = \sum_J (b_2^J - b_3^J) \frac{\ln \frac{M_{\mathrm{GUT}}}{M_J}}{\ln \frac{M_{\mathrm{GUT}}}{M_Z}} = B_{23} \qquad (8.6)$$

Analogously, if we subtract Eq. (8.3) from Eq. (8.4) we have:

$$0 = \alpha_2(M_Z) - \alpha_1(M_Z) + \sum_J (b_2^J - b_1^J) \ln \frac{M_{\mathrm{GUT}}}{M_J}$$

$$\alpha_2(M_Z) - \alpha_1(M_Z) = \sum_J (b_1^J - b_2^J) \ln \frac{M_{\mathrm{GUT}}}{M_J}$$

$$\left(\alpha_2(M_Z) - \alpha_1(M_Z)\right) \ln \frac{M_Z}{M_{\mathrm{GUT}}} = \sum_J (b_1^J - b_2^J) \frac{\ln \frac{M_{\mathrm{GUT}}}{M_J}}{\ln \frac{M_{\mathrm{GUT}}}{M_Z}} = B_{12} \qquad (8.7)$$

where we define coefficients B_{ij} as:

$$B_{ij} = \sum_J (b_i^J - b_j^J) r_J . \qquad (8.8)$$

Again, coefficients b_i^J are the β-function coefficients of a specific particle J with mass M_J and $r_J = \ln(M_{\mathrm{GUT}}/M_J)/\ln(M_{\mathrm{GUT}}/M_Z)$. The relevant b_i^J ($i = 1, 2, 3$) are given in Table (7.1).

Eqs. (8.6) and (8.7) yield the following two identities [112] that imply successful unification if simultaneously satisfied:

$$\frac{B_{23}}{B_{12}} = \frac{5}{8} \frac{\sin^2 \theta_W - \alpha(M_Z)/\alpha_S(M_Z)}{3/8 - \sin^2 \theta_W} , \qquad (8.9)$$

$$\ln \frac{M_{\mathrm{GUT}}}{M_Z} = \frac{16\pi}{5\alpha(M_Z)} \frac{3/8 - \sin^2 \theta_W}{B_{12}} . \qquad (8.10)$$

It is these equations that we need to solve for maximum possible value of M_{GUT} by varying parameters

r_J. Before we start to vary $M_J's$, there are three constraints we already mentioned, that one needs to pay attention to. Again, first one comes from symmetry breaking in $SU(5)$, regarding 15_F, whose three Standard Model multiplets need to satisfy mass relation:

$$M_{\Sigma_6} = 2M_{\Sigma_3} - M_{\Sigma_1}. \tag{8.11}$$

If one assumes that all the masses in Eq. (8.11) are positive, it is easy to show that these three masses are practically degenerate and thus converge to single mass scale when it comes to gauge coupling unification analysis. This is the scenario that we will investigate. Note, however, that there is a possibility that these masses could take negative values, which actually can open up an additional parameter space that we will not cover in this thesis. That would correspond to the scenario with degenerate Σ_6 and Σ_1 fields and light Σ_3. Second constraint refers to Eq. (7.5) where, again, we have degenerate heavy masses of Φ_1 and Φ_{10} and degenerate light masses of Φ_3 and Φ_6. Basically, there are thus only two mass scales for states in 35_H. Third constraint would refer to Λ_3, whose mass value we preliminary set to be at least 10^{12} GeV and vary it afterwards throughout the numerical analysis.

Once we implement these conditions, we can present available parameter space in two-dimensional plane spanned by masses of Φ_1 and Σ_1 due to the fact that neutrino mass spectrum depends on it via m_0 in Eq. (7.7).

Maximization of M_{GUT} value is accomplished via Eqs. (8.9) and (8.10), using Wolfram System Modeler, Mathematica [113]. To obtain unification points, we use $M_Z = 91.1876$ GeV, $\alpha_S(M_Z) = 0.1193 \pm 0.0016$, $\alpha^{-1}(M_Z) = 127.906 \pm 0.019$, and $\sin^2\theta_W = 0.23126 \pm 0.00005$ as our input parameters [114]. We present, as an example, in Fig. 8.1 obtained mass spectra and α_{GUT} for three specific points A ($M \geq 1$ TeV), A' ($M \geq 10$ TeV), and A'' ($M \geq 100$ TeV), where $M_{\Phi_1} = M_{\Sigma_1} = 10^{13.19}$ GeV.

In order to explain viable neutrino mass spectrum with perturbative couplings, we need to find appropriate part of space where this is possible. Therefore, we set λ' from Eq. (7.7) to be 1 in order to generate the curve of constant m_0 assuming that entries in matrices Y^a and Y^b cannot exceed one. More specifically, we vary M_{Φ_1}, M_{Σ_1}, and six phases from Eq. (7.12) to find a region where the product $\max(|Y_i^a|)\max(|Y_j^b|)$, $i,j = 1,2,3$, takes value of one at most. Parameter space where product $\max(|Y_i^a|)\max(|Y_j^b|)$, $i,j = 1,2,3$, is greater than 1 is excluded since there is no viable neutrino mass spectrum with perturbative couplings in that case.

Potentially viable parameter space to address neutrino mass can alternatively be found in the following way. From Eq. (7.7), we can write:

$$\frac{\lambda' v_5^2}{8\pi^2} \frac{M_{\Sigma_1}}{M_{\Sigma_1}^2 - M_{\Phi_1}^2} \ln\left(\frac{M_{\Sigma_1}^2}{M_{\Phi_1}^2}\right) = m_0 \tag{8.12}$$

where for our analysis we take $\lambda' = 1$, $v_5 = 174$ GeV. We can separately consider two cases, one for

$m_{\Sigma_1} \neq m_{\Phi_1}$ when:

$$m_0 = \frac{v_5^2}{8\pi^2} \frac{M_{\Sigma_1}}{M_{\Sigma_1}^2 - M_{\Phi_1}^2} \ln\left(\frac{M_{\Sigma_1}^2}{M_{\Phi_1}^2}\right) \tag{8.13}$$

and second one when $M_{\Sigma_1} = M_{\Phi_1}$ where we take logarithmic series expansion expression:

$$\ln\left(\frac{M_{\Sigma_1}^2}{M_{\Phi_1}^2}\right) = 2\ln\left(\frac{M_{\Sigma_1}}{M_{\Phi_1}}\right) = 2\ln\left(\frac{M_{\Sigma_1}}{M_{\Phi_1}} - 1 + 1\right) = 2\ln\left(\frac{M_{\Sigma_1} - M_{\Phi_1}}{M_{\Phi_1}} + 1\right)$$
$$= 2\frac{M_{\Sigma_1} - M_{\Phi_1}}{M_{\Phi_1}} - \cdots \tag{8.14}$$

to have:

$$m_0 = \frac{v_5^2}{4\pi^2} \frac{M_{\Sigma_1}}{M_{\Sigma_1}^2 - M_{\Phi_1}^2} \cdot \frac{M_{\Sigma_1} - M_{\Phi_1}}{M_{\Phi_1}} . \tag{8.15}$$

Expressions (8.13) and (8.15) allow us to obtain viable coordinates with respect to the neutrino mass generation, within M_{Φ_1}-M_{Σ_1} plane via requirement that

$$m_0 \geq \frac{\sqrt{\Delta m_{31}^2}}{2} , \tag{8.16}$$

where m_0 is given in Eqs. (8.15) and (8.13), and $\Delta m_{31}^2 \simeq 2.5 \times 10^{-3}\,\mathrm{eV}^2$ [115].

Since states in 15_F and $\overline{15}_F$ are all degenerate in mass, this means that change in mass of state Σ_1 does not effect the value M_{GUT}. In other words, M_{GUT} is constant for constant value of Φ_1 mass. On the other hand, α_{GUT} decreases for the fixed value of M_{Φ_1} with the increase of M_{Σ_1}. From this one can conclude that proton decay bound via gauge boson mediation in this model is more rigorous and strict as m_{Σ_1} decreases.

8.1.2   Yukawa coupling RGE running

The next step is to run the masses and mixing parameters of the Standard Model charged fermions to the GUT scale using exact mass spectra that maximize M_{GUT}. We have checked that the running of the neutrino observables gives negligable change, therefore we take their low-scale values instead to save on the computing time. Input data for RGE running is presented in Table 8.1.

We perform RGE running for each individual point of otherwise viable parameter space in M_{Φ_1}-M_{Σ_1} plane. In Fig. 8.3 we present the viable parameter space in the plane spanned by Φ_1 and Σ_1 masses, since these are the only relevant parameters for neutrino mass scale. Values for M_{Φ_1} and M_{Σ_1} are taken to go from $10^{10}\,\mathrm{GeV}$ to $10^{13.5}\,\mathrm{GeV}$ and from $10^7\,\mathrm{GeV}$ to $10^{14}\,\mathrm{GeV}$, respectively. More precisely, we use

Table 8.1: Experimental observables associated with charged fermions [116] and neutrinos for normal ordering [117] with $1\,\sigma$ uncertainties (except for charged leptons).

| $m(M_Z)$ (GeV)	Fit input	$\theta_{ij}^{\text{CKM,PMNS}}$ & δ^{CKM} & Δm_{ij}^2 (eV^2)	Fit input
$m_u/10^{-3}$	1.158 ± 0.392	$\sin\theta_{12}^{\text{CKM}}$	0.2254 ± 0.00072
m_c	0.627 ± 0.019	$\sin\theta_{23}^{\text{CKM}}/10^{-2}$	4.207 ± 0.064
m_t	171.675 ± 1.506	$\sin\theta_{13}^{\text{CKM}}/10^{-3}$	3.640 ± 0.130
$m_d/10^{-3}$	2.864 ± 0.286	δ^{CKM}	1.208 ± 0.054
$m_s/10^{-3}$	54.407 ± 2.873	$\Delta m_{21}^2/10^{-5}$	7.425 ± 0.205
m_b	2.854 ± 0.026	$\Delta m_{3\ell}^2/10^{-3}$	2.515 ± 0.028
$m_e/10^{-3}$	0.486576	$\sin^2\theta_{12}^{\text{PMNS}}/10^{-1}$	3.045 ± 0.125
m_μ	0.102719	$\sin^2\theta_{23}^{\text{PMNS}}$	0.554 ± 0.021
m_τ	1.74618	$\sin^2\theta_{13}^{\text{PMNS}}/10^{-2}$	2.224 ± 0.065

logarithmic scale from 10 to 13.5 and from 7 to 14 in units of $\log_{10}(M_{\Phi_1}/1\,\text{GeV})$ and $\log_{10}(M_{\Sigma_1}/1\,\text{GeV})$, respectively, with discretization step of 0.1 for both axes.

Recall, in first step, where gauge coupling unification analysis was conducted, the complete parameter space has been analyzed and reviewed point by point. In the second stage of numerical analysis, we take each of those points and use RGEs to evaluate Yukawa couplings at the GUT scale using associated mass spectrum of $\Phi_1, \Phi_3, \Phi_6, \Phi_{10} \in 35_H$, $\Sigma_1, \Sigma_3, \Sigma_6 \in 15_F$, $\phi_1, \phi_8 \in 24_H$, and $\Lambda_3 \in 5_H$. The renormalization group running for charged fermion masses is performed at the one-loop level for two reasons. First, at this level of accuracy, gauge coupling unification can be studied and performed separately from the running of the Standard Model charged fermion parameters. Second, this running gives feedback to the unification only at the two-loop level, while unification effects the Yukawa coupling running already at the one-loop level. Sample of RGE running of Yukawa couplings for τ, b quark, and t quark is given in Figure 8.2 for three specific points A $(M \geq 1\,\text{TeV})$, A$'$ $(M \geq 10\,\text{TeV})$, and A$''$ $(M \geq 100\,\text{TeV})$, where $M_{\Phi_1} = M_{\Sigma_1} = 10^{13.19}\,\text{GeV}$.

Numerical fit of the Standard Model variables is performed afterwards as we describe next.
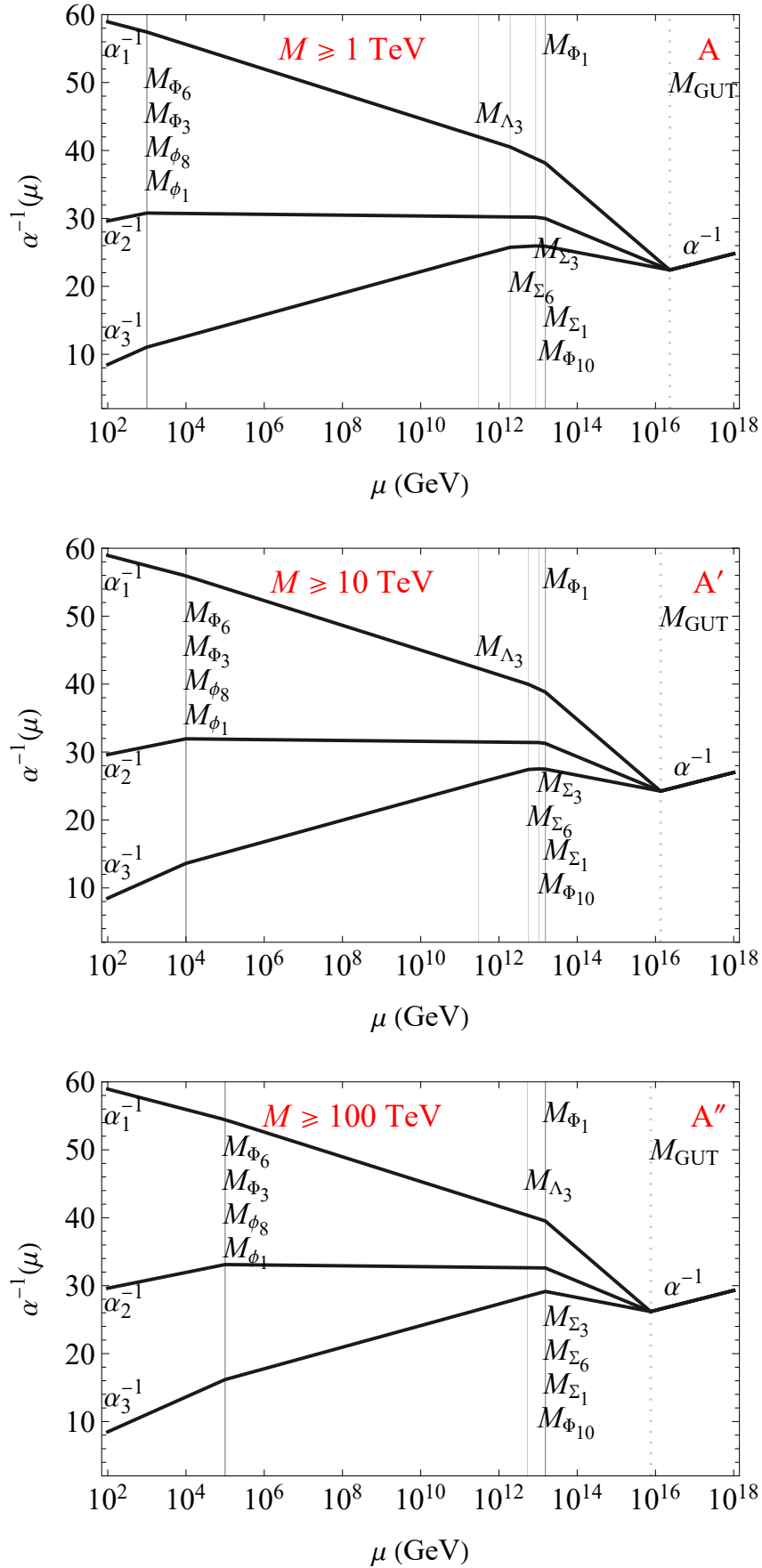
Figure 8.1: The gauge coupling unification spectra for unification points A ($M \geq 1\,\text{TeV}$), A' ($M \geq 10\,\text{TeV}$), and A'' ($M \geq 100\,\text{TeV}$), as indicated.
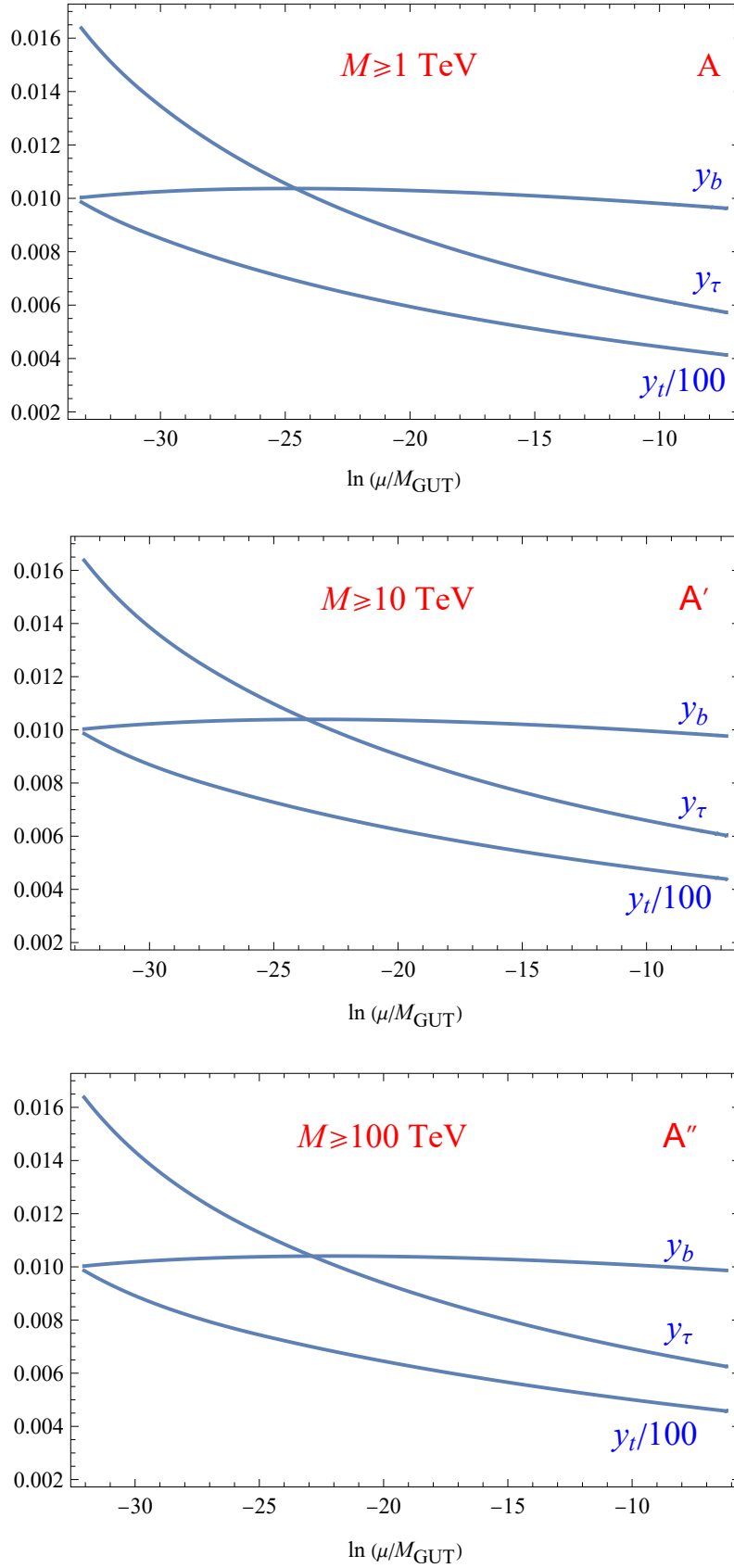
Figure 8.2: The running of Yukawa couplings for top quark, bottom quark and tau lepton for unification points A ($M \geq 1\,\mathrm{TeV}$), A′ ($M \geq 10\,\mathrm{TeV}$), and A″ ($M \geq 100\,\mathrm{TeV}$), as indicated.

8.1.3 Fermion mass fit

We work in the mass eigenstate basis for charged leptons. Hence, $E_L = E_R = \mathbb{1}$. This also means that charged fermion masses are automatically accommodated in our model. On the other hand, we need to simultaneously fit masses of down-type quarks and neutrinos together with PMNS matrix. Recall that one neutrino is massless particle in our model. Also, there is no need to numerically fit up-type quark sector, where, due to fact that $M_U = M_U^T$ we have that $U_L \sim U_R$. This simply means that we can always exactly reconstruct up-type quark masses and CKM mixing parameters once we know D_L from the fit.

Let us describe numerical fit of fermion masses in more detail. Recall that the Standard Model fermion masses in our model can be found from the following Lagrangian:

$$\mathcal{L} \supset -u^T M_U u^C - d^T M_D d^C - e^T M_E e^C - \frac{1}{2} \nu^T M_N \nu + \text{h.c.}, \tag{8.17}$$

where M_U, M_D, M_E, and M_N are given in Eqs. (7.17), (7.18), (7.19), and (7.9), respectively.

The fermion mass eigenstate basis, generally, can be defined through

$$M_U = U_L M_U^{\text{diag}} U_R^\dagger, \tag{8.18}$$

$$M_D = D_L M_D^{\text{diag}} D_R^\dagger, \tag{8.19}$$

$$M_E \equiv E_L M_E^{\text{diag}} E_R^\dagger, \tag{8.20}$$

$$M_N = N M_N^{\text{diag}} N^T, \tag{8.21}$$

where U_L, U_R, D_L, D_R, E_L, E_R, and N are the unitary transformation matrices defined in Chapter 5 in Eqs. (5.57)–(5.61).

We notice that down-type quark mass matrix of Eq. (7.18) and the neutrino mass matrix of Eq. (7.7) share the same Yukawa coupling row matrix Y^a. Hence the need for a combined data fit for these two sectors. For that reason, we minimize a χ^2 function which is defined as

$$\chi^2 = \sum_k P_k^2, \quad P_k = \frac{T_k - O_k}{E_k}, \tag{8.22}$$

where, T_k, O_k, and E_k represent theoretical prediction, measured central value, and experimental 1σ error for the observable k, respectively. This observable k will take values from neutrino and down-type quarks' sectors. In this fitting procedure, the Yukawa coupling matrices Y^a, Y^b, and Y^c are determined against three down-type quark masses, two neutrino mass-squared differences and three mixing angles in the neutrino sector. In other words, they will be output of our numerical fit. Again, we demand perturbativity and utilize the criteria $\chi^2/n \leq 1$ where $n(= 8)$ is the number of fitted observables.

The output of our fit are D_L, D_R, two Majorana phases and CP violating phase in PMNS matrix,

whereas model stipulates that

$$U_L = D_L \text{diag}(1, e^{i\eta_1}, e^{i\eta_2}) V_{\text{CKM}}^T \text{diag}(e^{i\kappa_1}, e^{i\kappa_2}, e^{i\kappa_3}) = D_L D(\eta) V_{\text{CKM}}^T D(\kappa) \tag{8.23}$$

$$U_R = U_L^* \text{diag}(e^{i\xi_1}, e^{i\xi_2}, e^{i\xi_3}) = U_L^* D(\xi), \tag{8.24}$$

$$E_L = \mathbb{1}, \tag{8.25}$$

$$E_R = \mathbb{1}, \tag{8.26}$$

$$N = \text{diag}(e^{i\gamma_1}, e^{i\gamma_2}, e^{i\gamma_3}) U_{\text{PMNS}}^* = D(\gamma) U_{\text{PMNS}}^* . \tag{8.27}$$

Here we introduce notation for four diagonal phase matrices $D(\eta)$, $D(\kappa)$, $D(\xi)$ and $D(\gamma)$. V_{CKM} is the mixing matrix with one CP violating phase (δ^{CKM}) and U_{PMNS} is the PMNS mixing matrix with one CP violating phase and two Majorana phases. Again, the connection between U_L and U_R in Eq. (8.24) is due to the fact that $M_U = M_U^T$. Note that the fit does not provide information on entries of $D(\eta)$, $D(\kappa)$ and $D(\xi)$. We will discuss if and when they enter proton decay predictions.

One of the outcomes of the numerical fit is that the neutrino sector exhibits normal mass hierarchy. This can be explained as follows. From Eq. (7.16) one can conclude that Yukawa matrix Y^d is a hierarchical diagonal matrix, where its entries are completely determined by the charged lepton Yukawa couplings. Again, we work in the mass eigenstate basis for the charged leptons. Since the matrix elements $(M_D)_{ij}$ are proportional to the linear combination of $(Y^d)_{ij}$ and $Y_i^c Y_j^a$, it is obvious that Y^a and Y^c should ideally both be hierarchical matrices to produce a good fit to data. This, on the other hand, is possible to achieve only for the normal ordering of the neutrino masses. Put differently, for the inverted scenario the entries in the first row and the first column of the neutrino mass matrix M_N are typically of the same order, whereas the lower 2×2 block is required to be somewhat smaller in magnitude. This, again, would be in conflict with hierarchical form of Y^a.

To summarize, this model accommodates charged lepton masses, the up-type quark masses, and the CKM parameters exactly. Combined numerical fit of the neutrino mass and mixing parameters, and the down-type quark masses yields D_L and D_R and consequently U_L and U_R. There are five unknown phases in U_L and three additional phases in U_R. However, in next section we show that for the analysis of the leading source of proton decay we only need two of these phases, i.e., η_1 and η_2 of Eq. (8.23), that reside in U_L.

Viable parameter spaces of our model for $M \geq 1\,\text{TeV}$, $M \geq 10\,\text{TeV}$, and $M \geq 100\,\text{TeV}$ scenarios are shown in panels of Fig. 8.3 in M_{Φ_1}-M_{Σ_1} plane together with contours of constant values of M_{GUT} and α_{GUT}. The contours for M_{GUT} are given in units of $10^{15}\,\text{GeV}$ and are shown as the vertical solid lines while the contours for α_{GUT} are given as dot-dashed lines that run horizontally. The parameter space that corresponds to $M_{\text{GUT}} \leq 6 \times 10^{15}\,\text{GeV}$ is discarded in this numerical study in all three instances due to the fact that such a low M_{GUT} is *a priori* not realistic with regard to the experimental input on the

proton decay lifetimes.

There are two dashed curves in all three plots of Fig. 8.3. With the outermost one we mark the boundary after which it is not possible to generate the correct mass scale for neutrinos with perturbative couplings, since their product exceeds value of 1 with certainty.

The region between the two dashed lines corresponds to the so-called "grey" zone of parameter space, meaning that in that region it is sometimes, but not always, possible, for some special choice of the six phases featured in Eq. (7.12), to find perturbative solution to the neutrino mass fit. The region to the left of the innermost dashed line gives correct neutrino mass fit for arbitrary choices of the six phases. Green solid contours are used to mark the naive bound on the correct neutrino mass scale. These green lines are generated by setting $2m_0/\sqrt{\Delta m_{31}^2}$ to 1, 10, and 100, as indicated in the plots of Fig. 8.3, for $\lambda' = 1$.

Note that there is already proton decay exclusion bound visible on all three panels in Fig. 8.3. This bound is actually provided by the numerical analysis of proton decay signatures and not some naive estimates.

Overall, the parameter space we investigate is in-between $M_{\mathrm{GUT}} = 6 \times 10^{15}\,\mathrm{GeV}$ and the outermost dashed line after which it is not possible to produce the neutrino mass observables with perturbative couplings.

8.1.4 Proton decay signatures

We have discussed proton decay in detail in Chapter 5, where we pointed out that amongst many types of proton decay, we would investigate two-body channels via gauge boson and scalar leptoquark mediations. After theoretical setup of how to evaluate proton decay widths, we conduct the numerical analysis where our idea is to accurately identify the most dominant channels for both types of proton decay, and compare these with current experimental limits and future expectations for a ten-year period of data taking at C.L. of 90 %.

Experimental bounds on proton decay lifetimes put constrain on allowed masses of associated mediators. The result of this numerical analysis is presented in Fig. 8.3. Namely, parameter space presented in Fig. 8.3 is constrained by experimental limit on the partial lifetime of $p \to \pi^0 e^+$ process due to the fact that it is the existing measurement of $p \to \pi^0 e^+$ that provides the most stringent bound. We will elaborate on this in the next paragraph.

Since the mass spectrum for all the particles is known in each unification point, as well as M_{GUT}, once we have accomplished the fermion sector fit, a lower bound for M_{GUT} can be set using experimental data on proton decay lifetimes. The region to the left from "proton decay bound" in Fig. 8.3 has been ruled out in this manner. It turns out that the partial lifetime limit of the process $p \to \pi^0 e^+$ is the most constraining one. Again, the decay width for this process [66] is:

$$\Gamma(p \to \pi^0 e^+) = \frac{m_p \pi}{2} \left(1 - \frac{m_\pi^2}{m_p^2}\right)^2 A_L^2 \frac{\alpha_{\text{GUT}}^2}{M_{\text{GUT}}^4}$$

$$\times \left(A_{SL}^2 \left|c(e^c, d)\langle\pi^0|(ud)_L u_L|p\rangle\right|^2 + A_{SR}^2 \left|c(e, d^c)\langle\pi^0|(ud)_R u_L|p\rangle\right|^2\right), \qquad (8.28)$$

where the relevant matrix elements are $\langle\pi^0|(ud)_L u_L|p\rangle = 0.134(5)(16)\,\text{GeV}^2$ and $\langle\pi^0|(ud)_R u_L|p\rangle = -0.131(4)(13)\,\text{GeV}^2$ [71]. Recall, the coefficients $c(e^C, d)$ and $c(e, d^C)$, in our model, are

$$c(e_\alpha^C, d_\beta) = e^{-i\xi_1}\left((D_L^*)_{11} + (U_L^T D_L^*)_{11}(U_L^*)_{11}\right), \qquad (8.29)$$

$$c(e, d^C) = e^{-i\xi_1}(D_R^\dagger)_{11}. \qquad (8.30)$$

Since these coefficients come under square in Eq. (8.28), the phase parameter ξ_1 vanishes and the only two relevant parameters that are not determined by the fermion mass fit are η_1 and η_2 from Eq. (8.23). Matrix elements of D_L and D_R are obtained through numerical fit and U_L can be expressed via D_L in relation to CKM matrix. Therefore, only η_1 and η_2 parameters survive to be varied in order to find the smallest possible value for $|c(e_\alpha^C, d_\beta)|$.

We present the viable parameter space in M_{Φ_1}-M_{Σ_1} plane in Fig. 8.3. Again, values for M_{Φ_1} and M_{Σ_1} are set from $10^{10}\,\text{GeV}$ to $10^{13.5}\,\text{GeV}$ and from $10^7\,\text{GeV}$ to $10^{14}\,\text{GeV}$, respectively, or in logarithmic scale from 10 to 13.5, and from 7 to 14 of $\log_{10}(M_{\Phi_1}/1\,\text{GeV})$ and $\log_{10}(M_{\Sigma_1}/1\,\text{GeV})$, respectively, with discretization step of 0.1 for both axes. One can observe three sets of contours for constant values of M_{GUT}, α_{GUT}, and m_0 for $|\lambda'| = 1$. In three panels in Fig. 8.3, one can see straight vertical, thin black lines which represent M_{GUT}, and almost horizontal dashed lines that represent α_{GUT}. Knowing this, due to the decay width dependence on M_{GUT} and α_{GUT}, i.e., $\Gamma \sim \alpha_{\text{GUT}}^2/M_{\text{GUT}}^4$, proton decay bound marked with pink line additionally denoted "proton decay bound" is presented on all three panels for different unification scenarios.

Proton decay via gauge bosons

Once we have determined the parameter space for $M \geq 1\,\text{TeV}$, $M \geq 10\,\text{TeV}$, and $M \geq 100\,\text{TeV}$ scenarios, we examine eight proton decay channels via gauge boson mediation for each of them. It was previously mentioned and explained that these decays depend on *a priori* two unknown parameters η_1 and η_2 except for the channels with antineutrinos in the final state. Hence, we use experimentally determined and observed values for all other parameters as input, while varying η_1 and η_2 for each point of interest in associated parameter space. Again, this will be performed for all three scenarios, i.e., $M \geq 1\,\text{TeV}$, $M \geq 10\,\text{TeV}$, and $M \geq 100\,\text{TeV}$. We thus vary η_1 and η_2 to find the maximum and minimum values of proton decay width for each channel. Once the minimum and maximum values for each decay channel

width are known, the plots that depict predicted ranges can be created.

We have taken one specific point, that is very close to the current proton decay bound, namely point Q featured in the upper panel of Fig. 8.3 with coordinates $M_{\Phi_1} = 10^{11.5}$ GeV and $M_{\Sigma_1} = 10^{8.7}$ GeV to showcase implementation of our approach. The results of our analysis for that point are given in left panel of Fig. 8.4. For channels with antineutrinos, i.e., $p \to \pi^+\bar{\nu}$ and $p \to K^+\bar{\nu}$, one can observe no flavor dependence as we have previously shown this in Eq. (5.27). Namely, with summation over neutrino flavors, any information associated with neutrino mixing parameters or any other phases vanishes from these proton decay signatures.

The channels with a charge lepton in final state exhibit dependence on η_1 and η_2, where η_2 effect can be neglected for all practical purposes. This can be seen in left panels of Fig. 8.5, where we give examples of η_1 and η_2 dependence for $p \to \pi^0 e^+$ and $p \to \eta^0 \mu^+$ at point Q. Note that even η_1 effect is rather mild. Explicit calculation of effects of η_1 and η_2 for point Q yields the following variations of decay widths: 2 % $(p \to \pi^0 e^+)$, 32 % $(p \to \pi^0 \mu^+)$, 0 % $(p \to \pi^+\bar{\nu})$, 2 % $(p \to \eta^0 e^+)$, 63 % $(p \to \eta^0 \mu^+)$, 2 % $(p \to K^0 e^+)$, 4 % $(p \to K^0 \mu^+)$, and 0 % $(p \to K^+\bar{\nu})$. These variations correspond to lengths of vertical blue bars of Fig. 8.4.

There are two proton decay channels shown in Fig. 8.4 — $p \to \pi^0 \mu^+$ and $p \to \eta^0 \mu^+$ — that exhibit the largest dependence on η_1. This is due to the fact that various contributions towards their decay widths are of approximately same magnitudes that even the smallest change in a single phase induces a large effect.
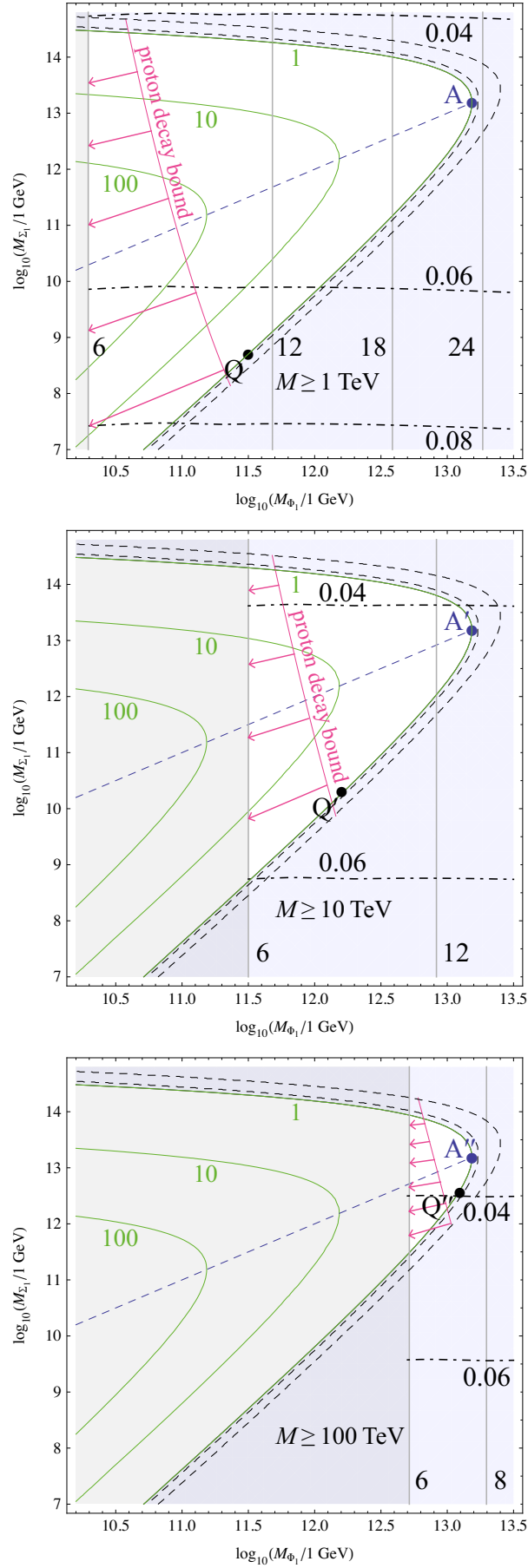
Figure 8.3: Experimentally viable parameter space of the model for scenarios when $M \geq 1\,\mathrm{TeV}$, $M \geq 10\,\mathrm{TeV}$, and $M \geq 100\,\mathrm{TeV}$, as indicated. For details, see the text.

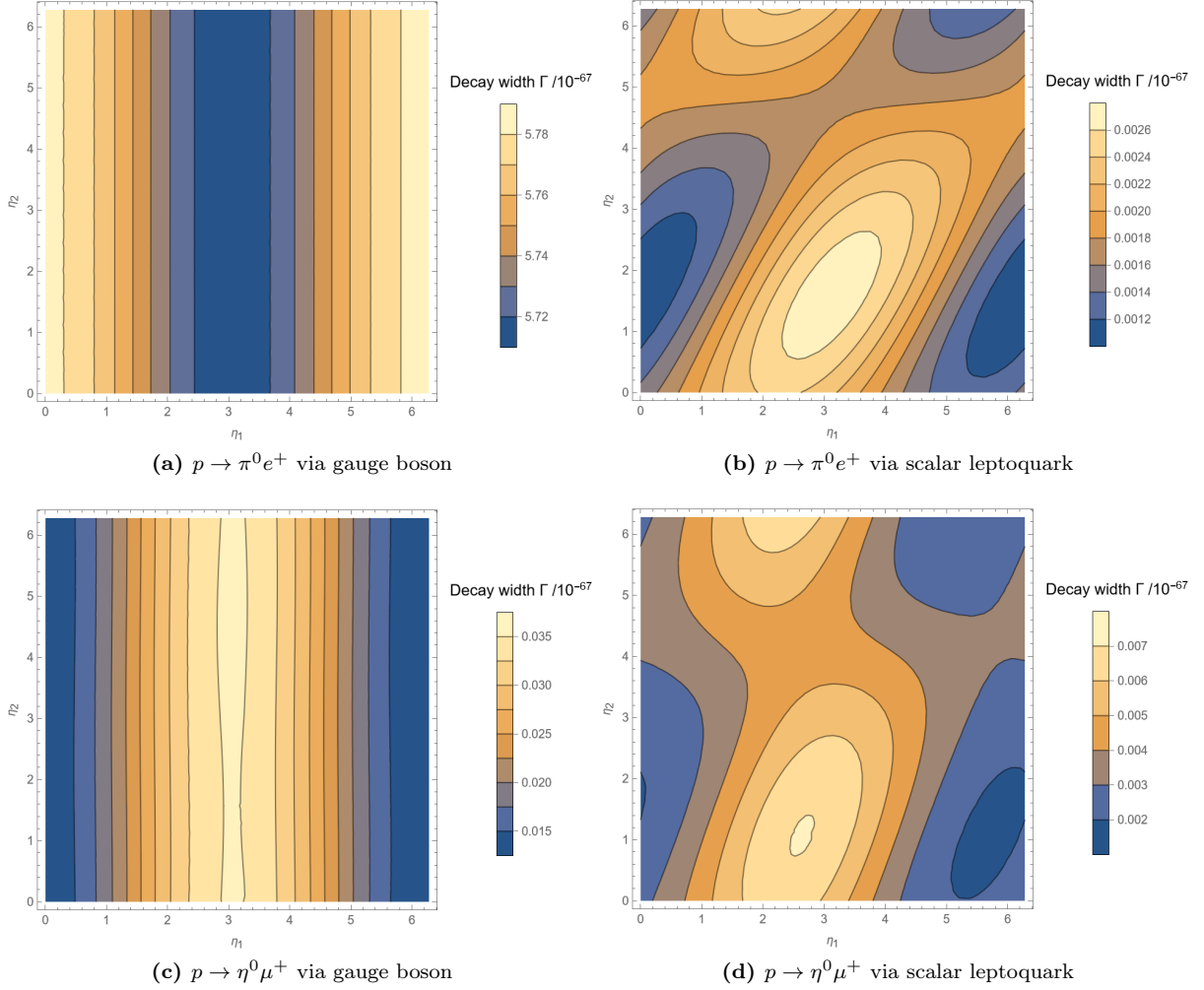**(a)** gauge boson mediation   **(b)** scalar leptoquark mediation
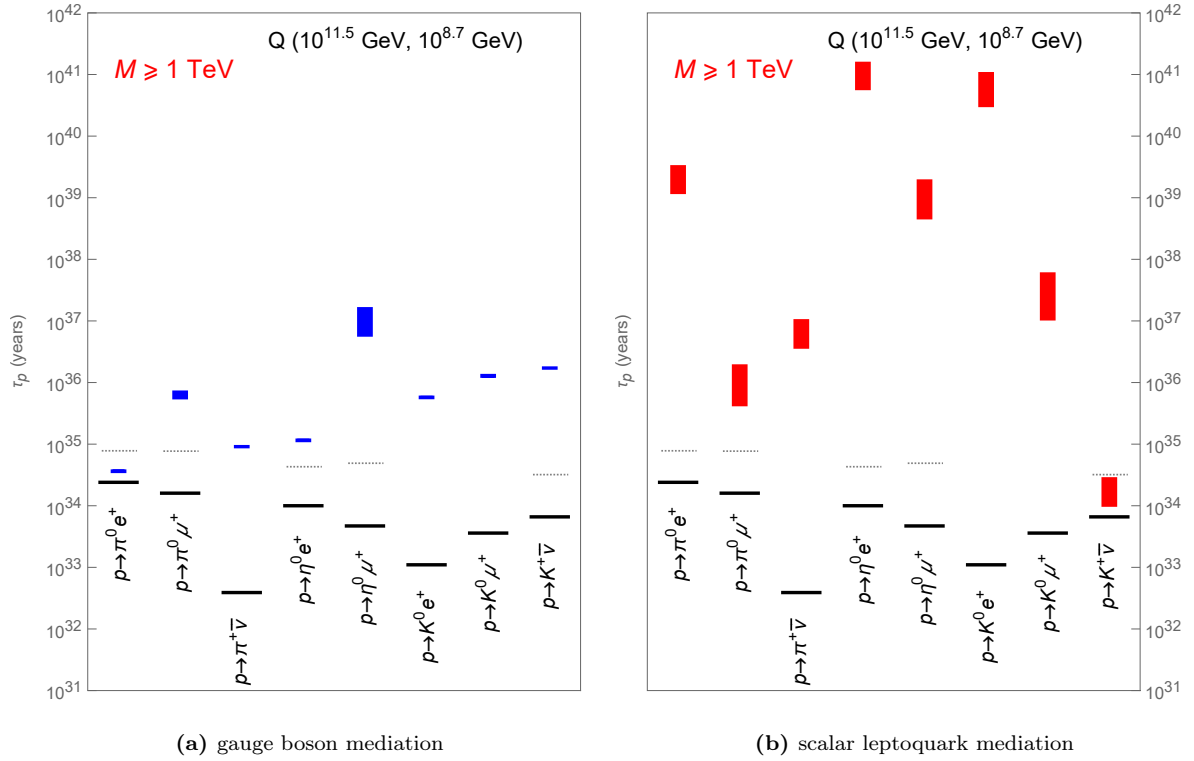
Figure 8.4: Proton decay widths for eight decay channels via **(a)** gauge boson and **(b)** scalar leptoquark mediations for point Q with coordinates of $M_{\Phi_1} = 10^{11.5}$ GeV and $M_{\Sigma_1} = 10^{8.7}$ GeV within $M \geq 1$ TeV scenario.

Proton decay via scalar leptoquark

The same numerical procedure can be performed to find proton decay widths via scalar leptoquark mediation. Note that we need to indicate the mass of scalar leptoquark. Hence, we set up initial value of Λ_3 to be 2×10^{12} GeV and proceed with the same numerical analysis as in the case of mediation via gauge boson for point Q of $M \geq 1$ TeV scenario. We, again, perform maximization and minimization for η_1 and η_2 parameters to plot predicted ranges using red bars as shown in right panel of Fig. 8.4. One can conclude that the only channel to be observed with certainty in experiments after a ten-year period of data taking is $p \to K^+ \overline{\nu}$. All other channels are not to be seen in decades to come in this model if scalar leptoquark mediation is the dominant source.

Uncertainty in prediction for proton decay widths for scalar leptoquark mediation is much more prominent than for gauge boson mediation. This is due to the fact that relevant widths depend not only on unitary transformations, but on Yukawa coupling matrix entries as well. We demonstrate the dependence on parameters η_1 and η_2 in Fig. 8.5 for $p \to \pi^0 e^+$ and $p \to \eta^0 \mu^+$. The variation of η_1 and η_2 yields the following decay width changes for point Q: 75 % ($p \to \pi^0 e^+$), 91 % ($p \to \pi^0 \mu^+$), 76 % ($p \to \pi^+ \overline{\nu}$), 76 % ($p \to \eta^0 e^+$), 94 % ($p \to \eta^0 \mu^+$), 81 % ($p \to K^0 e^+$), 92 % ($p \to K^0 \mu^+$), and 76 % ($p \to K^+ \overline{\nu}$).

(a) $p \to \pi^0 e^+$ via gauge boson

(b) $p \to \pi^0 e^+$ via scalar leptoquark

(c) $p \to \eta^0 \mu^+$ via gauge boson

(d) $p \to \eta^0 \mu^+$ via scalar leptoquark

Figure 8.5: Contour plots of proton decay widths in units of GeV scaled with factor of 10^{-67} for point Q as a function of η_1 and η_2 for $p \to \pi^0 e^+$ ((a) and (b)) and $p \to \eta^0 \mu^+$ ((c) and (d)) decay channels, where left panels correspond to mediation via gauge boson and right panels are for mediation via scalar leptoquark.

Correlation between two different proton decay mediations

In order to accomplish comparative study between gauge boson and scalar leptoquark mediation signatures for the partial proton decay lifetimes, we have chosen one particular point in viable parameter space for each of three scenarios $M \geq 1\,\text{TeV}$, $M \geq 10\,\text{TeV}$, and $M \geq 100\,\text{TeV}$ as our starting point. Namely, these are points Q, Q$'$, and Q$''$ in Fig. 8.3. Since we are interested in those parts of parameter space that could be probed, at least in principle, in future experiments, the points Q, Q$'$, and Q$''$ were chosen to be near to the current proton bound expressed as pink straight line in Fig. 8.3. We subsequently evaluate $\alpha_{\text{GUT}}^2/M_{\text{GUT}}^4$ at these points to be able to find all other points that satisfy criteria that the associated value of $\alpha_{\text{GUT}}^2/M_{\text{GUT}}^4$ at those points is within $\pm 3\,\%$ with respect to the values extracted for points Q, Q$'$, and Q$''$. This requirement is needed in order to capture enough points for our study, as our parameter space in Fig. 8.3 is given with lattice spacing of 0.1 for both M_{Φ_1} and M_{Σ_1} parameters. Once all these points are known, we evaluate gauge boson mediated proton decay widths for all eight channels where

114

we also vary η_1 and η_2 phases in a manner outlined before. The results for all three scenarios for gauge boson mediation obtained with this procedure is summarized in Fig. 8.6.

The points that are used to study proton decay signatures via gauge boson mediation are the same points we use to look at proton decay via scalar leptoquark mediation. To generate associated proton decay widths, we take that $M_{\Lambda_3} = 2 \times 10^{12}\,\text{GeV}$ for $M \geq 1\,\text{TeV}$ scenario and $M_{\Lambda_3} = 1.6 \times 10^{12}\,\text{GeV}$ for scenarios $M \geq 10\,\text{TeV}$ and $M \geq 100\,\text{TeV}$. These choices ensure that the scalar mediated proton decay signatures will be observed with certainty at future proton decay experiments. The outcome of this numerical analysis is presented in Fig. 8.7.

Finally, we place signatures for both types of mediation side by side in Fig. 8.8, where blue bars are used for gauge boson mediation predictions, red bars are used for predictions associated with scalar leptoquark mediation, current experimental limits are represented by thin black lines, and grey dashed lines stand for future expectations after a ten-year period of data taking at $90\,\%$ C.L., if and where available.

Several comments are in order. For gauge boson mediation the uncertainty in predictions for partial proton lifetimes with charged leptons in final state comes from three sources: (i) $\pm 3\%$ originates from the fact that $\alpha_{\text{GUT}}^2/M_{\text{GUT}}^4$ ratio is allowed to vary from point to point due to the discrete nature of our parameter space, (ii) unitary transformations, including CKM values, that also vary from point to point, and (iii) unknown phases η_1 and η_2. For antineutrinos in final states, the uncertainty originates only from first two sources.

When it comes to scalar leptoquark mediation, the uncertainty primarily originates from the fact that the fermion mass fit varies from point to point and the need to vary phases η_1 and η_2 to find accurate lower and upper bounds for associated proton decay widths. Note, however, that the uncertainties in proton decay widths associated with scalar leptoquark mediation are much larger than those associated with gauge boson mediation. This is primarily due to fact that gauge boson mediation is affected by unitary transformations of the Standard Model fermion fields whereas the scalar leptoquark mediation is proportional to products of Yukawa couplings of those fermions.

Side by side comparison of Fig. 8.8 leaves us with the following conclusions. If this model is realized in nature, and if proton is observed to decay to π^0 and e^+, the decay is mediated via gauge boson, and if it is observed to decay to K^+ and $\bar{\nu}$, the decay is mediated via scalar leptoquark. If both $p \to \pi^0 e^+$ and $p \to K^+ \bar{\nu}$ are observed, there is also a possibility to observe third process $p \to \pi^0 \mu^+$ within the ten-year period of data taking. This would also require fortuitous interference between the gauge and scalar leptoquark contributions at the amplitude level. The remaining five channels will be experimentally inaccessible in decades to come within this particular scenario.
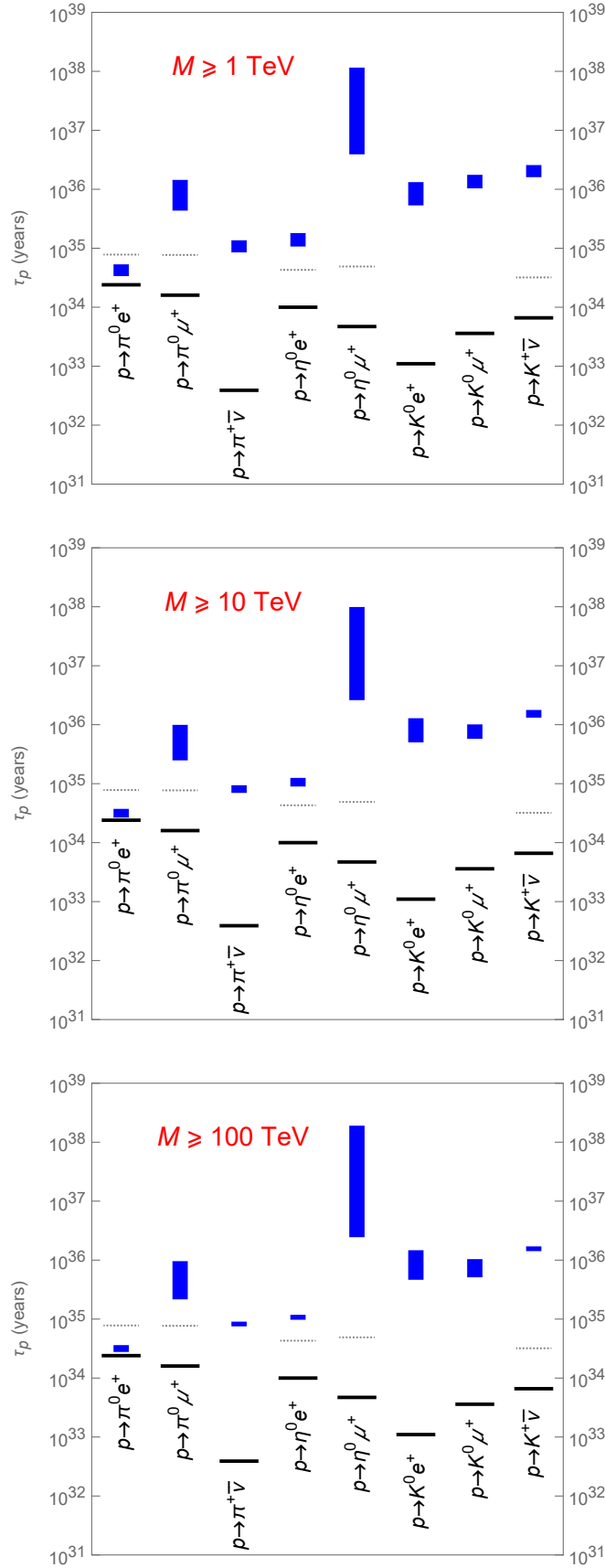
Figure 8.6: Proton decay channels via gauge boson mediation within $M \geq 1\,\text{TeV}$, $M \geq 10\,\text{TeV}$, and $M \geq 100\,\text{TeV}$ scenarios, where thin black horizontal lines represent current experimental limits, blue vertical bars stand for expected ranges within the model under consideration, and horizontal grey dashed lines represent future experimental sensitivities after a ten-year period of data taking at $90\,\%\,\text{C.L.}$
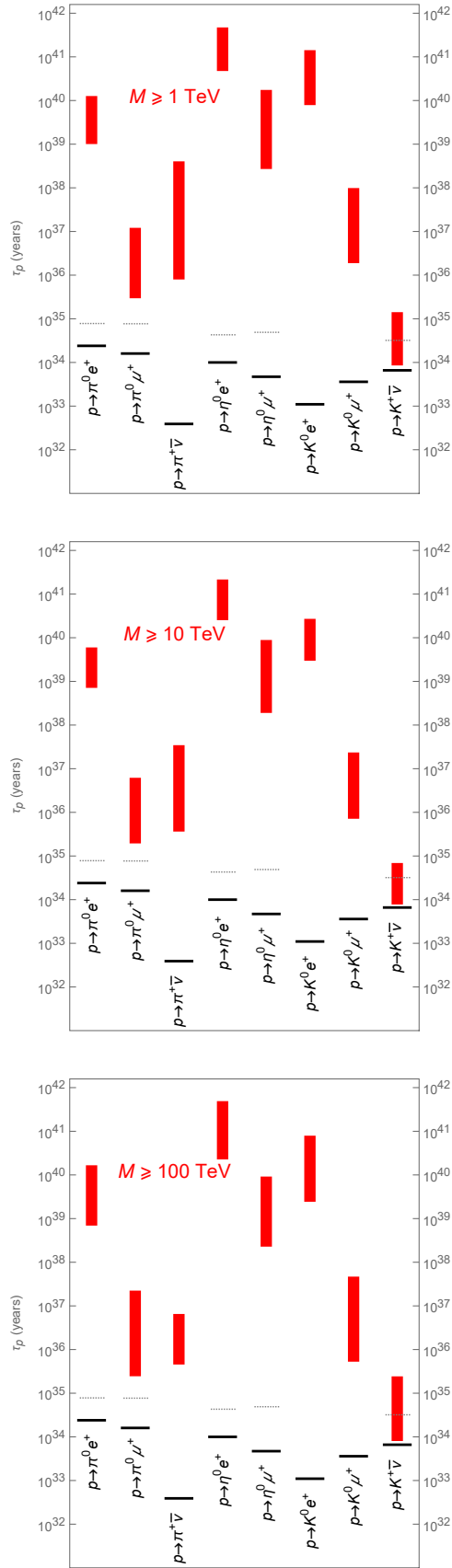
Figure 8.7: Proton decay channels via scalar leptoquark mediation within $M \geq 1\,\text{TeV}$, $M \geq 10\,\text{TeV}$, and $M \geq 100\,\text{TeV}$ scenarios, where thin black horizontal lines represent current experimental limits, red vertical bars stand for expected ranges within the model under consideration, and horizontal grey dashed lines represent future experimental sensitivities after a ten-year period of data taking at $90\,\%\,\text{C.L.}$
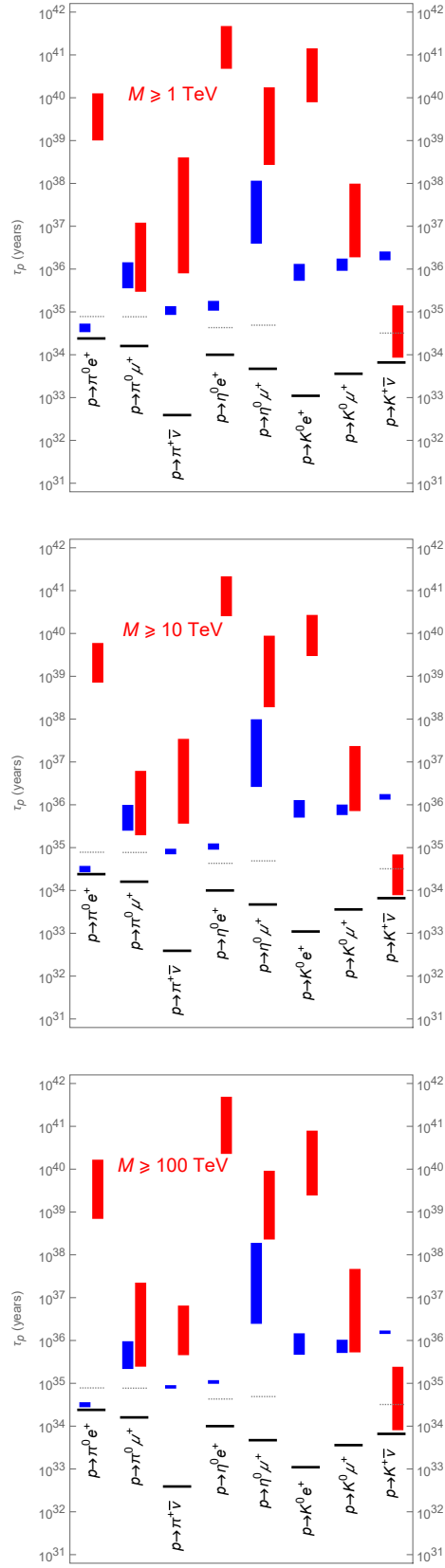
Figure 8.8: Correlation of proton decay signatures via gauge boson and scalar leptoquark mediation within $M \geq 1\,\text{TeV}$, $M \geq 10\,\text{TeV}$, and $M \geq 100\,\text{TeV}$ scenarios. Thin black lines represent current experimental limits, blue vertical bars are predictions for gauge boson mediation signatures, red vertical bars are corresponding predictions for scalar leptoquark mediations and grey dashed lines represent future experimental sensitivities after a ten-year period of data taking at $90\,\%$ C.L.

Part IV

Summary and conclusions

Chapter 9

Discussion

> A true student is like a sponge.
> Absorbing what goes on around
> him, filtering it, latching on to
> what he can hold. A student is
> self-critical and self-motivated,
> always trying to improve his
> understanding so that he can
> move on to next topic, the next
> challenge. A real student is also
> his own teacher and his own
> critic. There is no room for ego
> there.
>
> *Ryan Holiday*

À la fin...

Proton decay is an exciting and appealing hypothetical prediction with many facets. We have opted to investigate one particular path paved in a specific $SU(5)$ model. In that model, we have analyzed proton decay to two-body final states, and we have found accurate predictions for all eight possible decay channels via gauge boson and scalar leptoquark mediation. We briefly spell out our main findings in what follows.

9.1 Summary and conclusions

There are only two possible types of mediators of proton decay within the model in question. The anticipated experimental signal of these decay processes can, hence, originate solely from gauge boson

mediation, or entirely from scalar leptoquark mediation, or from combination of the two. Our analysis stipulates that we can conclude with certainty that if in experiments proton is observed to decay to π^0 and e^+, the decay is mediated via gauge boson, and if it is observed to decay to K^+ and $\overline{\nu}$, the decay is mediated via scalar leptoquark. If both $p \to \pi^0 e^+$ and $p \to K^+ \overline{\nu}$ are observed, there is also a possibility to observe third process $p \to \pi^0 \mu^+$ within the ten-year period of data taking. This would also require fortuitous interference between the gauge and scalar leptoquark contributions at the amplitude level. The remaining five channels will be experimentally inaccessible in decades to come. Again, two channels that might be observed in future experiments are $p \to \pi^0 e^+$ and $p \to K^+ \overline{\nu}$. If both are observed, then the third channel $p \to \pi^0 \mu^+$ might be accessible.

The beauty of a specific $SU(5)$ model we have been analyzing proton decay in, lies in its simplicity since the only parameters that are not determined via fermion mass fit that affect proton decay predictions are two phases η_1 and η_2. Moreover, in case of gauge boson mediation, almost all dependence falls solely on η_1.

The fact that the proton decay signatures from two different sources of new physics can be predicted at this level of accuracy has not been observed in other models of $SU(5)$ unification. Moreover, there does not exist a single correlation study of proton decay signatures via two different sources of new physics in the literature. This work can serve as an example of a self-consistent study of proton decay signatures and might be used as a guide on how to analyze models with similar features if and when they are identified. Finally, the tools developed in this analysis are applicable to other models of unification and can thus be of help in generating accurate predictions for expected proton decay signatures.

Appendices

Appendix A

Einstein index notation

A convenient notation in expressions with vectors, matrices and tensors is Einstein index notation. There are some rules that need to be followed in this notation:

- Any term in an expression can have each index only two times,

- Repeated indices are the ones summation is conducted over, and

- Each term must have identical not repeating indices.

For example, if one wants to do summation over index i in certain expression such as:

$$A = \sum_j B_{ij} r_j \tag{A.1}$$

then it would read as:

$$A = \sum_j B_{ij} r_j \equiv B_{ij} r_j \tag{A.2}$$

whereas this expression:

$$C = B_{ij}r_jp_j + q_i \tag{A.3}$$

would not be correct in this index notation due to the fact that first rule was not followed (index j is repeated more than two times in first term).

Another example of invalid expression in this notation is this:

$$D = B_{ijk}r_k + E_{il} \tag{A.4}$$

because first term has non-repeated index j and second l.

A.1 Free and dummy indices

Using Eq. (A.2), we can rewrite and add:

$$A = \sum_j B_{ij}r_j \equiv B_{ij}r_j = (\mathbf{Br})_i = \mathbf{q}_i \tag{A.5}$$

Free indices are indices present on both sides of equation, and in case of Eq. (A.5), that is for example, index i.

Dummy indices are indices present on one side of equation, but not on the other. Also, these indices come in an even amount of times in each product. In Eq. (A.5) that is index j.

A.2 The Kronecker δ, Levi-Civita ε_{ijk} and metric tensor $g_{\mu\nu}$

In writing expressions in Einstein's notation, but also in others as well, symbols mentioned in the title of this section, are not just useful but also inevitable when deriving expressions and doing calculations.

We will start with Kronecker δ symbol that reads like this:

$$\delta_{ij} = \begin{cases} 1 & i = j \\ 0 & i \neq j \end{cases} \tag{A.6}$$

or with Iverson brackets:

$$\delta_{ij} = [i = j] \tag{A.7}$$

The role of this symbol is to replace one index by another:

$$\delta_{ij} v_i = v_j \tag{A.8}$$

There are also these two properties:

$$v_i \delta_{ij} = v_j \tag{A.9}$$

$$\delta_{ik}\delta_{kj} = \delta_{ij} \tag{A.10}$$

from where we can conclude that δ matrix is identity matrix. For 3×3 it reads:

$$\delta_{ij} = \begin{pmatrix} 1 & 0 & 0 \\ 0 & 1 & 0 \\ 0 & 0 & 1 \end{pmatrix} \tag{A.11}$$

Levi-Civita ε_{ijk} symbol or tensor is a tensor that in dependence of permutation of indices gives three different values. Since we started with Levi-Civita in three-dimensional space, we will give its mathematical formulation in that specific case:

$$\varepsilon_{ijk} = \begin{cases} 1 & \text{if } (i,j,k) \text{ is } (1,2,3),\ (2,3,1) \text{ or } (3,1,2) \\ -1 & \text{if } (i,j,k) \text{ is } (1,3,2),\ (2,1,3) \text{ or } (3,2,1) \\ 0 & \text{if } i=j,\ j=k \text{ or } k=i \end{cases} \tag{A.12}$$

In four-dimensional space, it would read like this:

$$\varepsilon_{ijkl} = \begin{cases} 1 & \text{if } (i,j,k,l) \text{ is an even permutation of } (1,2,3,4) \\ -1 & \text{if } (i,j,k,l) \text{ is an odd permutation of } (1,2,3,4) \\ 0 & \text{otherwise} \end{cases} \tag{A.13}$$

For example:

$$\varepsilon_{1432} = -\varepsilon_{1234} = -1$$

$$\varepsilon_{2134} = -\varepsilon_{1234} = -1$$

$$\varepsilon_{4321} = -\varepsilon_{1324} = -(\varepsilon_{1234}) = -1$$

$$\varepsilon_{2132} = -\varepsilon_{2132} = 0 \tag{A.14}$$

In general case, in n dimensions, we can write it as:

$$\varepsilon_{a_1 a_2 a_3 \ldots a_n} = \begin{cases} 1 & \text{if } (a_1 a_2 a_3 \ldots a_n) \text{ is an even permutation of } (1, 2, 3, \ldots n) \\ -1 & \text{if } (a_1 a_2 a_3 \ldots a_n) \text{ is an odd permutation of } (1, 2, 3, \ldots n) \\ 0 & \text{otherwise} \end{cases} \tag{A.15}$$

In product of two vectors $\mathbf{a}$ and $\mathbf{b}$, we can use Levi-Civita in Einstein notation in the following form:

$$(\mathbf{a} \times \mathbf{b})^i = \varepsilon_{ijk} a^j b^k \tag{A.16}$$

In the triple scalar product, it is used in this form:

$$\mathbf{a} \cdot (\mathbf{b} \times \mathbf{c}) = \varepsilon_{ijk} a^i b^j c^k \tag{A.17}$$

Metric tensor $g_{\mu\nu}$ reads:

$$g_{\mu\nu} = \begin{pmatrix} 1 & 0 & 0 & 0 \\ 0 & -1 & 0 & 0 \\ 0 & 0 & -1 & 0 \\ 0 & 0 & 0 & -1 \end{pmatrix} = \begin{pmatrix} 1 & 0 \\ 0 & -I_3 \end{pmatrix} \tag{A.18}$$

We have further discussed, used and explained this tensor in appendices B and C.

Appendix B

Dirac algebra and gamma matrices

I seem to have been only like a
boy playing on the seashore, and
diverting myself in now and then
finding a smoother pebble or a
prettier shell than ordinary,
whilst the great ocean of truth
lay all undiscovered before me.

Isaac Newton

Paul Dirac introduces [57] a Hamiltonian linear regarding the momentum operator, for the purpose of having a relativistically covariant equation for the quantum mechanical wave function:

$$H = \gamma^0 \left(\gamma \cdot \mathbf{p} + m \right) \tag{B.1}$$

where m is the particle mass and $\mathbf{p}$ is the momentum operator. These γ^0 and γ matrices are dimensionless. Standard 4×4 Dirac matrices $\gamma^\mu = \{\gamma^0, \gamma^1, \gamma^2, \gamma^3\}$ represent the set of conventional matrices that generate the matrix representation of Clifford algebra. In Minkowski space, where metric $M = \{x^\mu\}$ is denoted as pseudo-euclidean, due to the form of the metric tensor $g_{\mu\nu}$:

$$g_{\mu\nu} = \begin{pmatrix} 1 & 0 & 0 & 0 \\ 0 & -1 & 0 & 0 \\ 0 & 0 & -1 & 0 \\ 0 & 0 & 0 & -1 \end{pmatrix} = \begin{pmatrix} 1 & 0 \\ 0 & -I_3 \end{pmatrix} \tag{B.2}$$

the column vectors on which the γ^μ matrices act become a space of spinors. Gamma matrices in Dirac representation are of this form:

$$\gamma^0 = \begin{pmatrix} 1 & 0 & 0 & 0 \\ 0 & 1 & 0 & 0 \\ 0 & 0 & -1 & 0 \\ 0 & 0 & 0 & -1 \end{pmatrix} \quad \gamma^1 = \begin{pmatrix} 0 & 0 & 0 & 1 \\ 0 & 0 & 1 & 0 \\ 0 & -1 & 0 & 0 \\ -1 & 0 & 0 & 0 \end{pmatrix}$$

$$\text{(B.3)}$$

$$\gamma^2 = \begin{pmatrix} 0 & 0 & 0 & -i \\ 0 & 0 & i & 0 \\ 0 & i & 0 & 0 \\ -i & 0 & 0 & 0 \end{pmatrix} \quad \gamma^3 = \begin{pmatrix} 0 & 0 & 1 & 0 \\ 0 & 0 & 0 & -1 \\ -1 & 0 & 0 & 0 \\ 0 & 1 & 0 & 0 \end{pmatrix}$$

In order for gamma matrices to generate Clifford algebra, they must obey the anticommutation relation:

$$\{\gamma^\mu, \gamma^\nu\} = \gamma^\mu \gamma^\nu + \gamma^\nu \gamma^\mu = 2g_{\mu\nu}I_4 \tag{B.4}$$

where I_4 denotes the unit matrix 4×4.

B.1 The fifth gamma matrix

The fifth gamma matrix is used in quantum mechanics' theories with the term of chirality. Namely, the projector of left and right handed states is defined with γ^5:

$$P_L = \frac{1 - \gamma_5}{2} \tag{B.5}$$

$$P_R = \frac{1 + \gamma_5}{2} \tag{B.6}$$

The matrix γ^5 itself is defined in the Dirac basis in the following form:

$$\gamma^5 = i\gamma^0\gamma^1\gamma^2\gamma^3 = \begin{pmatrix} 0 & 0 & 1 & 0 \\ 0 & 0 & 0 & 1 \\ 1 & 0 & 0 & 0 \\ 0 & 1 & 0 & 0 \end{pmatrix} \tag{B.7}$$

It has some interesting properties:

- Hermitian matrix:

$$\left(\gamma^5\right)^\dagger = \gamma^5 \tag{B.8}$$

- With eigenvalues ± 1:

$$\left(\gamma^5\right)^2 = I_4 \tag{B.9}$$

- Anticommutes with the other four gamma matrices:

$$\left\{\gamma^5,\,\gamma^\mu\right\} = \gamma^5\gamma^\mu + \gamma^\mu\gamma^5 = 0 \tag{B.10}$$

B.2 Trace properties and charge conjugation

There are several trace identities that apply for gamma matrices:

1. $\mathrm{Tr}\left(\gamma^0\right) = 0$

2. $\mathrm{Tr}\left(\gamma^{\mu_1}\cdots\gamma^{\mu_n}\right) = 0$ for $n = 2k+1$

3. $\mathrm{Tr}\left(\gamma^5\gamma^{\mu_1}\cdots\gamma^{\mu_n}\right) = 0$ for $n = 2k+1$

4. $\mathrm{Tr}\left(\gamma^\mu\gamma^\nu\right) = 4g_{\mu\nu}$

5. $\mathrm{Tr}\left(\gamma^\mu\gamma^\nu\gamma^\rho\gamma^\sigma\right) = 4\left(g_{\mu\nu}g_{\rho\sigma} - g_{\mu\rho}g_{\nu\sigma} + g_{\mu\sigma}g_{\nu\rho}\right)$

6. $\mathrm{Tr}\left(\gamma^5\right) = \mathrm{Tr}\left(\gamma^\mu\gamma^\nu\gamma^5\right) = 0$

7. $\mathrm{Tr}\left(\gamma^{\mu_1}\cdots\gamma^{\mu_n}\right) = \mathrm{Tr}\left(\gamma^{\mu_n}\cdots\gamma^{\mu_1}\right)$

Gamma matrices are also used in defining charge conjugation operator:

$$C\gamma^\mu C^{-1} = -(\gamma^\mu)^T \tag{B.11}$$

where $C = \gamma^0\gamma^2$ with a property $C^{-1} = C^\dagger = C^T = -C$.

In quantum field theory, in the studies and discussions on Dirac fields, it is often used Feynman slash notation or as it is sometimes referred as Dirac slash notation [118]:

$$\slashed{A} \overset{\text{def}}{=} \gamma^\mu A_\mu \tag{B.12}$$

There are specific identities in this notation, derived from identities that gamma matrices obey:

1. $\slashed{A}\slashed{B} = A \cdot B - iA_\mu\sigma^{\mu\nu}B_\nu$ with $\sigma^{\mu\nu} = \frac{i}{2}[\gamma^\mu,\gamma^\nu]$

2. $\slashed{A}\slashed{A} = A^\mu A^\nu \gamma_\mu\gamma_\nu = \frac{1}{2}A^\mu A^\nu(\gamma_\mu\gamma_\nu + \gamma_\nu\gamma_\mu) = \frac{1}{2}A^\mu A^\nu\,2\,g_{\mu\nu}I_4 = A^2$

3. $\slashed{\partial}^2 = \partial^2 \cdot I_4$

4. $\text{Tr}\,(\slashed{A}\slashed{B}) = 4\,(A \cdot B)$

5. $\text{Tr}\,(\gamma^5 \slashed{A}\slashed{B}) = 0$

6. $\gamma_\mu \slashed{A} \gamma^\mu = -2\slashed{A}$

7. $\gamma_\mu \slashed{A}\slashed{B} \gamma^\mu = 4\,(A \cdot B)$

8. $\text{Tr}\,(\slashed{A}) = \text{Tr}\,(\slashed{A}\slashed{B}\slashed{C}) = \text{Tr}\,(\slashed{A}\slashed{B}\slashed{C}\slashed{D}\slashed{E}) = 0$

Appendix C

Fierz Transformations

Life cannot have had a random beginning... The trouble is that there are about 2000 enzymes, and the chance of obtaining them all in a random trial is only one part in $10^{40\,000}$ an outrageously small probability that could not be faced even if the whole universe consisted of organic soup.

Fred Hoyle

Fierz identities or Fierz transformations [119] represent an useful tool in quantum field theory. More precise, we employ this tool in explicit calculations in four-fermion interactions. In this thesis, proton decay processes include four-fermion interactions.

For each particle involved, there is a corresponding spinor. In an expression to which we apply Fierz identities, there are two Dirac bilinears in a product that is usually called quadrilinear:

$$[\bar{\omega}_1 M \omega_2][\bar{\omega}_3 M' \omega_4] \tag{C.1}$$

Dirac bilinears can be placed in any order in its product, but the spinors cannot. Therefore, the order of appearance of four spinors is important and it will play the major role in Fierz identities.

In Appendix A we have presented Dirac matrices and algebra. Using these matrices, it is possible to construct set of 16 matrices in order to have 16-dimensional space of all the 4×4 matrices. The set usually [120] corresponds to matrices in the following way:

$$\Gamma_S^1 \equiv \mathbb{1},$$

$$\Gamma_V^1 \text{ to } \Gamma_V^4 \equiv \gamma^\mu,$$

$$\Gamma_T^1 \text{ to } \Gamma_T^6 \equiv \sigma^{\mu\nu}, \quad (\mu < \nu), \tag{C.2}$$

$$\Gamma_A^1 \text{ to } \Gamma_A^4 \equiv i\gamma^\mu\gamma_5,$$

$$\Gamma_P^1 \equiv \gamma_5,$$

where we have already known:

$$\gamma^5 = i\,\gamma^0\,\gamma^1\,\gamma^2\,\gamma^3 = \begin{pmatrix} 0 & 0 & 1 & 0 \\ 0 & 0 & 0 & 1 \\ 1 & 0 & 0 & 0 \\ 0 & 1 & 0 & 0 \end{pmatrix} \quad \text{and} \quad \sigma_{\mu\nu} = \frac{i}{2}\left[\gamma^\mu, \gamma^\nu\right]. \tag{C.3}$$

Since the form of the metric tensor $g_{\mu\nu}$ is given with:

$$g_{\mu\nu} = \begin{pmatrix} 1 & 0 & 0 & 0 \\ 0 & -1 & 0 & 0 \\ 0 & 0 & -1 & 0 \\ 0 & 0 & 0 & -1 \end{pmatrix} = \begin{pmatrix} 1 & 0 \\ 0 & -I_3 \end{pmatrix} \tag{C.4}$$

we can then write:

$$\left\{\gamma^\mu, \gamma^\nu\right\} = \gamma^\mu\gamma^\nu + \gamma^\nu\gamma^\mu = 2g_{\mu\nu}\mathbb{1} \tag{C.5}$$

Knowing these propreties:

$$\text{Tr}[\gamma_\mu] = 0,$$

$$\text{Tr}[\gamma_\mu\gamma_\nu] = 4g_{\mu\nu}$$

$$\text{Tr}[\gamma_\mu\gamma_\alpha\gamma_\nu] = 0 \tag{C.6}$$

$$\text{Tr}[\gamma_\mu\gamma_\alpha\gamma_\nu\gamma_\beta] = 4\left(g_{\mu\alpha}g_{\nu\beta} - g_{\mu\nu}g_{\alpha\beta} + g_{\mu\beta}g_{\alpha\nu}\right)$$

together with Eq. (C.2), we can deduce the basis for derivation of all Fierz identities:

$$\text{Tr}[\Gamma_I\Gamma^J] = \delta_I^J \tag{C.7}$$

where I and J can represent A, P, S, T and V.

Previously defined set of 16 matrices in Eq. (C.2) we can redefine in writing it in the following

way [121, 122]:

$$\Gamma^A = \left\{1, \gamma^0, i\gamma^1, i\gamma^2, i\gamma^3, \gamma^{01}, \gamma^{02}, \gamma^{03}, i\gamma^{12}, i\gamma^{13}, i\gamma^{23}, i\gamma^{012}, i\gamma^{013}, i\gamma^{023}, \gamma^{123}, i\gamma^{0123}\right\} . \tag{C.8}$$

Lower-order matrices are defined in Eq. (B.3), and higher-order matrices are built from these:

$$\gamma^{01} = \frac{1}{2}\left(\gamma^0\gamma^1 - \gamma^1\gamma^0\right)$$

$$\gamma^{02} = \frac{1}{2}\left(\gamma^0\gamma^2 - \gamma^2\gamma^0\right)$$

$$\gamma^{03} = \frac{1}{2}\left(\gamma^0\gamma^3 - \gamma^3\gamma^0\right)$$

$$\gamma^{12} = \frac{1}{2}\left(\gamma^1\gamma^2 - \gamma^2\gamma^1\right)$$

$$\gamma^{13} = \frac{1}{2}\left(\gamma^1\gamma^3 - \gamma^3\gamma^1\right)$$

$$\gamma^{23} = \frac{1}{2}\left(\gamma^2\gamma^3 - \gamma^3\gamma^2\right)$$

$$\gamma^{012} = \frac{1}{3}\left(\gamma^0\gamma^{12} - \gamma^1\gamma^{02} + \gamma^2\gamma^{01}\right)$$

$$\gamma^{013} = \frac{1}{3}\left(\gamma^0\gamma^{13} - \gamma^1\gamma^{03} + \gamma^3\gamma^{01}\right)$$

$$\gamma^{023} = \frac{1}{3}\left(\gamma^0\gamma^{23} - \gamma^2\gamma^{03} + \gamma^3\gamma^{02}\right)$$

$$\gamma^{123} = \frac{1}{3}\left(\gamma^1\gamma^{23} - \gamma^2\gamma^{13} + \gamma^3\gamma^{12}\right)$$

$$\gamma^{0123} = \frac{1}{4}\left(\gamma^0\gamma^{123} - \gamma^1\gamma^{023} + \gamma^2\gamma^{013} - \gamma^3\gamma^{012}\right)$$

$$\tag{C.9}$$

The identity we will be using in Fierz transformation is:

$$\left(\Gamma^A\right)_{ij}\left(\Gamma^B\right)_{kl} = \sum_{C,D} C^{AB}_{CD}\left(\Gamma^C\right)_{il}\left(\Gamma^D\right)_{kj} . \tag{C.10}$$

Eq. (C.10) is linear decomposition. This is viable since all Γ's form a complete basis for all 4×4 matrices. Our next step is to find coefficients C^{AB}_{CD}. Firstly, we will multiply Eq. (C.10) by $\left(\Gamma^E\right)_{li}\left(\Gamma^F\right)_{jk}$:

$$\left(\Gamma^E\right)_{li}\left(\Gamma^F\right)_{jk}\left(\Gamma^A\right)_{ij}\left(\Gamma^B\right)_{kl} = \sum_{C,D} C^{AB}_{CD}\left(\Gamma^E\right)_{li}\left(\Gamma^F\right)_{jk}\left(\Gamma^C\right)_{il}\left(\Gamma^D\right)_{kj} \tag{C.11}$$

$$\mathrm{tr}\left(\Gamma^E\Gamma^A\Gamma^F\Gamma^B\right) = \sum_{C,D} C^{AB}_{CD}\,\mathrm{tr}\left(\Gamma^E\Gamma^C\right)\mathrm{tr}\left(\Gamma^F\Gamma^D\right) \tag{C.12}$$

$$\mathrm{tr}\left(\Gamma^E\Gamma^A\Gamma^F\Gamma^B\right) = 16\,C^{AB}_{CD} \tag{C.13}$$

$$C^{AB}_{CD} = \frac{1}{16}\,\mathrm{tr}\left(\Gamma^C\Gamma^A\Gamma^D\Gamma^B\right) . \tag{C.14}$$

135

Eq. (C.13) was derived from completeness relation and eq. (C.14) comes from relabelling of indices. Next we directly apply matrix identity:

$$
\begin{aligned}
\left(\overline{\omega}_1 \Gamma^A \omega_2\right)\left(\overline{\omega}_3 \Gamma^B \omega_4\right) &= \left(\overline{\omega}_1\right)_i \left(\omega_2\right)_j \left(\overline{\omega}_3\right)_k \left(\omega_4\right)_l \left(\Gamma^A\right)_{ij} \left(\Gamma^B\right)_{kl} \\
&= \left(\overline{\omega}_1\right)_i \left(\omega_2\right)_j \left(\overline{\omega}_3\right)_k \left(\omega_4\right)_l \sum_{C,D} C_{CD}^{AB} \left(\Gamma^C\right)_{il} \left(\Gamma^D\right)_{kj} \\
&= \sum_{C,D} C_{CD}^{AB} \left(\overline{\omega}_1 \Gamma^C \omega_4\right)\left(\overline{\omega}_3 \Gamma^D \omega_2\right)
\end{aligned}
\tag{C.15}
$$

in order to derive the Fierz identities or transformations:

$$
\begin{aligned}
\left(\overline{\omega}_1 \omega_2\right)\left(\overline{\omega}_3 \omega_4\right) &= \sum_{C,D} C_{CD}^{11} \left(\overline{\omega}_1 \Gamma^C \omega_4\right)\left(\overline{\omega}_3 \Gamma^D \omega_2\right) \\
&= \sum_{C,D} \frac{1}{16} \operatorname{tr}\left(\Gamma^C \Gamma^D\right) \left(\overline{\omega}_1 \Gamma^C \omega_4\right)\left(\overline{\omega}_3 \Gamma^D \omega_2\right) \\
&= \frac{1}{4} \sum_C \left(\overline{\omega}_1 \Gamma^C \omega_4\right)\left(\overline{\omega}_3 \Gamma^C \omega_2\right)
\end{aligned}
\tag{C.16}
$$

$$
\begin{aligned}
\left(\overline{\omega}_1 \gamma^\mu \omega_2\right)\left(\overline{\omega}_3 \gamma_\mu \omega_4\right) &= \sum_{C,D} \frac{1}{16} \operatorname{tr}\left(\Gamma^C \gamma^\mu \Gamma^D \gamma_\mu\right) \left(\overline{\omega}_1 \Gamma^C \omega_4\right)\left(\overline{\omega}_3 \Gamma^D \omega_2\right) \\
&= \sum_{C',D'} \frac{1}{16} \operatorname{tr}\left(\Gamma^{C'} \Gamma^{D'}\right) \left(\overline{\omega}_1 \Gamma^{C'} \gamma_\mu \omega_4\right)\left(\overline{\omega}_3 \Gamma^{D'} \gamma^\mu \omega_2\right) \\
&= \frac{1}{4} \sum_C \left(\overline{\omega}_1 \Gamma^C \gamma^\mu \omega_4\right)\left(\overline{\omega}_3 \Gamma^C \gamma_\mu \omega_2\right)
\end{aligned}
\tag{C.17}
$$

where $\Gamma^{C'} = \Gamma^C \gamma^\mu$.

Bibliography

[1] J. C. Pati and A. Salam, "Is Baryon Number Conserved?," *Phys. Rev. Lett.* **31** (1973) 661–664.

[2] J. C. Pati and A. Salam, "Lepton Number as the Fourth Color," *Phys. Rev. D* **10** (1974) 275–289. [Erratum: Phys.Rev.D 11, 703–703 (1975)].

[3] H. Georgi and S. L. Glashow, "Unity of All Elementary Particle Forces," *Phys. Rev. Lett.* **32** (1974) 438–441.

[4] H. Georgi, H. R. Quinn, and S. Weinberg, "Hierarchy of Interactions in Unified Gauge Theories," *Phys. Rev. Lett.* **33** (1974) 451–454.

[5] H. Georgi, "The State of the Art—Gauge Theories," *AIP Conf. Proc.* **23** (1975) 575–582.

[6] H. Fritzsch and P. Minkowski, "Unified Interactions of Leptons and Hadrons," *Annals Phys.* **93** (1975) 193–266.

[7] I. Doršner and S. Saad, "Towards Minimal $SU(5)$," *Phys. Rev. D* **101** no. 1, (2020) 015009, `arXiv:1910.09008 [hep-ph]`.

[8] N. Oshimo, "Realistic model for SU(5) grand unification," *Phys. Rev.* **D80** (2009) 075011, `arXiv:0907.3400 [hep-ph]`.

[9] **Super-Kamiokande** Collaboration, A. Takenaka *et al.*, "Search for proton decay via $p \to e^+ \pi^0$ and $p \to \mu^+ \pi^0$ with an enlarged fiducial volume in Super-Kamiokande I-IV," *Physical Review D* **102** no. 11, (Dec, 2020) .

[10] **Hyper-Kamiokande** Collaboration, K. Abe *et al.*, "Hyper-kamiokande design report," 2018.

[11] **Super-Kamiokande** Collaboration, K. Abe *et al.*, "Search for nucleon decay into charged antilepton plus meson in 0.316 megaton years exposure of the Super-Kamiokande water Cherenkov detector," *Physical Review D* **96** no. 1, (Jul, 2017) .

[12] R. Brock *et al.*, "Proton Decay," in *Workshop on Fundamental Physics at the Intensity Frontier*, pp. 111–130. 5, 2012.

[13] **Kamiokande** Collaboration, R. Matsumoto *et al.*, "Search for proton decay via $p \to \mu^+ K^0$ in 0.37 megaton-years exposure of Super-Kamiokande," `arXiv:2208.13188 [hep-ex]`.

[14] **Super-Kamiokande** Collaboration, K. Abe *et al.*, "Search for nucleon decay via $n \to \bar{\nu}\pi^0$ and $p \to \bar{\nu}\pi^+$ in Super-Kamiokande," *Physical Review Letters* **113** no. 12, (Sep, 2014) .

[15] **Super-Kamiokande** Collaboration, V. Takhistov, "Review of Nucleon Decay Searches at Super-Kamiokande," 2016.

[16] **JUNO** Collaboration, A. Abusleme *et al.*, "JUNO Sensitivity on Proton Decay $p \to \bar{\nu}k^+$ Searches," *Chinese Physics C* **47** no. 11, (Nov, 2023) 113002.

[17] S. L. Glashow, "Partial-symmetries of weak interactions," *Nuclear Physics* **22** no. 4, (1961) 579–588.

[18] S. Weinberg, "A Model of Leptons," *Phys. Rev. Lett.* **19** (1967) 1264–1266.

[19] A. Salam, "Weak and Electromagnetic Interactions," *Conf. Proc. C* **680519** (1968) 367–377.

[20] B. Fornal, *Baryon Number Violation beyond the Standard Model*. PhD thesis, Caltech, 2014.

[21] S. Antusch and K. Hinze, "Nucleon decay in a minimal non-SUSY GUT with predicted quark-lepton Yukawa ratios," `arXiv:2108.08080 [hep-ph]`.

[22] S. L. Olsen, "The Curious Early History of CKM Matrix – miracles happen!," 2023.

[23] C.-N. Yang and R. L. Mills, "Conservation of Isotopic Spin and Isotopic Gauge Invariance," *Phys. Rev.* **96** (1954) 191–195.

[24] **ATLAS** Collaboration, G. Aad *et al.*, "Observation of a new particle in the search for the Standard Model Higgs boson with the ATLAS detector at the LHC," *Phys. Lett. B* **716** (2012) 1–29, `arXiv:1207.7214 [hep-ex]`.

[25] **CMS** Collaboration, S. Chatrchyan *et al.*, "Observation of a New Boson at a Mass of 125 GeV with the CMS Experiment at the LHC," *Phys. Lett. B* **716** (2012) 30–61, `arXiv:1207.7235 [hep-ex]`.

[26] **Kamiokande** Collaboration, Y. Fukuda *et al.*, "Solar neutrino data covering solar cycle 22," *Phys. Rev. Lett.* **77** (1996) 1683–1686.

[27] **Super-Kamiokande** Collaboration, Y. Fukuda *et al.*, "Evidence for oscillation of atmospheric neutrinos," *Phys. Rev. Lett.* **81** (1998) 1562–1567, `arXiv:hep-ex/9807003`.

[28] **Double Chooz** Collaboration, Y. Abe *et al.*, "Indication of Reactor $\bar{\nu}_e$ Disappearance in the Double Chooz Experiment," *Phys. Rev. Lett.* **108** (2012) 131801, `arXiv:1112.6353 [hep-ex]`.

[29] M. López-Corredoira, "Problems with the dark matter and dark energy hypotheses, and alternative ideas," in *Cosmology on Small Scales 2018: Dark Matter Problem and Selected Controversies in Cosmology.* 8, 2018. arXiv:1808.09823 [astro-ph.CO].

[30] A. Deur, "An explanation for dark matter and dark energy consistent with the Standard Model of particle physics and General Relativity," *Eur. Phys. J. C* **79** no. 10, (2019) 883, arXiv:1709.02481 [astro-ph.CO].

[31] A. Deur, "Implications of graviton–graviton interaction to dark matter," *Physics Letters B* **676** no. 1, (2009) 21–24.

[32] V. A. Kostelecky, "Gravity, Lorentz violation, and the standard model," *Phys. Rev. D* **69** (2004) 105009, arXiv:hep-th/0312310.

[33] G. Bhattacharyya, "The Hierarchy Problem and Physics Beyond the Standard Model," *Springer Proc. Phys.* **203** (2018) 17–20.

[34] C. Csáki and P. Tanedo, "Beyond the Standard Model," in *2013 European School of High-Energy Physics*, pp. 169–268. 2015. arXiv:1602.04228 [hep-ph].

[35] Lee, Hyun Min, "Lectures on physics beyond the Standard Model," *Journal of the Korean Physical Society* (May, 2021) , arXiv:1907.12409 [hep-ph].

[36] G.-y. Huang and S. Zhou, "Precise values of running quark and lepton masses in the standard model," *Phys. Rev. D* **103** (Jan, 2021) 016010.

[37] P. de Aquino, *Beyond Standard Model Phenomenology at the LHC.* PhD thesis, Louvain U., New York, 2012.

[38] M. C. Gonzalez-Garcia, M. Maltoni, and T. Schwetz, "NuFIT: Three-flavour global analyses of neutrino oscillation experiments," *Universe* **7** no. 12, (Nov, 2021) 459.

[39] I. Esteban, M. Gonzalez-Garcia, M. Maltoni, T. Schwetz, and A. Zhou, "The fate of hints: updated global analysis of three-flavor neutrino oscillations," *Journal of High Energy Physics* **2020** no. 9, (Sep, 2020) .

[40] R. Dermíšek, "Unification of gauge couplings in the standard model with extra vectorlike families," *Phys. Rev. D* **87** (Mar, 2013) 055008. https://link.aps.org/doi/10.1103/PhysRevD.87.055008.

[41] **Particle Data Group** Collaboration, K. A. Olive *et al.*, "Review of Particle Physics," *Chin. Phys. C* **38** (2014) 090001.

[42] D. R. T. Jones, "Two-loop β function for a $G_1 \times G_2$ gauge theory," *Phys. Rev. D* **25** (Jan, 1982) 581–582.

[43] J. Roy, "Calculating β-function coefficients of Renormalization Group Equations," 2019.

[44] Ellis, John and Kelley, S and Nanopoulos, Dimitri V, "Precision LEP data, supersymmetric GUTs and string unification," *Physics Letters B* **249** no. 3-4, (1990) 441–448.

[45] Amaldi, Ugo and de Boer, Wim and Fürstenau, Hermann, "Comparison of grand unified theories with electroweak and strong coupling constants measured at LEP," *Physics Letters B* **260** no. 3-4, (1991) 447–455.

[46] Ellis, John and Kelley, S and Nanopoulos, Dimitri V, "Probing the desert using gauge coupling unification," *Physics Letters B* **260** no. 1-2, (1991) 131–137.

[47] Schwichtenberg, Jakob, "Gauge coupling unification without supersymmetry," *The European Physical Journal C* **79** no. 4, (Apr, 2019) .

[48] R. Slansky, "Group Theory for Unified Model Building," *Phys. Rept.* **79** (1981) 1–128.

[49] Y. Nagashima, *Beyond the standard model of elementary particle physics*. Wiley-VCH, Weinheim, USA, 2014.

[50] T. Hübsch and S. Pallua, "Symmetry breaking mechanism in an alternative su(5) model," *Physics Letters B* **138** no. 4, (1984) 279–282.

[51] T. Hubsch, S. Meljanac, and S. Pallua, "A NONMINIMAL SU(5) MODEL," *Phys. Rev. D* **31** (1985) 2958.

[52] D. Croon, T. E. Gonzalo, L. Graf, N. Košnik, and G. White, "Gut physics in the era of the lhc," *Frontiers in Physics* **7** (2019) 76.

[53] K. Kang, "INTRODUCTION TO GRAND UNIFICATION THEORIES," in *15th Rencontres de Moriond: II: Electroweak and Unified Theory Predictions*, pp. 413–426. 1980.

[54] J. C. Pati and A. Salam, "Unified lepton-hadron symmetry and a gauge theory of the basic interactions," *Phys. Rev. D* **8** (Aug, 1973) 1240–1251.

[55] J. C. Pati and A. Salam, "Lepton number as the fourth "color"," *Phys. Rev. D* **10** (Jul, 1974) 275–289.

[56] A. D. Sakharov, "Violation of CP Invariance, C asymmetry, and baryon asymmetry of the universe," *Pisma Zh. Eksp. Teor. Fiz.* **5** (1967) 32–35.

[57] P. A. M. Dirac, "The quantum theory of the electron," *Proc. Roy. Soc. Lond. A* **117** (1928) 610–624.

[58] B. Bajc, "*Grand Unification and Proton Decay*," 2011. Accessed: 2021–07-16.

[59] W. Buchmüller and D. Wyler, "Effective lagrangian analysis of new interactions and flavour conservation," *Nuclear Physics B* **268** no. 3, (1986) 621–653.

[60] B. Grzadkowski, M. Iskrzyński, M. Misiak, and R. J., "Dimension-six terms in the Standard Model Lagrangian," *Journal of High Energy Physics* **85(2010)** (2010) 10, `arXiv:1008.4884 [hep-ph]`.

[61] M. Claudson, M. B. Wise, and L. J. Hall, "Chiral Lagrangian for Deep Mine Physics," *Nucl. Phys. B* **195** (1982) 297–307.

[62] F. Wilczek and A. Zee, "Operator Analysis of Nucleon Decay," *Phys. Rev. Lett.* **43** (1979) 1571–1573.

[63] N. Sakai and T. Yanagida, "Proton decay in a class of supersymmetric grand unified models," *Nuclear Physics B* **197** no. 3, (1982) 533–542.

[64] S. Weinberg, "Baryon and Lepton Nonconserving Processes," *Phys. Rev. Lett.* **43** (1979) 1566–1570.

[65] P. Fileviez Pérez, "Fermion mixings vs d=6 proton decay," *Physics Letters B* **595** no. 1, (2004) 476–483.

[66] P. Nath and P. F. Pérez, "Proton stability in grand unified theories, in strings and in branes," *Physics Reports* **441** no. 5-6, (Apr, 2007) 191–317.

[67] Y. Hara, S. Itoh, Y. Iwasaki, and T. Yoshié, "Proton decay and lattice qcd," *Phys. Rev. D* **34** (Dec, 1986) 3399–3404.

[68] K. C. Bowler, D. Daniel, T. D. Kieu, D. G. Richards, and C. J. Scott, "Nucleon Wave Functions From Lattice Gauge Theories: Measurements of Baryonic Operators," *Nucl. Phys. B* **296** (1988) 431–444.

[69] S. Aoki, M. Fukugita, S. Hashimoto, K.-I. Ishikawa, N. Ishizuka, Y. Iwasaki, K. Kanaya, T. Kaneda, S. Kaya, Y. Kuramashi, and et al., "Nucleon decay matrix elements from lattice qcd," *Physical Review D* **62** no. 1, (Jun, 2000) .

[70] Y. Aoki, E. Shintani, and A. Soni, "Proton decay matrix elements on the lattice," *Physical Review D* **89** no. 1, (Jan, 2014) .

[71] Y. Aoki, T. Izubuchi, E. Shintani, and A. Soni, "Improved lattice computation of proton decay matrix elements," *Physical Review D* **96** no. 1, (Jul, 2017) .

[72] J.-S. Yoo, Y. Aoki, T. Izubuchi, and S. Syritsyn, "Proton decay matrix element on the lattice with physical pion mass," 2018.

[73] Y. Aoki, P. Boyle, P. Cooney, L. Del Debbio, R. Kenway, C. M. Maynard, A. Soni, and R. Tweedie, "Proton lifetime bounds from chirally symmetric lattice qcd," *Physical Review D* **78** no. 5, (Sep, 2008) .

[74] I. Doršner, E. Džaferović-Mašić, and S. Saad, "Parameter space exploration of the minimal SU(5) unification," *Phys. Rev. D* **104** no. 1, (2021) 015023, `arXiv:2105.01678 [hep-ph]`.

[75] T. Nihei and J. Arafune, "The two loop long range effect on the proton decay effective lagrangian," *Progress of Theoretical Physics* **93** no. 3, (Mar, 1995) 665–669.

[76] **Particle Data Group** Collaboration, R. L. Workman *et al.*, "Review of Particle Physics," *PTEP* **2022** (2022) 083C01.

[77] **Particle Data Group** Collaboration, M. Tanabashi *et al.*, "Review of particle physics," *Phys. Rev. D* **98** (Aug, 2018) 030001.

[78] W. Buchmuller, R. Ruckl, and D. Wyler, "Leptoquarks in Lepton - Quark Collisions," *Phys. Lett. B* **191** (1987) 442–448. [Erratum: Phys.Lett.B 448, 320–320 (1999)].

[79] M. Claudson, M. B. Wise, and L. J. Hall, "Chiral lagrangian for deep mine physics," *Nuclear Physics B* **195** no. 2, (1982) 297–307.

[80] H. Adarkar, S. R. Dugad, M. R. Krishnaswamy, M. G. K. Menon, B. V. Sreekantan, Y. Hayashi, N. Ito, S. Kawakami, S. Miyake, and Y. Uchihori, "Experimental evidence for gut proton decay," `arXiv:hep-ex/0008074`.

[81] G. Battistoni, P. Campana, V. Chiarella, A. Ciocio, E. Iarocci, G. Murtas, G. Nicoletti, L. Satta, L. Trasatti, E. Bellotti, E. Fiorini, G. Liguori, P. Negri, A. Pullia, S. Ragazzi, M. Rollier, L. Zanotti, G. Bologna, G. Castagnoli, and M. Price, "Results on nucleon decay in the mont blanc nusex experiment,".

[82] M. Deakyne, K. Lande, C. K. Lee, R. Steinberg, and S. Sutton, "Homestake mine proton decay experiment,".

[83] C. Berger, A. HOFFMANN, F. Raupach, J. Tutas, G. Schmitz, B. Dudelzak, P. Eschstruth, G. Deuzet, S. Jullian, and D. Lalanne, "Search for proton decay in the frejus experiment,".

[84] J. L. Thron, "The Soudan-II Proton Decay Experiment," *Nucl. Instrum. Meth. A* **283** (1989) 642–645.

[85] R. C. Svoboda *et al.*, "The IMB Proton Decay Detector," in *International School of Cosmic Ray Astrophysics: Composition and Origin of Cosmic Rays.* 1982.

[86] P. Langacker, "Grand Unified Theories and Proton Decay," *Phys. Rept.* **72** (1981) 185.

[87] **Super-Kamiokande** Collaboration, K. Abe *et al.*, "Search for proton decay via $p \to \nu K^+$ using 260 kiloton · year data of Super-Kamiokande," *Physical Review D* **90** (Oct, 2014) 072005.

[88] P. N. Bhattiprolu, S. P. Martin, and J. D. Wells, "Statistical significances and projections for proton decay experiments," *Physical Review D* **107** no. 5, (Mar, 2023) .

[89] P. S. B. Dev, L. W. Koerner, S. Saad, S. Antusch, M. Askins, K. S. Babu, J. L. Barrow, J. Chakrabortty, A. de Gouvêa, Z. Djurcic, S. Girmohanta, I. Gogoladze, M. C. Goodman, A. Higuera, D. Kalra, G. Karagiorgi, E. Kearns, V. A. Kudryavtsev, T. Kutter, J. P. Ochoa-Ricoux, M. Malinský, D. A. M. Caicedo, R. N. Mohapatra, P. Nath, S. Nussinov, V. Pec, A. Rafique, J. R. Rondon, R. Shrock, H. W. Sobel, T. Stokes, M. Strait, R. Svoboda, S. Syritsyn, V. Takhistov, Y. T. Tsai, R. A. Wendell, and Y. L. Zhou, "Searches for Baryon Number Violation in Neutrino Experiments: A White Paper," 2022.

[90] S. Antusch, I. Doršner, K. Hinze, and S. Saad, "Fully testable axion dark matter within a minimal $SU(5)$ GUT," *Physical Review D* **108** no. 1, (Jul, 2023) .

[91] T. Ohlsson, "Proton decay," *Nuclear Physics B* **993** (2023) 116268.

[92] V. A. K. and, "Underground physics with DUNE," *Journal of Physics: Conference Series* **718** no. 6, (May, 2016) 062032.

[93] E. Chardonnet, "The DUNE dual-phase liquid argon TPC," *Journal of Instrumentation* **15** no. 05, (May, 2020) C05064.

[94] **ESSnuSB** Collaboration, A. Alekou *et al.*, "The ESSnuSB design study: overview and future prospects," `arXiv:2303.17356 [hep-ex]`.

[95] **ESSnuSB** Collaboration, E. Baussan, "The ESSnuSB High Intensity Neutrino Super Beam," *PoS* **ICHEP2022** (2022) 555.

[96] **ESSnuSB** Collaboration, O. Zormpa, "ESSnuSB detector performance," *PoS* **NuFact2021** (2022) 206.

[97] D. Castelvecchi, "Japan will build the world's largest neutrino detector.," *Nature* (2019) .

[98] F. D. Lodovico and on behalf of the Hyper-Kamiokande Collaboration, "The Hyper-Kamiokande Experiment," *Journal of Physics: Conference Series* **888** no. 1, (Sep, 2017) 012020.

[99] B. Jelmini, "Calorimetry in a Neutrino Observatory: The JUNO Experiment," *Instruments* **6** no. 3, (2022) .

[100] "JUNO physics and detector," *Progress in Particle and Nuclear Physics* **123** (Mar, 2022) 103927.

[101] **JUNO** Collaboration, M. Colomer Molla, "Physics potential with astrophysical neutrinos in JUNO," *PoS* **ICRC2023** (2023) 1192.

[102] I. Doršner, "Scalar leptoquark in $SU(5)$," *Physical Review D* **86** no. 5, (Sep, 2012) .

[103] S. Bilenky, "Neutrinos: Majorana or Dirac?," 2020.

[104] K. S. Babu, S. Nandi, and Z. Tavartkiladze, "New Mechanism for Neutrino Mass Generation and Triply Charged Higgs Bosons at the LHC," *Phys. Rev.* **D80** (2009) 071702, `arXiv:0905.2710 [hep-ph]`.

[105] G. Bambhaniya, J. Chakrabortty, S. Goswami, and P. Konar, "Generation of neutrino mass from new physics at TeV scale and multilepton signatures at the LHC," *Phys. Rev. D* **88** no. 7, (2013) 075006, `arXiv:1305.2795 [hep-ph]`.

[106] N. Oshimo, "Realistic model for $su(5)$ grand unification," *Physical Review D* **80** no. 7, (Oct, 2009) .

[107] P. F. de Salas, S. Gariazzo, O. Mena, C. A. Ternes, and M. Tórtola, "Neutrino Mass Ordering from Oscillations and Beyond: 2018 Status and Future Prospects," *Frontiers in Astronomy and Space Sciences* **5** (2018) .

[108] W. Zhang, E.-K. li, M. Du, Y. Mu, S. Ning, B. Chang, and L. Xu, "Detecting the neutrino mass and mass hierarchy from global data," 2019.

[109] M. Gonzalez-Garcia, M. Maltoni, and T. Schwetz, "Global analyses of neutrino oscillation experiments," *Nuclear Physics B* **908** (2016) 199–217. Neutrino Oscillations: Celebrating the Nobel Prize in Physics 2015.

[110] I. Cordero-Carrió n, M. Hirsch, and A. Vicente, "Master Majorana neutrino mass parametrization," *Physical Review D* **99** no. 7, (Apr, 2019) .

[111] I. Cordero-Carrió n, M. Hirsch, and A. Vicente, "General parametrization of Majorana neutrino mass models," *Physical Review D* **101** no. 7, (Apr, 2020) .

[112] A. Giveon, L. J. Hall, and U. Sarid, "SU(5) unification revisited," *Phys. Lett.* **B271** (1991) 138–144.

[113] W. R. Inc., "Mathematica, Version 13.3.". Champaign, IL, 2023.

[114] **Particle Data Group** Collaboration, K. A. Olive *et al.*, "Review of Particle Physics," *Chin. Phys.* **C38** (2014) 090001.

[115] P. de Salas, D. Forero, C. Ternes, M. Tórtola, and J. Valle, "Status of neutrino oscillations 2018: 3σ hint for normal mass ordering and improved CP sensitivity," *Physics Letters B* **782** (2018) 633–640.

[116] S. Antusch and V. Maurer, "Running quark and lepton parameters at various scales," *JHEP* **11** (2013) 115, `arXiv:1306.6879 [hep-ph]`.

[117] I. Esteban, M. C. Gonzalez-Garcia, M. Maltoni, T. Schwetz, and A. Zhou, "The fate of hints: updated global analysis of three-flavor neutrino oscillations," *JHEP* **09** (2020) 178, `arXiv:2007.14792 [hep-ph]`.

[118] S. Weinberg, *The Quantum theory of fields. Vol. 1: Foundations.* Cambridge University Press, 6, 2005.

[119] M. Fierz, "Über die relativistische Theorie kräftefreier Teilchen mit beliebigem Spin," *Helv. Phys. Acta* **12** no. 1, (1939) 3–37.

[120] J. F. Nieves and P. B. Pal, "Generalized fierz identities," *American Journal of Physics* **72** no. 8, (Aug, 2004) 1100–1108.

[121] M. E. Peskin and D. V. Schroeder, *An Introduction to quantum field theory.* Addison-Wesley, Reading, USA, 1995.

[122] Z.-Z. Xianyu, *A Complete Solution to Problems in "An Introduction to Quantum Field Theory" by Peskin and Schroeder.* Harvard University, 2016.